

PRECAMBRIAN GEOLOGY
OF THE UPPER BRAZOS BOX AREA,
RIO ARRIBA COUNTY, NEW MEXICO

by

Joan L. Gabelman

Submitted in Partial Fulfillment
of the Requirements for the Degree of
Master of Science in Geology

New Mexico Institute of Mining and Technology

Socorro, New Mexico

May, 1988

ABSTRACT

Early Proterozoic (c.a. 1650-1750 Ma) supracrustal and plutonic rocks are exposed along and within the upper Brazos Box in the northern Tusas Mountains, Rio Arriba County, New Mexico. These Precambrian units are unconformably overlain by a sequence of Tertiary conglomerates, and volcanic and volcanoclastic rocks. The volcanic and volcanoclastic rocks represent a southern extension of the San Juan Volcanic Field into northern New Mexico. Quaternary to Recent landslides locally disrupt the Tertiary stratigraphy.

Proterozoic supracrustal rocks exposed in the upper Brazos Box are subdivided, from oldest to youngest, into three lithostratigraphic units: 1) the Moppin Metavolcanics (MMS), 2) the Metasedimentary and Metavolcanic package (MSMR), and 3) the Ortega Group. Intrusive into the lower portions of the Moppin Metavolcanics is a trondhjemite locally known as the trondhjemite of Rio Brazos. All of these rocks are multiply deformed and have experienced regional metamorphism from upper greenschist to lower amphibolite facies.

The MMS (Barker, 1958; Wobus, 1985) contains felsic to mafic schists and phyllites. Relict features such as bedding, pillows, flow breccias and vesicles are common in the lowermost portions of the exposed section. These rocks are interpreted to represent mafic to felsic volcanics and volcanoclastics. Compositionally, these rocks range from basalt to rhyolite; chemically, they are sub-alkaline.

The MSMR package unconformably overlies the MMS. The basal unit of this group is a thin metaconglomerate, which is overlain by the Burned Mountain metarhyolite. Flattened fragments believed to represent relict pumice, embayed quartz eyes, and the unit's great areal extent suggest the Burned Mountain metarhyolite was deposited as an ash flow tuff. The Burned Mountain metarhyolite has a reported U/Pb zircon age of $1,700 \pm 25$ MA (Silver in Reed et al., 1987). Above the metarhyolite horizon the MSMR package grades upward from a phyllitic metaconglomerate to a micaceous quartzite with numerous phyllite pebble interbeds.

The Ortega Group conformably overlies the MSMR package. The lower portion consists of a transitional quartzite with rare isolated phyllite pebbles that resemble those in the underlying MSMR package. The upper Ortega Group unit is a clean vitreous cross-bedded quartzite, the lower portion of which is slightly more micaceous.

The lower exposed portion of the Moppin Metavolcanics is intruded by the trondhjemite of Rio Brazos. An intrusive relationship is indicated by highly irregular contacts, chilled margins, dikes of trondhjemite in the MMS, and MMS xenoliths in the trondhjemite. Barker et al (1974) report a Rb-Sr whole-rock age for this rock of $1,654 \pm 34$ Ma.

Proterozoic rocks in the region have experienced at least three regionally-significant phases of ductile deformation. The first phase of deformation isoclinally folded and sheared supracrustal rocks, resulting in transposed-bedding and a layer-parallel foliation that strikes WNW and dips steeply south. A distinct mylonitic zone 3 m above the unconformable (?) contact between the MMS and MSMR is related to D1 and indicates that the Ortega Group and the MSMR package were sheared northward over the MMS. Offset along this mylonitic zone has not been determined. The second phase of deformation produced both mesoscopic and macroscopic open upright folds with shallow axial plunges. The third phase of deformation is evident in a NE-striking and steeply south-dipping fracture cleavage along Gavilan Creek.

The Moppin Metavolcanics are believed to have accumulated in an arc setting. Trace element geochemistry suggests that the Burned Mountain metarhyolite has many similarities to modern rhyolites formed in extensional settings in or near continental crust. The poorly sorted metaconglomerate in the base of the MSMR may have also been deposited in an extensional environment. The MSMR grades upsection from a poorly sorted metaconglomerate into a micaceous quartzite. The Ortega Group grades upsection from a micaceous quartzite into a clean vitreous quartzite. Cross-beds in the Ortega Group indicate that it was deposited in 3-4 m-deep water on an inner shelf where tidal processes dominated (Soegaard and Eriksson, 1985). The evolution of the poorly sorted metaconglomerate at the base of the MSMR package into the vi-

treous quartzite of the Ortega Group may represent the stabilization of a craton. The present proximity of the MMS and the overlying MSMR and Ortega Group may not reflect original spatial relationships, or original depositional and tectonic settings, if movement along the mylonitic zone has been substantial (Grambling et al., 1988, in press).

Table of Contents

Abstract	ii
Table of Contents	v
List of Plates	vii
List of Figures	vii
List of Tables	ix
Acknowledgements	x
INTRODUCTION	1
Location	1
Purpose	1
Methods	3
Previous Work	3
GENERAL GEOLOGY	11
Geologic setting	11
Phanerozoic Geologic History	11
Precambrian Stratigraphy of the Tusas Mountains	13
Precambrian Structures	15
Regional Metamorphism	16
Economic Geology	16
PROTEROZOIC LITHOLOGIES	18
Supracrustal Rocks	18
Moppin Metavolcanics	18
Intermediate to Mafic Rocks	20
Amphibole Schist	20
Plagioclase-Chlorite Schists	26
Muscovite-Chlorite Phyllite	28
Biotite-Amphibole Schist	30
Chlorite-Quartz Schist	32
Chlorite-Quartz-Muscovite Phyllite	33
Felsic Metavolcanics	34
Chlorite-Plagioclase-Quartz Schist	34
Muscovite-Quartz Schist	37
Possible Depositional Environment	38
Metasedimentary and Metarhyolite Package	39
Phyllite Pebble Metaconglomerate	40
Chlorite-Muscovite-Quartz Phyllonite	44
Burned Mountain Metarhyolite	46
Quartz-muscovite Phyllite	49
Chlorite Schist	50
Possible Depositional Environment	51

Ortega Group	51
Transitional Quartzite	52
Vitreous Quartzite	53
Quartz-Muscovite Phyllite	59
Chlorite Schist	60
Possible Depositional Environment	61
Intrusive Rocks	62
Trondhjemite of Rio Brazos	62
Hornblendite	67
Dikes	68
Quartz Veins	69
TERTIARY GEOLOGY	70
El Rito Formation	70
Ritito Conglomerate	70
Conejos Formation	71
Treasure Mountain Formation	72
Los Pinos Formation	73
AEROMAGNETIC DATA	75
STRUCTURAL GEOLOGY	77
Proterozoic Structures	77
Foliations	80
Domains 1 and 2	80
Domains 3 and 4	83
Domains 5 and 6	85
Domain 7	88
Folds	91
Lineations	92
Discussion	92
Tertiary Structures	96
Lineaments	99
METAMORPHISM	102
Regional Metamorphism	102
Spillitization	107
GEOCHEMISTRY	109
Methods	109
Alteration	109
Classification Diagrams	110
Tectonic Discrimination Diagrams	110
DISCUSSION	119
Depositional and Tectonic Setting(s) of the North Tusas Precambrian	119
Moppin Metavolcanics	119
Metasedimentary and Metarhyolite Package	121

Ortega Group	123
Trondhjemite of the Rio Brazos	124
Evolution of Settings in the North Tusas Mountains	125
Relationship of the North Tusas Proterozoic Rocks to Regional Proterozoic Rocks	128
SUMMARY	130
Geologic History	130
Recommendations for Future Work	133
References Cited	134
Appendix A- Thin Section Descriptions	140
Appendix B- Geochemical Analyses	163

List of Plates

	Page
Geologic Map	in pocket
Geologic Cross Section	in pocket

List of Figures

	Page
F.1 Locality map of the Upper Brazos Box study area	2
F.2 Geographic correlation of areas mapped by previous workers	4
F.3 Generalized stratigraphic column for Proterozoic rocks in the study area	19
F.4 Bedded amphibole schist from the lower MMS section	22
F.5 Pillow structure in an amphibole schist from the lower MMS section	23
F.6 Amygdules in a brecciated amphibole schist from the lower MMS section	24
F.7 Siderite porphyroblasts in a plagioclase-chlorite schist from the upper MMS section	29

F.8	Amphibole pseudomorph of a pyroxene crystal in a biotite-amphibole schist from the central portion of the MMS section	31
F.9	Flow banded felsic volcanic from the chlorite-plagioclase-quartz schist in the lower MMS section	35
F.10	Phyllite pebble metaconglomerate from the base of the MSMR section	42
F.11	Micaceous beds separated by phyllite pebble interbeds from the upper MSMR section	43
F.12	Chlorite-muscovite-quartz phyllonite from the base of the MSMR section	45
F.13	Photomicrograph of the Burned Mountain metarhyolite	48
F.14	Photomicrograph of the Ortega Group transitional quartzite	54
F.15	Jawbone Syncline	55
F.16	Ortega Group vitreous quartzite	57
F.17	Trondhjemite of the Rio Brazos intruding the MMS and crosscut by S_2	63
F.18	MMS xenoliths in the Trondhjemite of Rio Brazos	64
F.19	Aeromagnetic map	76
F.20	Index map of structural domains	78
F.21	Generalized map of structures in the study area	79
F.22	Stereonet of foliations from domain 1	81
F.23	Stereonet of foliations from domains 1 and 2	82
F.24	Stereonet of foliations from domains 3 and 4	84
F.25	S_1 and S_2 in an amphibole schist from the lower MMS section	86
F.26	S_1 and S_2 in a quartz-plagioclase-chlorite schist from the lower MMS section	87
F.27	Stereonet of foliations from domains 5 and 6	89
F.28	Stereonet of foliations from domain 7	90
F.29	Stereonet of extension lineations from domains 3 and 4	93

F.30	Tectonized zone in the Ortega Group micaceous quartzite	98
F.31	Satellite mosaic of northern New Mexico	101
F.32	Metamorphic paragenesis	103
F.33	Metamorphic temperature-pressure diagrams	106
F.34	Jensen cation plot	111
F.35	Zr/TiO ₂ vs Nb/Y plot	112
F.36	An-Or-Ab diagram	113
F.37	Ti vs Cr plot	114
F.38	Ti-Zr-Y diagram	115
F.39	Ti vs Zr plots	117
F.40	Nb vs Y plot	118
F.41	Generalized sequence of geologic events	131

List of Tables

		Page
T.1	Correlation of unit names	5
T.B1	Geochemical analyses	164
T.B2	Accuracy of Geochemical Analyses	169
T.B3	Precision of Geochemical Analyses	170
T.B4	Detection Limits of Some Trace Elements	171

ACKNOWLEDGEMENTS

I would like to thank the New Mexico Bureau of Mines and Mineral Resources for the financial support that made this study possible. I am grateful to my advisors, Dr. James M. Robertson, Dr. Christopher K. Mawer, and Dr. Kent C. Condie for their stimulating discussions, critical reviews of the thesis, and encouragement throughout the project. I would like to thank Dr. Jon Callender for his great help and enthusiasm in the field. Dr. Antonius Budding contributed a lot to the petrographic and metamorphic studies. Mr. John Blagbrough was very generous in advising me on periglacial processes and landforms. Dr. Richard Chamberlin helped me to understand modern ash flows. My appreciation is also extended to Mr. Lin Cordell for providing the aeromagnetic data of my study area and a critiquing of my interpretation. I am thankful to Dr. Bill Muelhberger for providing a stimulating review of my geologic map.

I am particularly grateful to Michael Knoper for the discussions we had and the help he provided on every aspect of this project. I owe Isaac Boadi and Stewart Smith a great deal of thanks for the many discussions of the Tusas Mountain geology that we had. Ron Linden and Michael Williams offered much advise on the structural aspects of this project. Paul Bauer also helped me in the structural aspects of this project and helped to prepare me for my defense. Paul Singer was very generous in advising me on aeromagnetic data.

I am very thankful to the Peterson family for allowing me to map and camp on their land for two summers. Mostly, I am grateful to Louise for all those wonderful days in the Brazos and cups of hot coffee.

And finally, I am tremendously grateful to my parents, Olive and John Gabelman, for their encouragement and support throughout this project.

**PRECAMBRIAN GEOLOGY
OF THE UPPER BRAZOS BOX AREA,
RIO ARRIBA COUNTY, NEW MEXICO**

INTRODUCTION

LOCATION

The upper Brazos Box study area is located in the Tusas Mountains of north-central New Mexico (Figure 1, Plate 1). The area lies on the north side of U.S. Highway 64 twenty-five miles west of Tres Piedras and twenty-five miles east of Tierra Amarilla. It is situated between north latitudes $36^{\circ} 51'$ and $36^{\circ} 45'$ and west longitudes $106^{\circ} 22'$ and $106^{\circ} 15'13''$ on the USGS Lagunitas Creek (7.5 minute) quadrangle. Geographically, the southern edge of the study area is Gavilan Creek and the western boundary extends beyond the western rim of the upper Brazos Box. The northern edge of the field area is south of San Antonio Creek and the eastern edge is the Carson National Forest boundary.

Access to the field area is by a private road from the Peterson cow camp. A portion of the Carson National Forest road was also used.

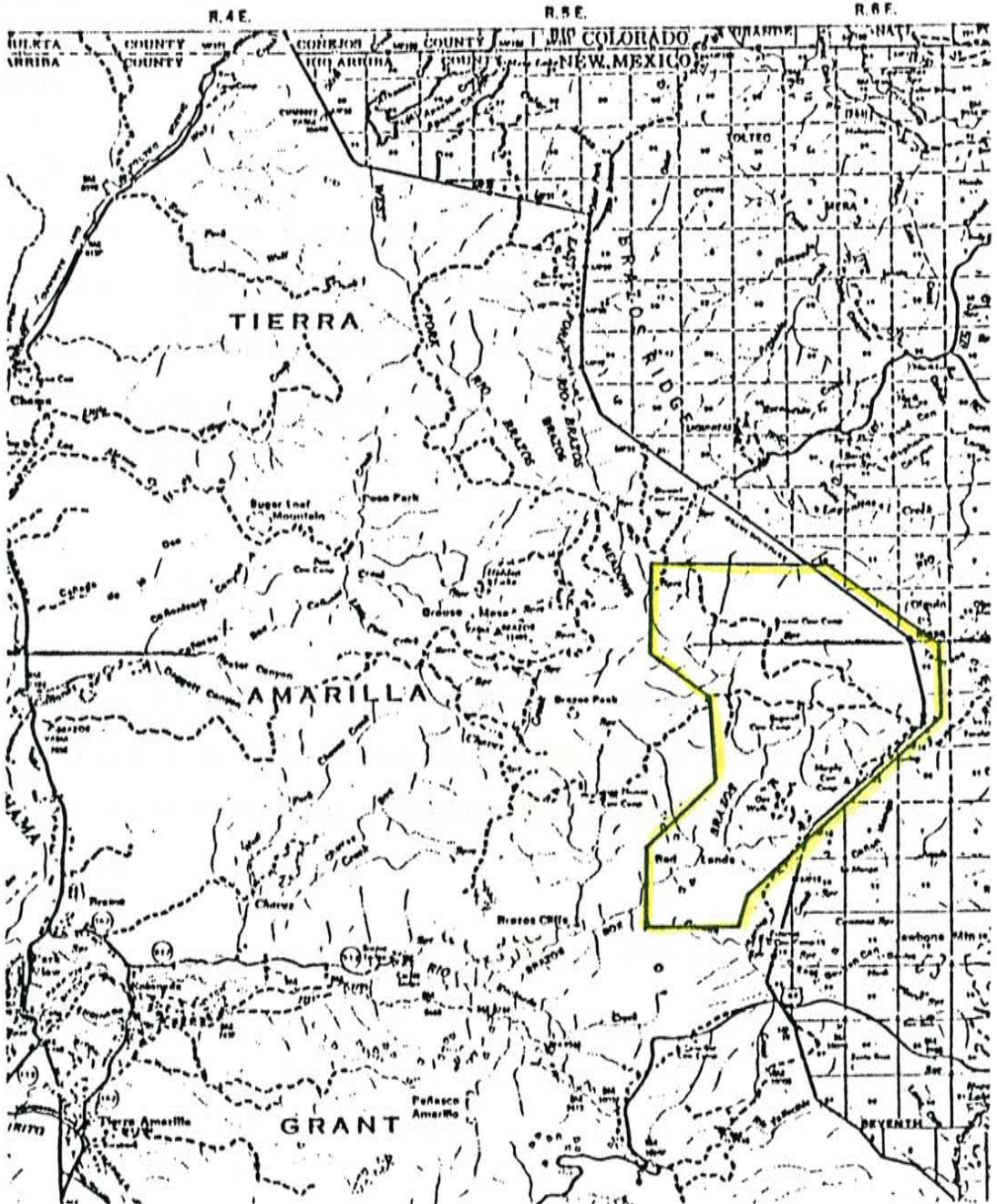
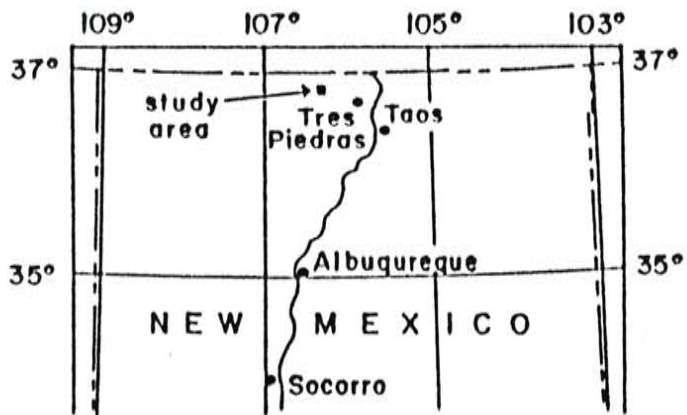
PURPOSE

This work is part of a continuing study of Proterozoic rocks in the Tusas Mountains of northern New Mexico. Specific objectives are:

- 1) to map at a scale of 1:12,000 Proterozoic rocks which had previously been mapped at a 1:48,000 scale in reconnaissance style (Muehlberger, 1968);

FIGURE 1

Location map of the Upper Brazos Box Study Area. Base map is Carson National Forest Service map.



- 2) to recognize and characterize Precambrian age deformational events and their resulting structures and fabrics;
- 3) to understand the nature of the contacts between major units;
- 4) to determine the grade of regional metamorphism ;
- 5) to chemically characterize the major lithologies;
- 6) to evaluate depositional environments and formulate a possible tectonic history for the area.

METHODS

The study area was mapped during the summers of 1986 and 1987 at a scale of 1:12,000 using standard pace and compass techniques and a Thommen altimeter. The USGS Lagunitas Creek (7.5 minute) quadrangle was used as a base map. Color air photos were used to supplement topographic maps. Petrology and micro-structures were examined in seventy-three thin sections. Thirty-one samples were analyzed by x-ray fluorescence for major, minor and trace elements.

PREVIOUS WORK

Many geologists have worked in the Tusas Mountains since the late 1930's. Figure 2 illustrates the relationships between geographic areas mapped in the Tusas Mountain area and Table 1 correlates the nomenclature of units used by various workers.

The earliest geologic investigation of northern New Mexico's Proterozoic rocks was by Just (1937), who studied non-metallic minerals associated with pegmatites in the Picuris-Petaca area. He named many of the major units including: the Hopewell Series- a group of mafic metavolcanic

FIGURE 2

Geographic correlation of areas in the Tusas Mountains that previous geologists have worked in. Base map is from the USGS index to topographic maps of New Mexico.

AUTHOR	YEAR	AREA
Just	1937	-----
Barker	1958	-----
Bingler	1965, 1974	-----
Muhelberger	1968	-----
Doney	1968	-----
Gresends & Stensrud	1974	-----
Kent	1980	-----
Gibson	1981	-----
Wobus	1982, 1985	-----
Boadi	1986	-----
Smith	1986	-----
Gabelman	1988	-----

105°

106°

107°

A

R

O

L

O

C

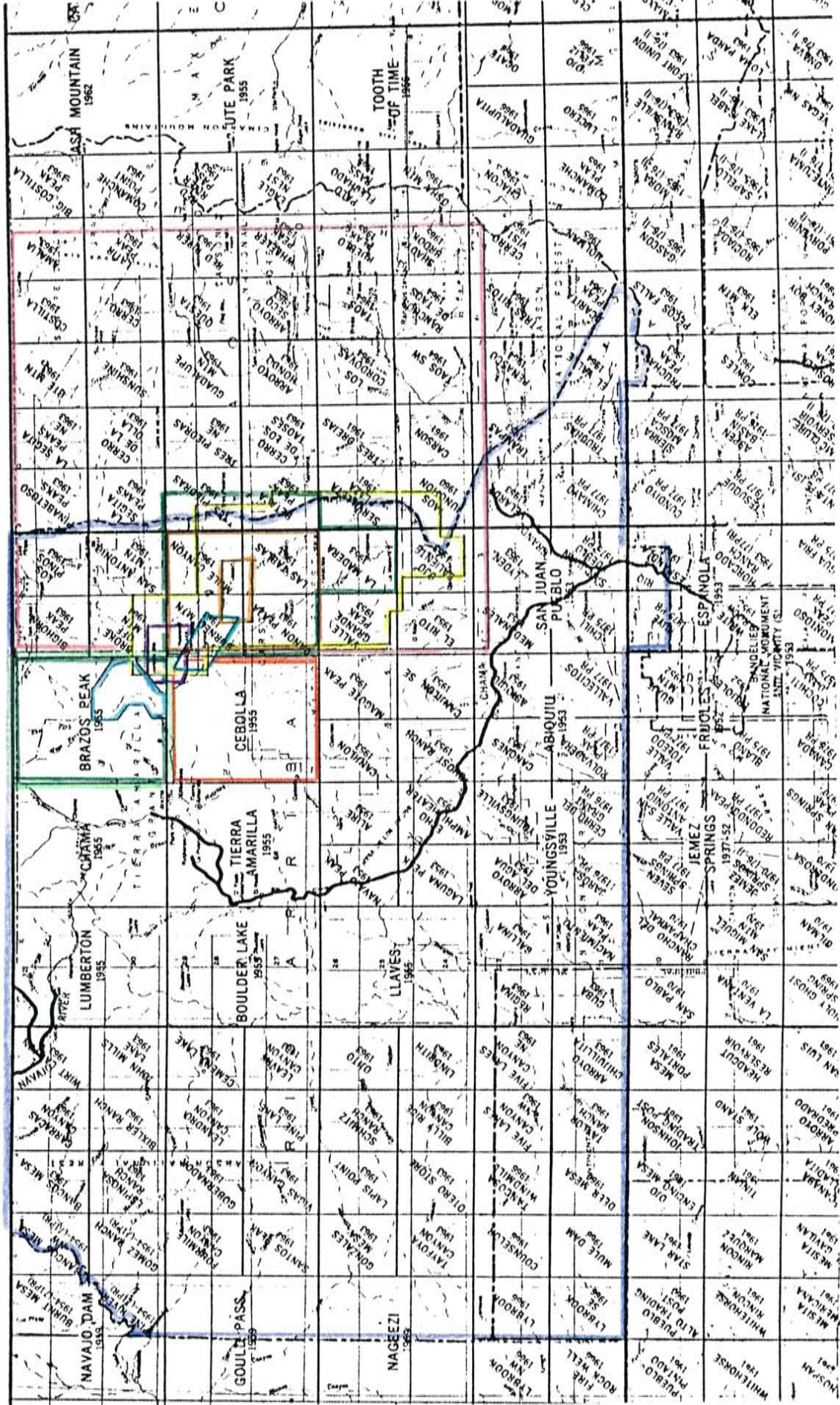


TABLE 1

Correlation of unit names used by previous geologists in the Tusas Mountains; work done by Just (1937) in the Picuris is also included. No stratigraphic sequences are implied. The correlation of metasedimentary units after Kent with those before Kent is tentative.

Just (1937)	Montgomery (1953)	Barker (1958, 1974)	Bingler (1965, 1974)	Muenberger (1968)	Gresens & Stensrud (1974)	Wobus (1982, 1985)	Kent (1980)	Gibson (1981)	Boadi (1986)	Smith (1986)	Williams (1987)	This Study
Ortega Quartzite		Ortega Qtzite, Kiawa Mt. Fm. upper qtzite memb. Jawbone cg. memb. amphibolite memb. Big Rock cg. memb. lower qtzite memb.	quartzite	quartzite	Ortega Quartzite	Ortega Quartzite	vitreous qtzite, subarkose arkose	vitreous qtzite.	Ortega Qtzite.	vitreous qtzite.	Ortega Group	Ortega Group
Vallecitos Rhy.		BMR	feldspathic sch. (65) lepites (74)		metahyalite and interbedded metasediments	BMR	feldspathic schist	feldspathic metaseds.	metacq.	micaceous metaseds.	Vadito	metased. & metahyalite package (BMR)
Hopewell Series		Moppin Metavolcanic Series	qtz.-musc.-bio. schist	musc.-bio. schist		Moppin Metavolcanics (includes the amphibolite member of the Kiawa Mt. Fm.)	Moppin Series	Moppin Series	Moppin Series	Moppin Metavolcanic Series	Mafic Sequence(s)	Moppin Metavolcanics
Plouris Basalts			hb.-chl. schist (includes amphibolite memb. of the Kiawa Mt. Fm.)	hb. schist chl. schist								
Tusos Granite		Maquinita Granodiorite Tres Piedras Granite	Qtz. diorite gneiss (may include Granite of Hopewell Lake)		Maquinita Granodiorite Tres Piedras Granite	Tusos Mt. Gr. Tres Piedras Gr.		linedated gd.		Maquinita Granodiorite		
		Trondhjemite of Rio Brazos	Granite porphyry	quartz-eye granite								Trondhjemite of Rio Brazos

and metasediments; the Ortega Quartzite- a clean quartzite; the Picuris Basalts-andesite and basalt flows interbedded with the upper Hopewell Series and lower Ortega Quartzite; and the Vallecitos Rhyolite. Just believed the Ortega Quartzite over- lay the Hopewell Series but was unable to discern the nature of the contact. He thought that flow bands, a fine-grained groundmass, and interbedded conglomerates indicated the Vallecitos Rhyolite was extrusive in origin.

Montgomery (1953) defined significant units in the Picuris Range which correlate with units in the Tusas Mountains. He discontinued usage of the Hopewell Series (Just, 1937) and defined the Vadito Formation, a series of interbedded metasediments and meta-igneous rocks in which felsites dominate the lower portion and amphibolites dominate the upper portion of the unit. He suggested that the Vadito Formation is a partial equivalent of the Hopewell Series.

Barker (1958) mapped the Las Tablas 15-minute quadrangle in Rio Arriba County. He changed the name of the Hopewell Series to the Moppin Metavolcanic Series and the Vallecitos Rhyolite to the Burned Mountain metarhyolite. Barker postulated that this metarhyolite was intrusive due to its abrupt margins. Based on cross-beds, he subdivided the Ortega Quartzite into two units: the Ortega Quartzite, which he interpreted as being older than the Moppin Metavolcanic Series, and the Kiowa Mountain Formation, which he believed to be younger than the metavolcanics. Barker recognized two northwest trending and plunging folds in the Las Tablas quadrangle- of which the Hopewell Anticline is exposed in the study area (Plate 1, Figure 22).

Bingler mapped Proterozoic rocks of the La Madera (7.5-minute) quadrangle (1965); and mapped both Proterozoic and Phanerozoic rocks of Rio Arriba County (1968). He described metamorphic rock types instead of using

formation names, and proposed no protoliths for the rocks. Bingler recognized three periods of deformation in the Proterozoic rocks. The first involved shearing and pervasive flowage of material, resulting in isoclinal folds which plunge gently to the south-southwest. The second episode transposed earlier axial planar cleavage into nearly isoclinal folds with south to southwest plunges and dips. The third episode, which is described as cataclastic, resulted in wide-spaced step folds with nearly vertical, west-trending axial planes. Bingler cautioned that the extensive deformation obscured original stratigraphic relationships and produced tectonic structures that may appear to be original sedimentary features, such as compositional layering and cross-beds.

Muehlberger (1968) mapped the Brazos Peak quadrangle (15-minute). He used lithologic descriptions as nomenclature for rock units. Muehlberger stated that because Proterozoic stratigraphic relationships are obscured by block faulting and Tertiary cover, only a probable sequence of formations could be inferred. He believes that the mafic schists are overlain by the metarhyolite which is, in turn, overlain by the quartzite. Muehlberger described the quartz-eye granite which intrudes the mafic schists in the east-central portion of his map as a possible variant of the Tres Piedras granite (Barker, 1958).

Doney (1968) mapped the Cebolla Quadrangle (15-minute). Proterozoic rocks in this area are dominated by the Ortega Quartzite. He recognized outwash and periglacial features from three episodes of glaciation.

Barker and Irving (1974) redefined the quartz-eye granite of Muehlberger (1968) as trondhjemite and analyzed a number of samples for major, minor, and trace-elements, and oxygen isotopes (1974, 1976, 1979). Barker et al. (1974) obtained a Rb-Sr whole-rock date of $1,654 \pm 34$ Ma for the trondhjemite of the Rio Brazos.

Gresens and Stensrud (1974) noted significant metarhyolite occurrences in both the Picuris and the La Madera-Las Tablas areas which had been severely altered to quartz-muscovite schists by metasomatism and deformation, or made apparently granite-like by recrystallization. They correlated the vitreous upper quartzite member and Jawbone Conglomerate Member of the Kiowa Mountain Formation (Barker, 1958) with the Ortega Quartzite. Gresens and Stensrud also recognized that what Montgomery (1953) believed to be the basal part of the Ortega Group in the Picuris Range is instead an altered metarhyolite. This enabled them to return to the original model of Just (1937) in which a series of metavolcanics are stratigraphically overlain by a single quartzite. They also suggested that the Petaca schist is an altered metarhyolite not related to the Ortega Quartzite, and that the Big Rock Conglomerate and lower quartzite member of the Kiowa Mountain Formation are metarhyolites belonging to the Burned Mountain metarhyolite. Gresens and Stensrud (1974) believed that the contact between the Ortega and overlying metasediments represents a hiatus in time (ie: a disconformity or an angular unconformity) and that during deformation the contact was sheared and disrupted while the quartzite itself acted as a competent unit.

Wobus (1985) provided structural evidence supporting a single quartzite model for the Ortega Quartzite. He proposed abandonment of the Kiowa Mountain Formation and Petaca Schist, reallocating the rocks into more suitable units as well as dropping "Series" from the Moppin Metavolcanic Series.

Manley and Wobus have produced several reconnaissance geologic maps (7.5-minute) in Rio Arriba county. These include the Mule Canyon Quadrangle (Manley and Wobus, 1982a) and the Las Tablas Quadrangle (Manley and Wobus, 1982b). Wobus and Manley (1982) mapped the Burned Mountain

Quadrangle.

A series of Master's theses on the Proterozoic rocks of the Tusas Uplift have been produced by students at the New Mexico Institute of Mining and Technology. Kent (1980) mapped the Tusas Mountain area. She recognized that deformation had been complex, and documented one period of isoclinal folding. Gibson (1981) mapped the Burned Mountain-Hopewell Lake area. He documented three deformations, the first two of which resulted in tight to isoclinal folds and the third in a crenulation cleavage. Smith (1986) mapped the Jawbone Mountain area. He reported two fabrics, an early bedding-parallel foliation and a later foliation axial planar to the Jawbone Syncline. Boadi (1986) studied the gold mineralization at Hopewell Lake.

Metamorphic studies (Grambling and Williams 1984; Grambling, 1986) have shown that most Proterozoic rocks in northern and central New Mexico experienced nearly uniform metamorphism evidenced by a subhorizontal kyanite-sillimanite (-andalusite) isograd. Al-silicate triple point assemblages are present when a Mn-bearing andalusite marker horizon crosses this isograd. However, the Tusas Mountains are an exception to this in that metamorphic conditions increase from 400 °C and 2-3 kb in the northwest to 585-600 °C and 5-6 kb in the Cerro Colorado area (Grambling et al., 1988b).

William's dissertation (1987) is a stratigraphic, structural and metamorphic overview of Proterozoic rocks in northern New Mexico. He redefined the Vadito Group (1985) as a package of feldspathic schists and gneisses with protoliths that are interpreted to be feldspathic metavolcanics and feldspathic metasediments. The Burned Mountain metarhyolite is included in this group. He recognized the Vadito Group in the Tusas, Picuris, and Rio Mora uplifts.

Soegaard and Eriksson (1985) determined by studies of sedimentary structures in the Ortega Group near Jawbone ridge that this quartzite was deposited in a shallow shelf environment which was influenced by tide, wave, and storm action.

Grambling et al. (in press, 1988a) have defined six Proterozoic terranes in New Mexico as "fault-bounded entities" which have a geologic history separate from the surrounding terranes. They have incorporated the MMS into the Taos terrane, and the MSMR and Ortega Group into the Truchas terrane.

GENERAL GEOLOGY

GEOLOGIC SETTING

The Tusas Mountains in northern New Mexico are part of a regional tectonic element called the Brazos uplift. It forms a long-lived structural high that trends northwest from Ojo Caliente into southern Colorado, and forms the divide between the Chama Basin to the west and the San Luis Valley to the east. The uplift is cored by Precambrian crystalline rocks and capped by Tertiary sediments and volcanics. The Brazos uplift is an extension of the San Juan Mountains in Colorado, and is also part of the southern Rocky Mountain physiographic province. This uplift is one of many that bound the Rio Grande depression (Baltz, 1976).

Precambrian rocks exposed in the Brazos uplift are generally similar lithologically, structurally, and in age to several other uplifts, which are part of a major belt of Proterozoic exposures from Mexico to Wyoming (Williams, 1987). Just (1937) and Montgomery (1953) were two of the early workers to recognize lithologic similarities between the Tusas and Picuris Mountains. Proterozoic rocks in the Pecos Greenstone belt of the Sangre de Cristo Mountains (Robertson et. al., in review; Robertson and Moench, 1979), the Needle Mountains in Colorado (Tewksbury, 1985; 1986), and the Gunnison area, in Colorado (Condie and Nuter, 1981; Bickford and Boardman, 1984; Knoper and Condie, 1988) are also generally similar in lithology, deformational style and age to Proterozoic rocks of the Tusas Mountains.

PHANEROZOIC GEOLOGIC HISTORY

The present day Brazos uplift has been a positive area in northern New Mexico throughout most of the Phanerozoic. Doney (1968) and Baltz (1976)

report that this uplift was part of the Ancestral Rocky Mountains. The oldest Paleozoic rocks in the Brazos Peak quadrangle are Pennsylvanian marine sediments that wedge out against the west side of the Brazos uplift along Chavez Box (Muehlberger, 1968). Permian rocks are not present in the region.

The Uncompahgre uplift, of which the Brazos uplift was a part, continued to be positive during most of the Mesozoic. This is evidenced by land vertebrate bones in the Chinle Formation, by the northeast thinning of the aeolian Entrada Sandstone, and by deposition of the littoral Dakota Sandstone directly on the Proterozoic basement near the headwaters of Chavez Creek in the Brazos Peak quadrangle.

The Laramide orogeny raised the San Juan and Tusas Mountains during late Cretaceous to Eocene time (Doney, 1968; Muehlberger, 1968). Baltz (1976) states that the Brazos and Sangre de Cristo uplifts were part of a single large, roughly north-south trending geanticline at this time. In the Brazos Peak quadrangle Muehlberger (1968) documents Laramide movement of down-to-the-east on the West Brazos Peak fault, Chavez Creek fault, and the Lagunitas Creek Fault. During the Cenozoic, movement on the major faults was up-to-the-east.

The Proterozoic surface was eroded in the late Eocene and its clasts were deposited in depressions as the El Rito Formation. The late Eocene and possibly early Oligocene was a time when the climate was temperate to subtropical and lateral planation by streams beveled both basement rocks and early Eocene formations, producing an extensive southeast-dipping erosional surface in the southern Rocky Mountains (Epis and Chapin, 1975). The uniform southeast dipping paleo-surface that dominates the uplands of the Tusas Mountains is probably an extension of this northern Late Eocene erosional surface.

The Oligocene was a time of extensive intermediate to silicic volcanism known as the "Mid-Tertiary ignimbrite flare-up" (Baltz, 1978). In northern New Mexico this volcanism is represented by the San Juan and Questa magmatic centers. Volcanism in the upper Oligocene and lower Miocene produced dominantly rhyolitic ash-flows, with some basalts and andesite flows, and associated derivative gravels (Lucas and Ingersoll, 1981). These mid-Tertiary volcanics are represented in the study area by the Conejos Formation and Treasure Mountain Formation.

The formation of the Rio Grande rift began in the early Miocene. The Sangre de Cristo Mountains were raised up from the eastern margin of the Uncompahgre uplift forming the eastern boundary of the rift (Muehlberger and Muehlberger, 1982). The Los Pinos sandstones, gravels and basalts are equivalents to early rift deposits such as the Abiquiu Tuff. In northern New Mexico, the Rio Grande flows in actively subsiding blocks of the Taos Plateau and Espanola Basin (Muehlberger and Muehlberger, 1982)

Late Pleistocene basalt flows and cinder cones are present in the Brazos Peak quadrangle (Muehlberger, 1968). The cold climate during the Pleistocene produced many glacial and periglacial features in the Tusas Mountains (Doney, 1968). Glaciers may have existed only as far south as Brazos Peak (Hawley, 1988, personal communication). Periglacial features such as rock streams, altiplanation terraces and stone circles are best developed on crystalline basement rocks. Present freeze-thaw cycles are sufficient to continue some of the fracturing processes that began in the Pleistocene.

PRECAMBRIAN STRATIGRAPHY OF THE TUSAS MOUNTAINS

The oldest rock formation in the Tusas Mountains is the Moppin Metavol-

canics (Barker, 1958). This unit is a heterogeneous series of mafic to felsic metamorphosed volcanics, volcanoclastics, intrusions and sediments. Mafic rocks are more abundant than either felsic or intermediate ones. The MMS is most abundant in the northern Tulas Mountains. The southern most exposures of the MMS are quartz-muscovite-biotite schists and hornblende-chlorite schists in the southeast portion of the La Madera quadrangle (Bingler, 1965). Exposures increase in thickness from less than 12 m in the La Madera quadrangle (Bingler, 1965) to 2.9 km thick in the Lagunitas Creek quadrangle.

Several plutons intrude the MMS. The largest is the informally-named trondhjemite of Rio Brazos (Barker, 1974). Two other significant plutons are the granite of Hopewell Lake, which has a Rb/Sr date of 1,467 Ma (Boadi, 1986), and the Maquinita granodiorite, which has a U-Pb date of 1,755 Ma (Silver in Reed et al., 1987). Late to post tectonic granites, such as the Tres Piedras granite, are also present in the Tulas Mountains.

The Metasedimentary and Metarhyolite rock package (MSMR) is separated from the MMS by an apparent unconformity. A major mylonitic zone is slightly above the contact. It is unclear how much the mylonite has influenced the contact, how much movement has taken place along the mylonite, or how much of the section has been removed. The MSMR contains coarse metaconglomerates, metasubarkoses, pelitic schists (including hornblende gneisses, amphibolites, and mica schists), and micaceous quartzites (Kent, 1980; Gibson, 1981; Smith, 1986; Williams, 1987). In the central Tulas Mountains, south of Kiawa Mountain the exposed MSMR is more than several kilometers thick (Williams, 1988), yet in the Lagunitas Creek quadrangle it is only 230 m-thick. Near the base of the package is the Burned Mountain metarhyolite, which has been dated at 1,700 Ma (Silver, in Reed et al., 1987).

Outcrops of the Burned Mountain metarhyolite range from 10 m-thick in the Lagunitas Creek quadrangle to 300 m-thick in the La Madera quadrangle (Bingler, 1965), although the thicker sections may have been repeated by folding.

The MSMR package is transitional into the Ortega Group, which is a sequence of upward-maturing quartzites. It contains a basal conglomerate and an overlying fine- to medium-grained vitreous quartzite, originally mapped by Barker (1958) as the Jawbone conglomerate member and the Upper Quartzite member of the Kiawa Mountain formation respectively. The Ortega quartzite is more than 1 km thick (Williams, 1987), although this may be complicated by deformation.

PRECAMBRIAN STRUCTURES

Precambrian rocks in the Tusas Mountains have been multiply deformed. Bingler (1965) describes three deformational events and the resulting folding and fabric development: 1) shearing associated with isoclinal folds that transposed bedding into parallelism with the S_1 foliation and destroyed stratigraphic continuity; 2) the formation of macroscopic, non-planar, cylindrical, asymmetrical, nearly-isoclinal, similar folds; 3) development of a wide-spaced fracture cleavage and associated low amplitude warps. Williams (1987) believes that Proterozoic rocks in northern New Mexico experienced "thin-skinned" deformation comprising northward thrusting and north-south shortening during a single progressive deformation. He documents three "end-member" deformational styles in the Tusas Mountains: 1) a single complex schistosity in the Cerro Colorado area which is composed of transposed remnants of earlier foliations; 2) three generations of superimposed folds in the Big Rock area; and 3) preserved sedimentary textures which are deformed into fold-fault pairs in the

Ortega quartzite. Common to each end-member area are north-south extension lineations, folds that have east-west striking and south dipping axial planes, and a continuity between deformation and metamorphism. Williams believes that the variety of deformational styles results from lithologic character and proximity to the Ortega quartzite.

REGIONAL METAMORPHISM

Proterozoic rocks in northern New Mexico generally preserve a nearly horizontal, slightly north dipping kyanite-sillimanite (-andalusite) isograd (Grambling, 1986; Grambling and Williams, 1984). Metamorphic conditions peaked after the youngest folding event as indicated by porphyroblasts and isograds that cut related deformational fabrics. Triple point assemblages are present wherever a Mn-andalusite bearing horizon crosses the kyanite-sillimanite isograd.

The Tusas Mountains, however, record a great increase in metamorphic conditions from the north to the southeast. Metamorphic conditions are estimated to be 380° and 2-3 kb in the northern Tusas Mountains, whereas they reach 580-600° in the south (Grambling et al., in press, 1988). Kyanite is ubiquitous throughout the Tusas Mountains, andalusite is limited to the northwest, and sillimanite is present only in the southeast reflecting this southward increase in metamorphic grade.

ECONOMIC GEOLOGY

Most of the economic mineralization in the Tusas Mountains occurs in the Hopewell and Bromide districts. Ore deposits there are of four types: "hydrothermal sulfide replacement veins, gold-bearing quartz veins, and placer deposits of alluvial gold" (Bingler, 1968, p. 71). Most hydrothermal mineralization is

hosted by the MMS and most of the gold ore from the Hopewell District was produced from placer deposits along Placer Creek.

Iron Mountain and Cleveland Gulch contain minor iron deposits within the MMS (Bingler, 1968; Smith, 1986).

Major non-metallic deposits of economic importance in the Tusas Mountains are the Petaca district pegmatites and the kyanite deposits from La Jarita Mesa (Bingler, 1968). The pegmatites are hosted by Precambrian muscovite schists, biotite schists, rhyolites, granite gneisses, and amphibolites. Minerals of economic interest in the pegmatites are: mica, beryl, columbite-tantalite, samarskite, bismuthite, and monazite. Kyanite deposits are present as accessories in the quartzite and as quartz-kyanite veins in the quartzite (Bingler, 1968). For more information on mineral resources of Rio Arriba county see Bingler, 1968.

PROTEROZOIC LITHOLOGIES

SUPRACRUSTAL ROCKS

Supracrustal rocks in the study area are regionally metamorphosed to greenschist facies. In some cases the protoliths are obvious while in others they are not. In most cases metamorphic rock names will be used to identify units. Multiple mineral prefixes are given in order of increasing abundance. Also, for purposes of simplification, the supracrustal succession in the study area is assumed to be a single, younging-to-the-southwest, sequence such that individual lithologies can be roughly located as "toward the top" or "toward the bottom" of a particular package. Inter-package folding and faulting within the MMS make this only a crude approximation. Figure 3 presents a generalized stratigraphic section of Precambrian rocks in the upper Brazos Box study area.

MOPPIN METAVOLCANICS

The Moppin Metavolcanics (MMS) is the oldest supracrustal package present in the study area. It underlies the central portion of the map area from north of the confluence of the Rio Brazos with Bull Canyon to just south of the lower Bagwell cow camp in the west and to the Carson National Forest gate in the east (Plate 1).

The MMS forms steep cliffs and slopes along the Rio Brazos. On gentle slopes and on the rolling uplands it occurs as float with rare small outcrops. All rocks in the MMS contain a dominant WNW trending foliation. Up to two other foliations may also be present. These foliations form conjugate relationships at approximately 30° to the dominant foliation. Outcrop character is controlled by the competency of the rocks and the number of foliations present. The more phyllitic to highly schistose members weather easily to talus, whereas

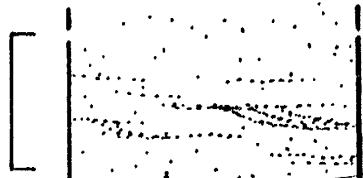
FIGURE 3

Generalized stratigraphic column of Proterozoic rocks from the upper Brazos Box study area.

STRUCTURAL
DOMAINS

GENERALIZED
STRATIGRAPHIC COLUMN

1



ORTEGA
GROUP
vitreous
quartzite

tectonized
zone

2



transitional
quartzite

3



MSMR
quartzite
conglomerate
BMR

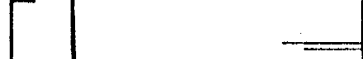
mylonite

4

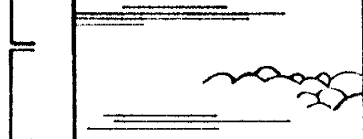


MMS

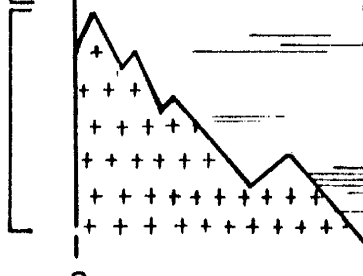
5



6



7



Trondhjemite of
Rio Brazos

?

?

competent units form bold outcrops. If all foliations are present outcrops may weather into distinctive diamond-shaped patterns.

The MMS contains two dominant lithologies: 1) mafic to intermediate volcanics, sediments and igneous rocks (95%); and 2) felsic volcanics (5%). The mafic to intermediate group is comprised of 32% amphibole schists, 32% plagioclase-chlorite schists, 20% muscovite-chlorite phyllites, 10% biotite-amphibole schists, 5% chlorite-quartz schists, and less than 1% chlorite-quartz-muscovite schist. The felsic volcanics contain 95% plagioclase-quartz schists and 5% muscovite-quartz schists (metarhyolites). The mafic to intermediate rocks are distributed throughout the the MMS section, while felsic rocks are present only in the lower exposed portion of the MMS section.

INTERMEDIATE TO MAFIC ROCKS

Amphibole Schist

The term amphibole schist is used to describe rocks that contain mostly actinolite and plagioclase even though the foliation in many of these samples is very subtle. This terminology was used so as not to imply a metamorphic grade.

Amphibole schists are most abundant from the central portion of the main canyon to the sharp west bend in the Rio Brazos near the north end of the canyon. They occur as massive units from 0.3 to 4.5 m thick which are inter-layered with all other members of the series as well as with the trondhjemite dikes in its southern exposures. Contacts are parallel to both the dominant foliation and contacts of the other major map units. Where exposed they are abrupt. The exception to this is in the lower portion of the section where bedded amphibolite schists and the S_1 foliation that parallels it strikes N50°E and

dips steeply southeast, while the outcrop foliation (S_2) strikes east-west and dips steeply south.

Two varieties of amphibole schists are present: a fine-grained dark green uniformly textured type and a fine grained green type with large darker green actinolite spots (3.0×1.0 mm). The amphibole schists commonly contain no primary fabrics, except near the base of the exposed section where the fine-grained amphibole schists display three distinct relict textures. The first texture is banding that ranges from 1 to 10 cm in width and darkens upward (Figure 4). This banding is present in only three outcrops. The second important texture is elongate close-spaced pillow-shaped forms that average 8×12 cm in diameter (Figure 5). Cusped forms are present at the bottom of each pillow shape and dark cracks are present near the top of the pillow-like forms. The third distinct texture is abundant, close-spaced, spherical to slightly elongate dark green and white forms 1.0×1.0 to 2.5×3.0 mm in size (Figure 6). They are most commonly in or near the pillow-shaped and brecciated amphibole schists.

Another variation in original compositional layering is present in the central portion of the canyon. There massive fine-grained amphibolite schists alternate with biotite-amphibole schists containing large pseudomorphs of pyroxene. Beds range from 0.6 to 4.5 m-thick. Contacts in this area parallel the major foliation. They are abrupt and commonly accentuated by weathering. Because the crystal-rich unit is interpreted to be a mafic intrusion (biotite-amphibole schist) these may be sills interlayered with original layering or other intrusions. However, no intrusive relationships were found.

Actinolite or actinolitic hornblende and plagioclase constitute most of the amphibolite schists. Pleochroic blue-green to yellow-green actinolite or actinoli-

FIGURE 4

Bedded amphibole schist from near the base of the exposed MMS section. The S_1 foliation is parallel to bedding and the S_2 foliation crosscuts both bedding and S_1 at a high angle. The pen is 14 cm long.

S₀/S₁

S₂



S₂

S₀/S₁

FIGURE 5

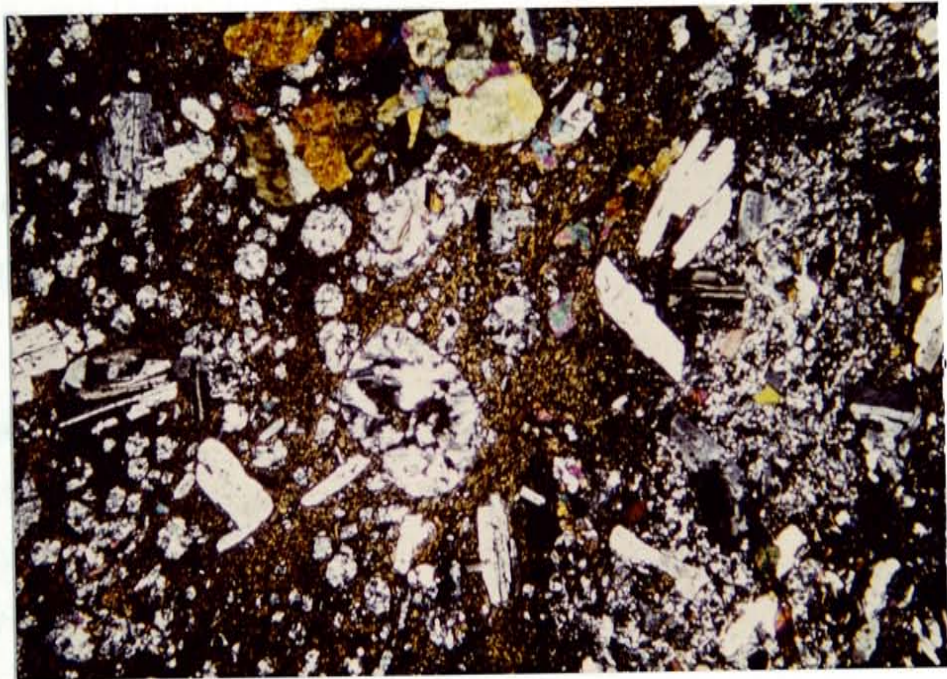
Pillow structure in the MMS amphibole schist near the base of the exposed section. Pillows average 8×12 cm in size. Note the chlorite-filled shrinkage cracks near the stratigraphic top of the pillow structures. The pencil is 15 cm long.



FIGURE 6

Photomicrograph of amygdules in an MMS brecciated amphibole schist. The amygdules are filled with patchy plagioclase. Also present are clustered plagioclase crystals contained in a fine-grained groundmass of felted actinolite needles. The brecciated areas (whiter) contain quartz, plagioclase, and actinolite. The longest amygdule is 1.8 mm in width. Crossed polarized light.

...
... ..
... ..



—
~ 1 mm

tic hornblende occurs as felted mats containing larger rectangular actinolite crystals and/or clusters of crystals. The large crystals display square cross sections with rare truncated corners and relict twinning that indicate they were originally pyroxene crystals. The groundmass contains interstitial xenoblastic quartz, plagioclase, epidote, biotite, chlorite, and carbonate, with minor clinozoisite, zoisite, magnetite and ilmenite. Plagioclase is albite to oligoclase in composition. It occurs in two forms: as irregularly shaped crystals that are erratically dispersed throughout a fine-grained matrix; and as medium-sized (0.2×0.7 mm) intergrown laths with smaller actinolite crystals filling the interstices. The matrix consists of discontinuous cleavage bands defined by oriented chlorite and actinolite crystals that alternate with microlithons of xenoblastic quartz and feldspar.

In thin section, the 1-10 cm-thick banding is seen to be the result of abrupt variations in plagioclase and actinolite content, and no fining sequence can be determined. Material in these bands is poorly sorted and contains abundant irregular to angular shaped feldspar crystals. The 1-3 mm in diameter spherical forms are filled with patchy to radiating plagioclase and/or epidote, +/- chlorite, +/- biotite.

The 1-10 cm-thick actinolite-rich and plagioclase-rich bands are interpreted to be relict beds of fine grained pyroclastic material containing broken feldspar crystals. The pillow-shaped forms are interpreted to be pillow structures that resulted from subaqueous eruption of mafic lava. The small round forms are interpreted to be relict vesicles which are often associated with pillow structures and brecciated units. The brecciated vesiculated units are interpreted as brecciated flow tops. The vesicles show little to no flattening, indicating that they were filled before deformation and/or that the deformation was minimal in

these localities.

Pillows, vesicles, and breccias indicate that some of the amphibole schists originated as mafic subaqueous flows which were vesiculated and brecciated in places. The long plagioclase laths enclosing small actinolite needles in several samples are reminiscent of primary diabasic textures and imply that some amphibole schists formed as flows or hypabyssal intrusions. Samples interpreted as displaying original bedding, are poorly sorted and contain broken crystals. These samples suggest that yet another type of amphibole schist may have originated through volcanoclastic processes. Near the northern end of the Brazos Box, pillowed, vesiculated, and brecciated mafic volcanic rocks are commonly associated with fine-grained bedded volcanoclastic sediments.

Plagioclase-Chlorite Schist

Plagioclase-chlorite to chlorite-plagioclase phyllites and schists are distributed randomly throughout the MMS. They occur as 0.3 to 6 m-thick interlayers between all other rock types as well as within the trondhjemite in its southernmost exposures. Contacts range from sharp to gradational.

Rocks in this unit form small isolated folds preserved in several places, such as on the hill labeled with an elevation of 10062-T feet. Because this unit is relatively incompetent it forms talus slopes.

This group of rocks displays a wide variety of textures from finely banded light and dark green phyllites to uniformly green coarsely schistose rocks to crystal-rich rocks with only a subtle foliation. One especially distinctive rock type is a crystal-rich chlorite-plagioclase schist in which large (2.0×2.0 mm) white to light green crystals stand out in relief on weathered surfaces. It is possible that some of the fine-grained chlorite-plagioclase phyllites and schists may

represent sheared members of this crystal-rich unit.

Plagioclase-quartz schists contain mostly plagioclase, chlorite, quartz, and muscovite, with some epidote and carbonate. Accessory minerals include biotite, clinozoisite, magnetite, and ilmenite.

In thin section some samples are seen to contain whole to broken plagioclase crystals in a poorly sorted groundmass of quartz, and minor biotite. Other samples contain intergrown plagioclase laths with interstitial xenoblastic epidote, chlorite, and carbonate. The large plagioclase crystals are equant in shape and are greatly altered to sericite and epidote, as is common in all plagioclase-chlorite schists. Plagioclase composition ranges from An_{3-11} , with albite as the most common type. In thin section all foliations are highly variable from anastomosing to lamellar and continuous to discontinuous. Cleavage bands, which vary from 1 to 0.04 mm in width are composed of idioblastic to subidioblastic muscovite and chlorite, while microlithons contain polygonal quartz, xenoblastic plagioclase, and small idioblastic muscovite and chlorite. Irregular lenses of calcite elongated in the foliation plane are common.

Metamorphism and deformation have greatly obscured original textures in many of these rocks, making evaluation of their protoliths difficult. Samples that contain broken crystals probably originated by pyroclastic processes or are sediments derived from pyroclastic sources, without much weathering. The large equant plagioclase crystals are probably relict phenocrysts. Samples that have intergrown plagioclase laths with interstitial chlorite and epidote as well as the crystal-rich samples probably formed as flows or hypabyssal intrusions. The fine bands in the phyllites are probably the result of metamorphic mineral segregations.

Muscovite-Chlorite Phyllite

This unit is most abundant in the upper portion of the MMS, although it also occurs interlayered with the trondhjemite in the southern exposures. It forms layers 0.3 to 6 m-thick with distinct to gradational contacts with adjacent rocks.

These phyllites are dark green in color and always strongly foliated. One distinct variety of the chlorite phyllite contains siderite rhombohedra which weather out leaving rhombohedral cavities filled with limonite. Although most common to this unit, these carbonates are not unique to it.

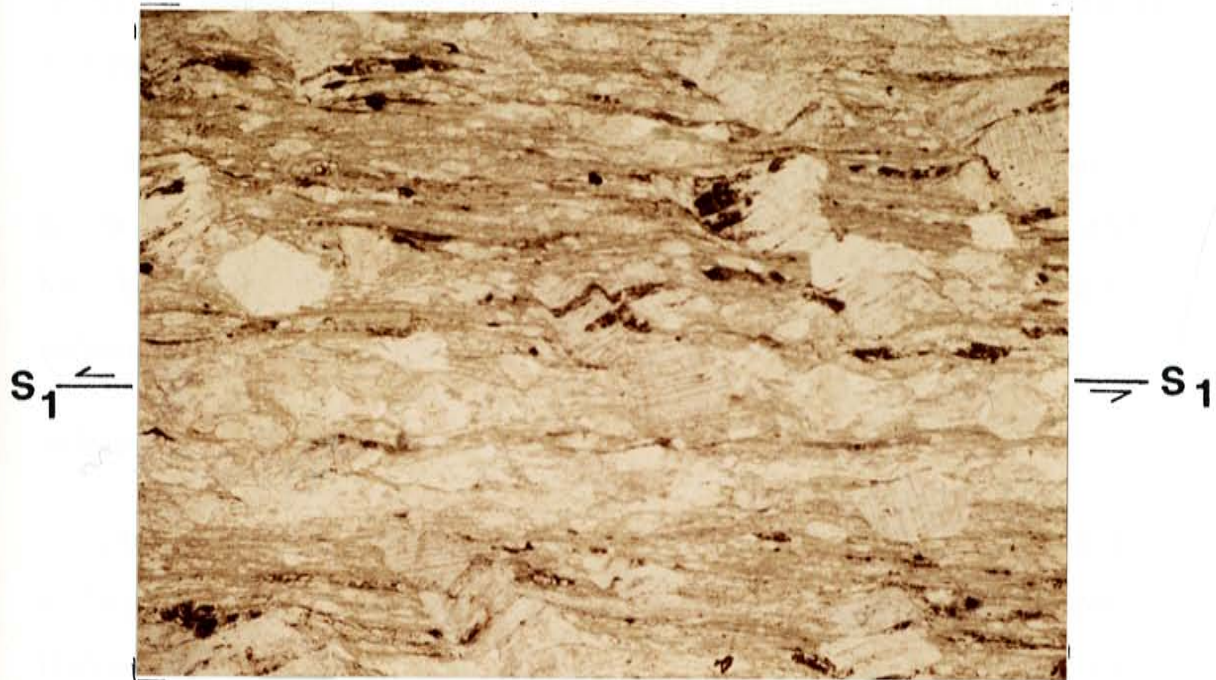
Muscovite-chlorite phyllites contain mostly chlorite, muscovite/sericite, quartz, and plagioclase. When carbonate rhombohedra (siderite) are present they may comprise up to 20% of the rock. Accessory epidote, rutile, and rare sphene are present.

Fine-grained rocks contain a continuous laminar foliation defined by a mixture of idioblastic to subidioblastic chlorite and muscovite, alternating with coarser-grained chlorite. As the quartz and feldspar content increase the microlithons become distinct and the foliation becomes discontinuous. Magnetite, opaque dust and hematite are present along foliation planes in some samples. Minor alteration of albite and oligoclase to sericite and/or epidote has occurred.

In thin section, the siderite rhombohedra are subidioblastic to xenoblastic and range from 2.0×2.0 mm to 1.2×0.77 mm in size (Figure 7). These rhombohedra contain abundant irregular patches of feldspar suggesting that the formation of the carbonate is partially the result of the alteration of plagioclase. Because the siderite are nearly rhombohedral in shape they must also be part-

FIGURE 7

Photomicrograph of siderite rhombohedra in the MMS plagioclase-chlorite schist in plane polarized light. The thin section is cut parallel to the extension lineation. Trains of opaque minerals indicate that the carbonate crystals have rotated northward (top towards the left). The long dimension of the photomicrograph is 1.7 cm.



~ 1 mm

ially the result of the nucleation of carbonate growth around a feldspar or carbonate core (Grambling, 1988, personal communication). Trains of opaque minerals contained in the carbonates are at a high angle to similar trains in the matrix which define the foliation. In the margins of the crystals the trains of opaque iron oxides are transitional between the orientation of mineral trains within the crystal and those in the foliation. This indicates that the carbonate crystals have rotated synkinematically in a northerly direction.

It is proposed that the fine-grained mica-rich material represents metasediments of a pelitic nature and that poorly-sorted samples with broken crystals have been derived from a pyroclastic source. The origin and distribution of the carbonate is not understood.

Biotite-Amphibole Schist

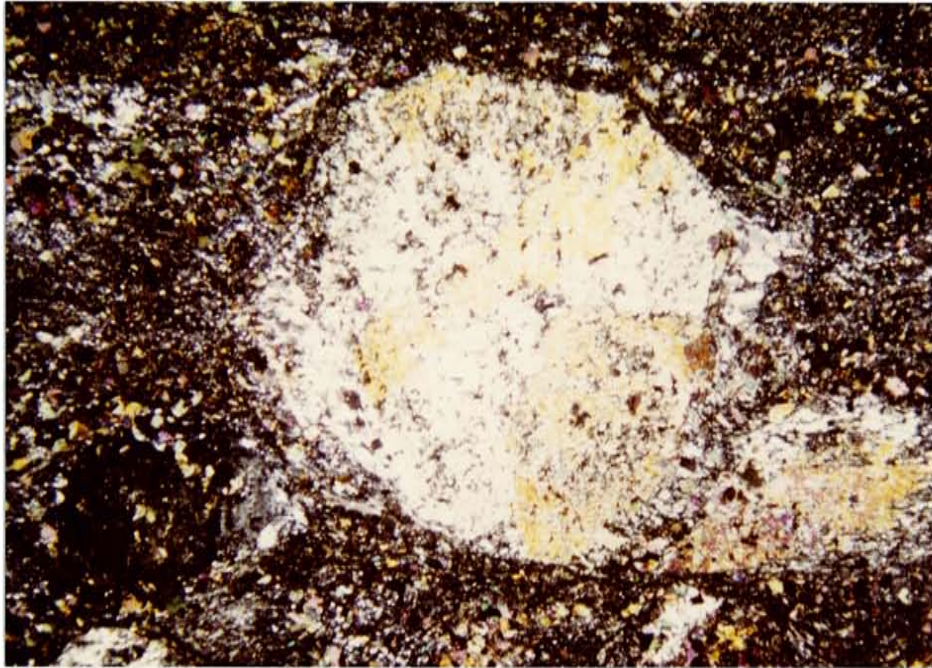
The term biotite-amphibole schist was used instead of amphibolite so as not to imply a metamorphic grade, although these rocks are only weakly foliated. Biotite-amphibole schists are most common in the middle portion of the canyon. The biotite-amphibole schist form prominent outcrops 0.6 to 4.5 m-thick layers between amphibole schists. Contacts are always abrupt and are best seen on weathered surfaces.

The typical biotite-amphibole schist is a dark green unit with up to 15% blackish green amphibole megacrysts that average 7.0×5.0 mm in size. The megacrysts are randomly oriented.

In thin section, the green to yellowish green actinolite or actinolitic hornblende megacrysts are extremely poikiloblastic and generally rectangular in shape (Figure 8). Some crystals contain relict twinning. They are often fringed by chlorite and/or have carbonate pressure shadows. Greenish brown biotite is

FIGURE 8

Photomicrograph of an amphibole pseudomorph after pyroxene in the MMS biotite-amphibole schist. The amphibole poikilitically encloses chlorite, greenish-brown biotite, and minor quartz. It is fringed by chlorite. Carbonate pressure shadows are in the upper left and lower right. Note the relict twin. The groundmass contains fine-grained chlorite, epidote, and plagioclase. The foliation is delineated by aligned chlorite crystals. Amphibole crystal is 4.6 mm in diameter. Crossed polarized light.



—
~ 1 mm

poikilitically enclosed in the actinolitic hornblende. The groundmass is comprised of idioblastic to subidioblastic chlorite and biotite, subidioblastic to granular epidote, xenoblastic to polygonal quartz, and xenoblastic carbonate. The alignment of chlorite forms an subtle anastomosing foliation.

Rectangular outlines of individual or clustered actinolite megacrysts indicate that this actinolite has formed pseudomorphs after pyroxene. The large amphibole pseudomorphs as well as the crystal-rich nature of this unit suggest that it must have originated as a crystal-rich mafic intrusion.

Chlorite-Quartz Schist

Chlorite-quartz to quartz-chlorite phyllites to schists are present throughout the MMS section. They form 0.3 to 1.5 m-thick interlayers with all other MMS units. Contact relationships are distinct to gradational. These rocks weather easily to talus.

The chlorite-quartz phyllites which contain tan and green colored bands and lenses are one of the most typical rock types in the MMS. All samples contain a strong continuous or discontinuous foliation.

The chlorite-quartz schist contains mostly quartz and chlorite with variable amounts of muscovite, carbonate, plagioclase, clinozoisite, rutile, and hematite. The foliation, which ranges from 1.2-0.02 mm-wide, is defined by cleavage bands of idioblastic to subidioblastic chlorite and muscovite, and microlithons of polygonal to xenoblastic quartz, minor subidioblastic to xenoblastic oligoclase, and rare xenoblastic carbonate lenses. Some samples contain dispersed larger broken to rounded oligoclase crystals. It is impossible to tell if the rounded character of these crystals is primary or tectonic.

One chlorite-schist contains large subidioblastic blue-green actinolitic hornblende crystals that are superimposed on what is interpreted to be an S_2 foliation. These crystals appear to have grown at the expense of chlorite, but have overgrown quartz. In addition, the actinolitic hornblende is randomly oriented indicating that these minerals, which probably correspond to the peak of metamorphism, formed after the formation of the S_2 foliation.

The chlorite-quartz schists which contain broken feldspar crystals may have originated as pyroclastic rocks that may have been reworked. Some chlorite-quartz phyllites are laminated and very fine-grained suggesting that they were metasediments.

Chlorite-Quartz-Muscovite Phyllite

Chlorite-quartz-muscovite phyllite is found in the upper most portion of the MMS section. It is dark green phyllite that contains distinct small white asymmetrically elongated quartz and feldspar crystals, which appear "fish-shaped" even in hand sample. A near vertical, wide-spaced, small-amplitude crenulation is present in this unit near the top of the metavolcanic section.

The quartz-chlorite-muscovite phyllites contain muscovite, chlorite, quartz, and plagioclase. Minor opaque iron oxides and epidote are also present. In thin section, the foliation is defined by idioblastic muscovite. Tectonized magnetite crystals and opaque dust are distributed along the foliation plane. Larger asymmetrical subidioblastic to rounded quartz and feldspar crystals are elongated in the plane of the foliation. Quartz has recrystallized as equant polygons in lenses and as tails around asymmetrical crystals.

The small-scale foliation and broken to strained crystals indicate that these samples have undergone extensive shearing. This intense deformation has

masked the protolith, although the metamorphic mineralogy is reminiscent of a mafic protolith. Chemically these rocks plot as sub-alkaline basalts (Floyd and Winchester, 1978).

FELSIC METAVOLCANICS

Chlorite-Plagioclase-Quartz Schist

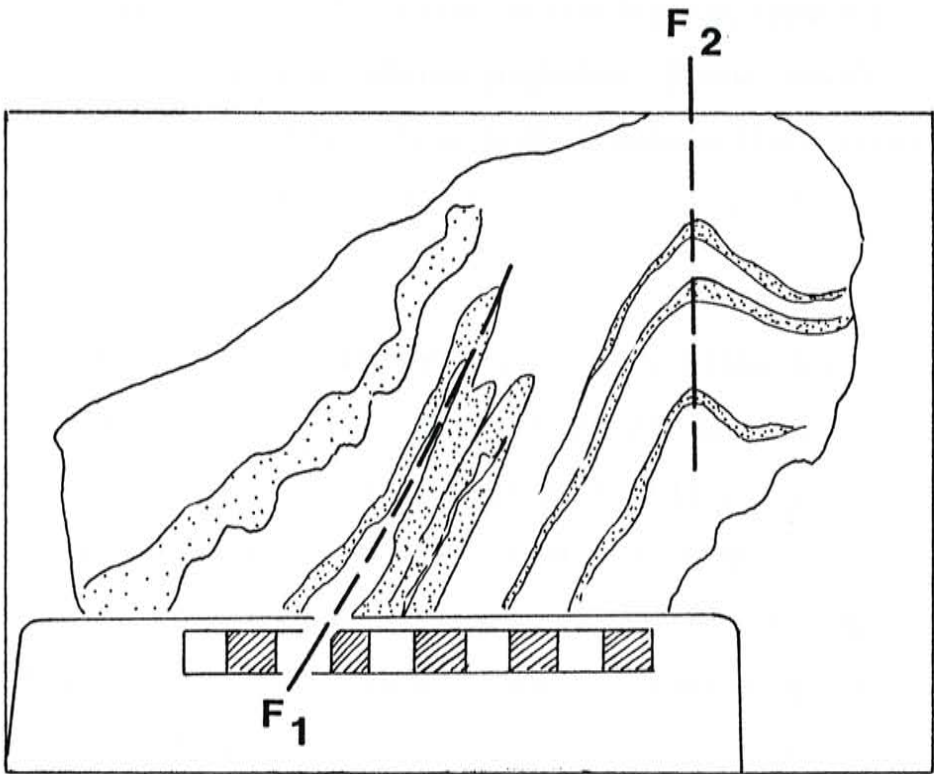
The chlorite-plagioclase-quartz schists are present in the lower exposed portion of the MMS section located on the hill labeled 10062-T. This schist occurs as interlayers 0.6-3 m-thick with chlorite-plagioclase, quartz-chlorite, muscovite-quartz schists and trondhjemite. Contacts are distinct when exposed.

Silica contents up to 77% and dense nature of these chlorite-plagioclase schists influences the bold character of the outcrops, although these rocks still break crudely along the plane of the major foliation.

Chlorite-plagioclase-quartz schists occur as three distinctly different textural types. It is most common as a green chlorite-rich matrix with thin cream colored bands that range from 0.2 to 12 mm-wide. The bands are folded into isoclinal folds which are refolded into open disharmonic folds (Figure 9). These folds vary greatly in size, but generally do not have wavelengths greater than 10 cm or amplitudes greater than 20 cm. The second distinct texture in the chlorite-plagioclase schist is a strongly flattened green and white spotted unit. The third type is a breccia with a dark green matrix that encloses light pink clasts which range from 3.5×1.5 mm to 2.0×1.0 mm in size. These clasts are irregular in shape and are strongly flattened in the plane of the major foliation. Rare pink and green banded clasts are present. This rock type is present only at the top of the hill with an elevation labeled 10062-T.

FIGURE 9

Flow bands in the MMS chlorite-plagioclase-quartz schist. Isoclinally folded (F_1) flow bands are refolded into open folds (F_2).



The chlorite-plagioclase-quartz schist contains mostly quartz, plagioclase, and chlorite, with minor biotite, muscovite, epidote, clinozoisite, carbonate and opaque iron oxides. The most distinct aspect of this unit in thin section are alternating bands and lenses of cryptocrystalline quartz and plagioclase, and coarser-grained bands of subidioblastic plagioclase and polygonal quartz. Some bands and lenses of chlorite + /- muscovite and subidioblastic to xenoblastic epidote + /- carbonate are oriented in the foliation plane. The cryptocrystalline bands are the cream colored bands in outcrop and the polygonal bands with chlorite are the green colored bands in outcrop. Large idioblastic to slightly subidioblastic plagioclase crystals and broken plagioclase crystals occur as isolated crystals and in clusters. These crystals commonly have their long axes in the foliation direction. Plagioclase is mostly albite to oligoclase in composition, although some andesine is present. While most plagioclase contains only minor sericite, rectangular masses of idioblastic to subidioblastic epidote + /- muscovite could represent completely altered plagioclase. Biotite, chlorite, and magnetite occur in clusters. Because large nearly idioblastic biotite crystals are superimposed on fine-grained chlorite masses, it is assumed that the biotite is prograde.

This unit is interpreted to be a felsic volcanic for several reasons. First, the abundant quartz and plagioclase along with the lack of potassium feldspar is consistent mineralogically with a dacite protolith. Chemically these rocks plot as rhyodacites or dacites (Floyd and Winchester, 1978). Second, the fine grained matrix of cryptocrystalline quartz and feldspar probably represent a devitrifying felsic volcanic. Third, these bands correlate with what is interpreted as flow banding in outcrop. Fourth, the breccia present on the hill labeled 10062-T is interpreted to be a primary feature because the clasts are similar in composition to the matrix and they are strongly flattened in the foliation plane.

Muscovite-Quartz Schist

Muscovite-quartz schists occur in the lower portion of the exposed MMS section at the top of the hill with elevation labeled 10062-T. This unit is present as layers up to 4 m-thick.

On the top of the hill with an elevation labeled 10062-T feet two 4×20 m layers, which parallel each other are separated by 15 m of chlorite phyllite and cover. Along the canyon rim east of the Rio Brazos the muscovite-quartz schist occur as as 15 cm to 2.5 m-thick layers that are isoclinally folded with 2.5 cm to 1 m-thick layers of a chlorite phyllite. This folding pinches out into the MMS. Directly across the Rio Brazos, on strike from this exposure, is a single 1 m-thick unit of muscovite-quartz schist. These exposures may be associated, although no muscovite-quartz schists were found along the bottom of the canyon.

Quartz-muscovite schists are pink on both fresh and weathered surfaces. They are distinguished by large quartz eyes (1.0×2.0 mm) that stand out in relief and less prominent feldspar crystals (0.4×0.6 mm). Near the river, this unit is strongly foliated and breaks easily along foliation planes. Muscovite on these surfaces has a light green tint and is strongly crenulated. Muscovite-quartz schists at the top of the hill labeled 10062-T are dense and only weakly foliated.

These muscovite-quartz schists contain up 9% quartz phenocrysts and 6% plagioclase megacrysts which are contained in a fine grained groundmass of quartz and muscovite. The quartz crystals are rounded and strongly embayed indicating they are relict phenocrysts. Feldspar is mostly oligoclase in composition, although minor albite is also present. Plagioclase crystals are partly to

wholly altered to sericite and/or epidote. Minor amounts of chlorite, biotite, epidote, carbonate, magnetite and hematite are present.

A discontinuous spaced anastomosing foliation is defined by irregular bands and lenses of fine grained xenoblastic quartz and feldspar with indistinct fuzzy grain boundaries, which alternate with bands of polygonal quartz, minor subidioblastic to xenoblastic feldspar and idioblastic muscovite. Chlorite is present as individual crystals adjacent to quartz phenocrysts and in the foliation. Subidioblastic biotite is usually oriented at a high angle to the foliation and therefore believed to be altering to chlorite, which is parallel to the foliation. Magnetite is rimmed by chlorite.

Embayed rounded quartz crystals and large feldspar crystals indicate that the muscovite-quartz schists are felsic volcanics. Chemically these rocks plot as rhyolites (Floyd and Winchester, 1978).

Possible Depositional Environment

Pillowed amphibole schists, rhyolite beds and flow banded felsic volcanics suggest that some of the rocks were deposited as mafic to felsic flows and ash flows, at least some of which were subaqueous. Fine-grained, thinly bedded parts of the MMS may be turbidites. The poorly sorted nature of many of the MMS rocks and the abundant broken crystals suggest that some of the MMS rocks are the result of pyroclastic processes. A few MMS rocks contain rounded grains suggesting they have been reworked. Textures reminiscent of diabases suggest that other MMS rocks were intrusive. In summary, the MMS was deposited as felsic to mafic flows, volcanoclastics, sediments, and intrusions in a dominantly submarine environment.

METASEDIMENTARY AND METARHYOLITE PACKAGE

The Metasedimentary and Metarhyolite package (MSMR) is exposed for 230 m along the Rio Brazos north of the confluence with Bull Canyon (Plate 1). Both upper and lower contacts parallel bedding, compositional layering, the S_1 foliation, and a mylonite near the base of the unit. The contact between the MSMR and the overlying Ortega Group is transitional. The MMS-MSMR contact appears to be both unconformable and tectonic.

In detail, the base of the MSMR consists of the Burned Mountain metarhyolite, underlain by an approximately 8 m-thick mylonite zone (now a chlorite-muscovite-quartz phyllonite), underlain by a 3 m-thick phyllite pebble metaconglomerate. Below the metaconglomerate are rocks clearly belonging to the MMS. At present, it is not known if the phyllite pebble metaconglomerate beneath the mylonite is part of the MSMR package, or if it is unrelated to any of the surrounding lithologies. Above the metarhyolite the MSMR grades upsection from a poorly sorted phyllite pebble metaconglomerate into a micaceous quartzite with isolated phyllite pebbles and phyllite pebble interbeds. Several thin (1-3 m-thick) intermediate to mafic horizons are present in the upper portion of the MSMR rocks.

The MSMR package of supracrustal rocks contains: 88% phyllite pebble metaconglomerates, 10% Burned Mountain metarhyolite, 2% chlorite-muscovite-quartz phyllonite, <1% micaceous interbeds and <1% chlorite schists.

The contact between the MMS and the MSMR may be unconformable because pebble conglomerates in the basal MSMR contain clasts that are similar in lithology to the underlying MMS. Kent (1980) has described MMS beds in

the Tusas Mountain area that are truncated by the Burned Mountain metarhyolite, and Smith (1986) has described the thickness of the Burned Mountain metarhyolite in the Jawbone Mountain area as extremely variable, and missing altogether in one place. The variation in unit thicknesses and the truncation of units may be the result of an unconformity, or may be the result of shearing (Mawer, 1988, personal communication). Approximately 3 m above the contact between the MMS and the MSMR is a distinct mylonitic zone. While most of the deformation between the two units must have taken place along the mylonite, shear indicators such as rotated crystals are present in units above and below the mylonite in both the MMS and the MSMR. Therefore the contact itself has been tectonized. It is difficult to determine the amount of shear that has taken place along the mylonite zone, or how much, if any, of the section has been removed.

The MSMR rock package forms steep rocky cliffs on the west side of the canyon, whereas on the eastern side of the canyon portions of the slopes are grass-covered with talus. All rocks contain a strong WNW foliation and most contain a later cross-cutting foliation. Many rocks contain a third foliation which along with the second one forms a conjugate relationship to the prominent foliation.

Phyllite Pebble Metaconglomerate

Two sections of phyllite pebble metaconglomerate are present along the Rio Brazos, a 3 m-thick section beneath the mylonite that appears to rest unconformably upon the MMS, and a 100 m-thick unit that extends from above the Burned Mountain metarhyolite to the confluence of the Rio Brazos and Bull Canyon. It is unclear if these pebble conglomerates are part of a single lithologic succession or are instead, parts of two distinctly different successions that

have been juxtaposed tectonically. The upper metaconglomerate grades from a pebble-rich, matrix-supported conglomerate with rare cobbles into a micaceous quartzite with isolated phyllite pebbles and phyllite interbeds. The upper metaconglomerate consists of approximately 46 m of the pebble-rich metaconglomerate, overlain by approximately 54 m of the micaceous quartzite beds with isolated pebbles and pebble interbeds. The lower pebble-rich portion of this section contains up to 80% green phyllite, red and black chert, and white bull quartz pebbles (Figure 10). This grades upsection (downstream) into the micaceous quartzite beds containing as little as 8% pebbles that are separated by phyllite pebble interbeds at the top of the section (Figure 11). Between some conglomerate beds are thin 1-2 cm-thick interbeds of micaceous phyllite with no pebbles. Upsection the thickness of individual conglomerate beds decreases to an average of 6 m in the middle of the unit, and 0.5 m near the top of the unit. The lower metaconglomerate beneath the mylonite is a sandy phyllite that contains about 15% quartz, phyllite, chert pebbles.

The only difference in the lower and upper metaconglomerate is the amount of pebbles present, therefore both units will be described together. Pebbles in the metaconglomerate are 96% green chlorite and pink muscovite phyllite, 2% black and red chert, and 2% bull quartz. All pebbles are well-rounded and strongly elongated in a easterly dipping extension direction. Pebbles range from $50 \times 20 \times 2$ mm to $15 \times 7 \times 5$ mm in size. Rare quartz cobbles reach $150 \times 100 \times 100$ mm size. All conglomerates are bimodal and matrix supported.

In this section the matrix is seen to contain rounded to well-rounded quartz and rare plagioclase grains. The quartz is either undulatory or polygonal. Muscovite is a prominent constituent. The amount of quartz and muscovite

FIGURE 10

Outcrop of the phyllite pebble metaconglomerate in the basal MSMR section. Phyllite pebbles are strongly elongated in an easterly direction. The hammer is 27 cm long.



FIGURE 11

Outcrop of the uppermost MSMR package. Micaceous beds (.5 m-thick) contain some isolated phyllite pebbles and are separated by phyllite pebble interbeds. The pen is 14 cm long.



vary inversely, quartz being more abundant upsection and muscovite most abundant downsection. Some of the plagioclase has altered completely to epidote + /- clinozoisite. Rounded hematite grains have accumulated on bedding planes. Epidote, chlorite, and carbonate are accessories. The foliation is delineated in these rocks by flattened pebbles and grains, and aligned muscovite crystals and lenses.

The poorly-sorted bimodal lower MSMR metaconglomerate could have been deposited by a fluvial system or a near-shore marine system. If deposition was by fluvial processes, it was probably in a near-shore setting, because the unit grades vertically into shallow marine rocks over a very short interval.

Chlorite-Muscovite-Quartz Phyllonite

The chlorite-muscovite-quartz phyllonite makes up 2% of the MSMR package of supracrustal rocks. This 8 m-thick unit lies beneath the Burned Mountain metarhyolite and above the thin pebble-rich horizon which lies directly on the MMS rocks. The phyllonite contacts are indistinct.

The chlorite-muscovite-quartz phyllonite is a thinly laminated, pink and grey rock that is strongly foliated and weathers easily to talus. "Fish-shaped" lenses of dark grey opaque-rich material, pink muscovite-rich material, and cream colored quartz-rich material average 15×2 mm in size and help define a strong mylonitic fabric. The asymmetry of these "fish-shaped" lenses indicate that shear has been north-directed in this unit. The S_1 foliation plane contains a strong east dipping extension lineation and a crenulation.

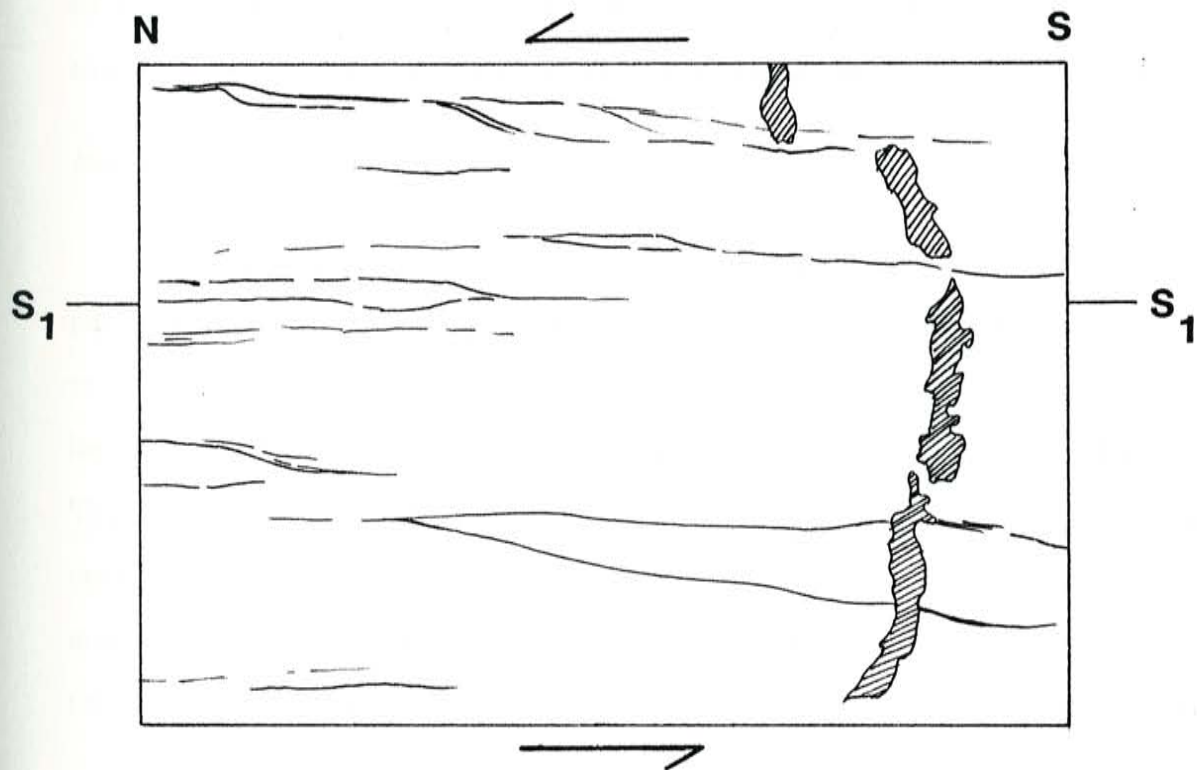
The strong fine-spaced continuous foliation in this rock is delineated by the alignment of muscovite and lenses of material (Figure 12). Two types of lenses

FIGURE 12

Photomicrograph of the mylonitic chlorite-muscovite-quartz phyllonite near the basal portion of the MSMR section. The thin section is cut parallel to the extension lineation. The shearing has produced "fish-shaped" lenses that contain quartz, feldspar, and opaque iron oxide; and chlorite and/or muscovite. Structural fabrics were formed by north-directed shear. The long dimension of the photomicrograph is 1.7 cm. Plane polarized light.



~ 1 mm



are present: one contains medium-sized (0.6×0.6 mm) equidimensional quartz, albite-oligoclase, and carbonate; the other contains chlorite and/or muscovite (0.06×0.15 mm). Single larger plagioclase crystals (0.8×0.8 mm) and smaller magnetite and garnet (almandine ?) have been strongly tectonized and their fragments are distributed along the shear planes. Brown irregular to rhombohedral siderite (1×1 mm) are common in this unit. The carbonates are not strained and contain trains of magnetite crystals oriented similarly to magnetite trains in the foliation that indicate the carbonate formed after the major foliation was established.

The strongly foliated nature of this unit, the "fish-shaped" lenses, and broken crystals are indicative of a mylonite. Field relationships, textures, and mineralogy suggest that this phyllonite may have been formed tectonically from the basal portion of the Burned Mountain metarhyolite and the upper portion of the phyllite pebble metaconglomerate beneath it. Structural fabrics indicate that this mylonite has experienced north-directed shear.

Burned Mountain Metarhyolite

The Burned Mountain metarhyolite constitutes 10% of the MSMR rock package. It forms a competent 10 m-thick unit along the Rio Brazos about 200 m north of the confluence with Bull Canyon. One 5×5 m block of metarhyolite is present in the easternmost gully that drains south into the Bad Lands. The Burned Mountain metarhyolite lies directly above and may grade into the previously described mylonite. It is difficult to determine if the pebble-poor metaconglomerate beneath the metarhyolite contains metarhyolite pebbles or if the apparent clasts are portions of deformed isoclinal folds.

The Burned Mountain metarhyolite is a muscovite-quartz schist with ubi-

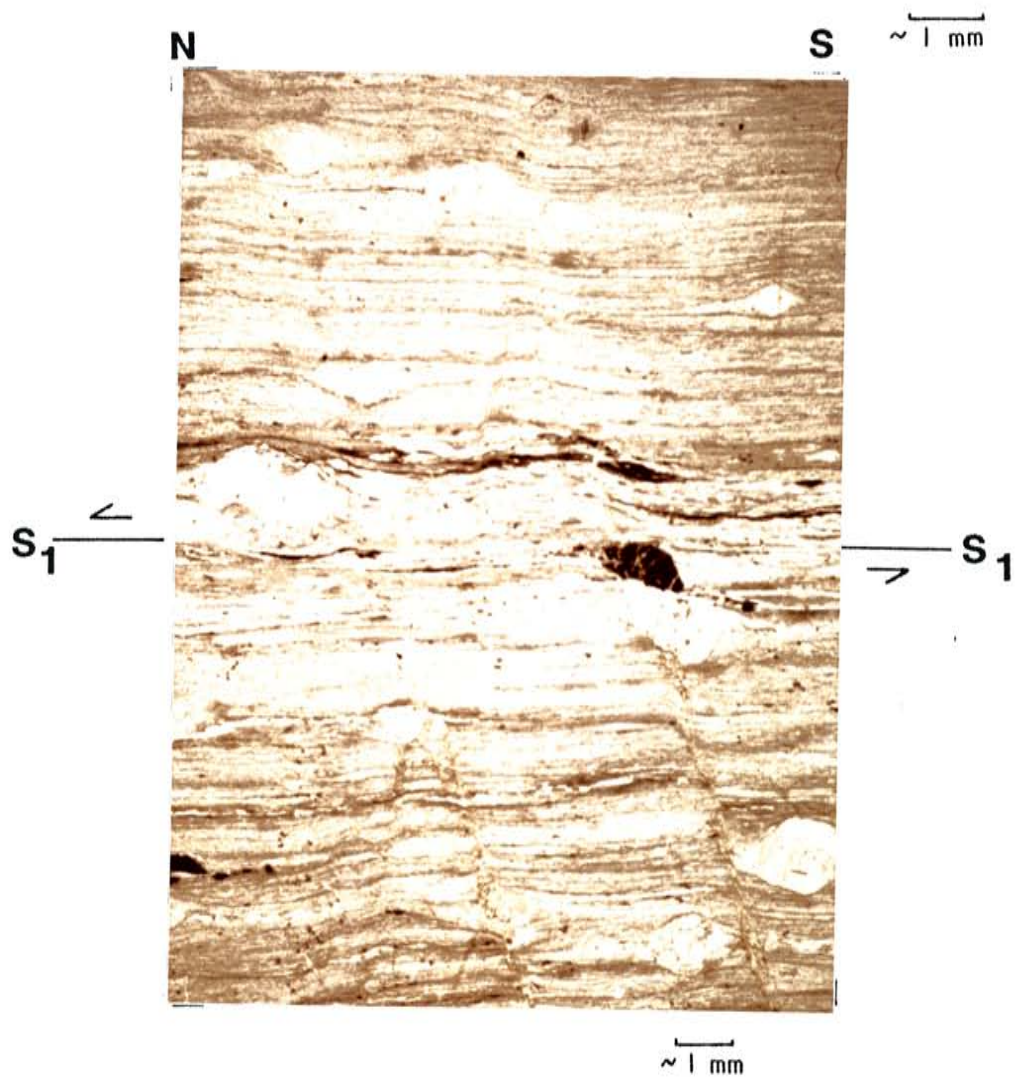
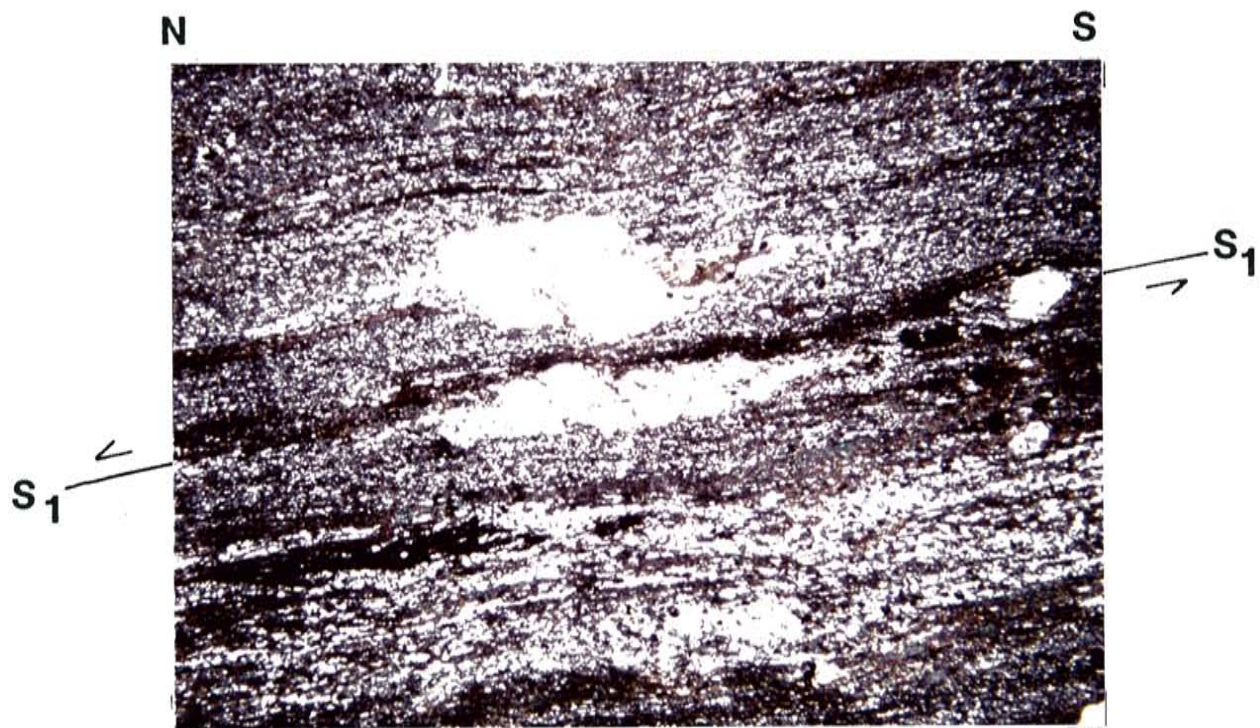
quitous quartz "eyes" that average 2×2 mm in size . In outcrop the metarhyolite is a dense, brick red to pink rock with gray blue quartz and smaller pink feldspar crystals. This unit contains a strong foliation, along which the rock breaks easily. The foliation planes contain a strong east-dipping mineral lineation and a set of conjugate crenulations.

Quartz and microcline phenocrysts are enclosed in a well-foliated, fine-grained matrix of polygonal quartz, equant feldspar, and idioblastic muscovite (Figure 13). The quartz crystals, which make up two-thirds of the phenocrysts, are rounded and strongly embayed. Rare near bipyramidal quartz crystals are also present. Quartz phenocrysts range from not recrystallized to completely recrystallized smaller polygonal grains. Many of the quartz and microcline crystals have been deformed. Medium-sized (0.5×0.5 mm), nearly polygonal quartz, equant feldspar, and xenoblastic carbonate are found adjacent to phenocrysts in pressure shadows and as lenses in the matrix. Rare albite is present in the lenses. Magnetite is a common accessory. A distinct foliation is delineated by the presence of muscovite-rich cleavage bands and lenses alternating with fine-grained bands of quartz, feldspar, muscovite, and carbonate.

Several possible explanations exist for the formation of the textures present in this metarhyolite and the felsic volcanics at the base of the MMS section. Minerals adjacent to phenocrysts and in lenses may have been formed from the crystallization of a vapor phase in primary voids (Chamberlin, 1988, personal communication); or they may be the result of growth in pressure shadows and metamorphic differentiation respectively. Broken and apparently sheared crystals can be a primary volcanic feature (Vernon, 1986; Chamberlin, 1988, personal communication); or they may be the result of tectonism. It is also possible that primary volcanic processes as well as metamorphic and deformational

FIGURE 13

Photomicrographs of the Burned Mountain metarhyolite. Thin sections are cut parallel to the extension lineation: a) Embayed quartz crystal (2.3 mm in length) and sheared feldspar. Shear is north-directed. Crossed polarized light; b) Quartz phenocrysts indicating north-directed shear. Conjugate crenulations also present. Photomicrograph is 1.7 cm long. Plane polarized light.



processes all contributed to the formation of these textures. Because this unit lies above a mylonitic zone and rocks in the general area are strongly deformed, it is assumed that these fabrics are mostly the result of deformation and are reliable shear indicators. Asymmetrical crystals, asymmetrical distribution of minerals in pressure shadows, and asymmetrical distribution of sheared minerals along foliation planes reveal that north-directed shear was significant in this unit.

Xenoblastic carbonate probably formed from the alteration of plagioclase and regional carbonization.

This author agrees with previous workers (Bingler, 1965; Kent, 1980; Gibson, 1981; Smith, 1986) in interpreting the Burned Mountain metarhyolite as an ash flow tuff. This conclusion is supported by:

- 1.) the presence of large feldspar and embayed quartz crystals, interpreted to be relict phenocrysts, which are contained in a fine-grained matrix of quartz and feldspar;
- 2.) thin laterally extensive rhyolite units that range from 30-100 m-thick and extend for up to 20 km in length (Barker, 1958; Doney, 1978; Gibson, 1981; Smith, 1986);
- 3.) medium-grained quartz and rare plagioclase adjacent to phenocrysts and in lenses that may represent crystallization from a vapor phase (Chamberlin, 1988, personal communication).

Quartz-muscovite phyllite

Quartz-muscovite phyllites occur as 1-2 cm-thick interbeds between more competent quartz-rich beds in the upper MSMR section. In outcrop these phyllites are dark grey. These rocks contain a bedding-parallel foliation and at least

one other crosscutting foliation.

The quartz-muscovite phyllites contain small visible quartz grains and are finely laminated. These phyllites are comprised of up to 20% well rounded quartz and hematite grains that are enclosed in a well-foliated muscovite matrix. Both the quartz and hematite are elongated in the plane of the S_1 foliation.

These quartz-muscovite phyllites are probably sand-rich mudstones that were deposited during quiet times (Soegaard and Eriksson, 1985).

Chlorite schist

Chlorite schists are present at three locations in the MSMR package: north of the confluence of the Rio Brazos and Bull Canyon, along Bull Canyon 10 m below the Los Pinos contact, and at the MSMR-Ortega Group contact.

Chlorite schists are mostly competent 1-10 m-thick units that parallel bedding in the MSMR package. Along Bull Canyon the chlorite schist is highly foliated and intensely deformed.

The chlorite schist is dark forest green in color and contains darker green chlorite spots that average 1×0.4 mm in size and are elongated in foliation plane. The strongly deformed rocks along Bull Canyon are chlorite phyllites, some of which contain darker green chlorite spots.

In thin section this rock is a quartz-plagioclase-chlorite schist. It contains abundant albite-oligoclase and chlorite with subequal portions of quartz, epidote, and carbonate. Up to 5% subidioblastic sphene is present in some samples. Carbonate is rhombohedral to xenoblastic in shape and rarely contains irregular shaped plagioclase patches. The rock contains a prominent foliation del-

ineated by the orientation of discontinuous patches of chlorite, and quartz and plagioclase. Sphene crystals have their long axes oriented in the foliation plane.

The chlorite schists are intermediate to mafic horizons that were either deposited during the formation of the MSMR package or later intruded as sills.

Possible Depositional Environment

The MSMR package is predominantly a poorly sorted metaconglomerate that grades upsection into a micaceous quartzite with isolated phyllite pebbles and phyllite pebble interbeds. The Burned Mountain metarhyolite is a single 10 m-thick volcanic unit near the base of the MSMR. The decrease upsection in pebbles and increase in quartz content represents a maturing of the MSMR rocks which is probably related to the stabilization of a depositional environment and the beginning of a marine transgression. Because the metaconglomerate above and below the Burned Mountain metarhyolite may have been fluvial or nearshore it is difficult to determine if the ash flow was deposited in a near-shore subaerial or marine environment. Never-the-less, the close proximity of marine sediments suggests that the metarhyolite was deposited subaqueously. It is unclear if the mafic horizons are sills or flows deposited during the deposition of the MSMR. The source of the mafic horizons is unknown.

ORTEGA GROUP

The Ortega Group is the youngest of the supracrustal rock packages in the study area (Just, 1935; Wobus, 1985; Smith, 1986; Williams, 1987). It is exposed along both the Rio Brazos south of the confluence with Bull Canyon and Gavilan Creek (Plate 1). The total quartzite section in the Tusas Mountains is more than one km-thick (Williams, 1987).

The Ortega Group is a maturing-upward quartzite sequence that lies conformably on the MSMR package. The basal unit of the Ortega has been termed a transitional quartzite because it contains minor phyllite-pebble-bearing interbeds and isolated phyllite pebbles that are similar to those in the underlying MSMR rocks. Above the transitional quartzite is a vitreous quartzite that matures upsection into a very clean cross-bedded quartzite. Throughout the Ortega Group competent quartz-rich beds 0.5-1.0 m-thick are separated by thin 1-2 cm-thick micaceous interbeds. Intermediate to mafic horizons of chlorite schist 1-2 m-thick are present in the vitreous quartzite. Superimposed on the lower more micaceous base of the vitreous quartzite is a brittlely deformed zone.

Proportionally, the Ortega Group consists of: 25% transitional quartzite, 70% vitreous quartzite, 4% micaceous interbeds, and 1% chlorite schist.

Transitional Quartzite

The transitional quartzite is a 900 m-thick section that extends from north of the confluence of the Rio Brazos and Bull Canyon to the northern edge of the Bad Lands. Because the decrease in phyllite pebble interbeds and isolated pebbles, and the increase in quartz content is gradational, the contact between the units was placed half way between distinct end members of each rock type. As defined in this study, the upper contact with the overlying vitreous quartzite is tectonic.

This unit contains 0.5-1.0 m-thick competent beds separated by 1-2 cm-thick micaceous interbeds. In the lower most 25 m of this unit the beds are thinly laminated; the remainder contains numerous cross-beds. Thin pebbly-horizons and isolated pebbles are most abundant in the basal 100 m of the section and diminish in abundance upward.

The transitional quartzite is a grey medium- to fine-grained micaceous quartzite. Laminations and cross-beds are dark grey to black in color. The quartzite contains flattened pink and green phyllite pebbles, and milky quartz and chert pebbles.

The transitional quartzite contains up to 67% rounded quartz. Minor albite and muscovite are present. Hematite, zircon, sphene, and rutile define primary lamina or cross-beds (Figure 14). All samples are framework supported and many are bimodal in thin section. The two populations of quartz grains average 0.4 and 4 mm in diameter. Quartz grains are either undulatory or have recrystallized to polygonal subgrains. All rocks contain a strong bedding-parallel foliation defined by elongated grains, quartz overgrowths, and oriented muscovite.

Vitreous Quartzite

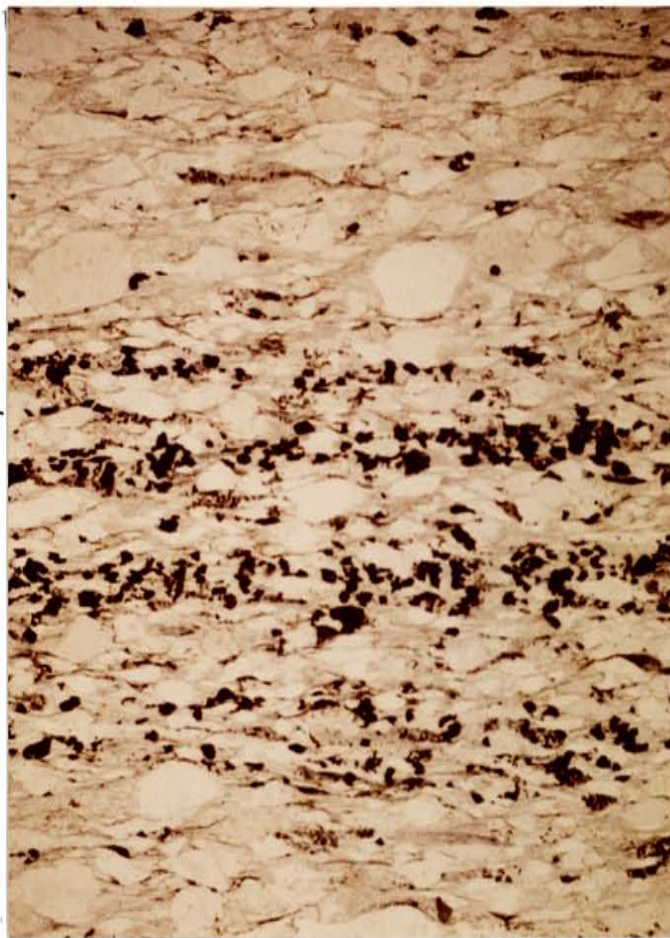
The study area contains only a small portion of the vitreous quartzite present in the northern Tusas Mountains. The vitreous quartzite is exposed along the Rio Brazos canyon south of the northern border of the Bad Lands, and along Gavilan Creek. The vitreous quartzite grades from a relatively micaceous quartzite at the base up into a very clean mature quartzite containing only a few percent of mica. The Jawbone syncline and the Hopewell anticline fold the vitreous quartzite in the southern part of the field area. Superimposed on the lower more micaceous portion of the vitreous quartzite is a brittlely deformed zone. This tectonized quartzite occupies a thin zone apparently only as wide as the Rio Brazos canyon and extending for 760 m across the Bad Lands.

The vitreous quartzite is very competent and forms steep near vertical cliffs along the Rio Brazos and Gavilan Creek (Figure 15). Stratigraphic facing can be determined by cross-beds which are tangential to the base of the quartzite

FIGURE 14

Photomicrograph of the Ortega Group transitional quartzite. Hematite defines bedding. Muscovite crystals are aligned and quartz grains elongated parallel S_0/S_1 foliation. Photomicrograph is 1.7 cm in length. Plane polarized light.

S_0/S_1

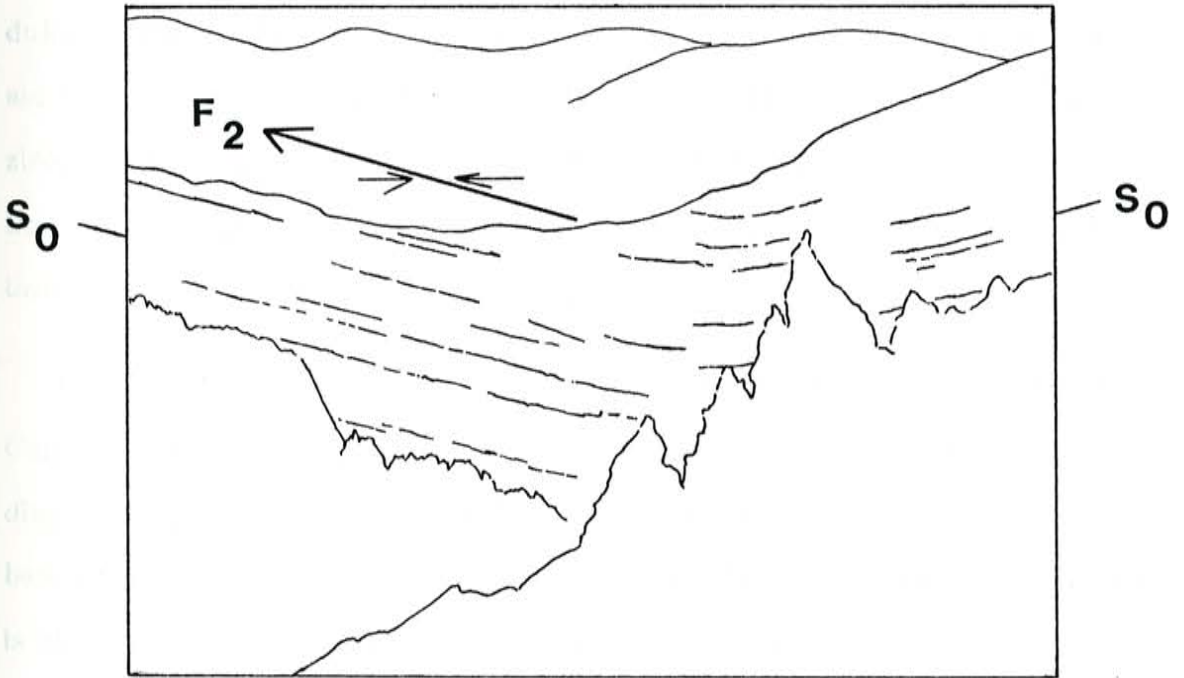


S_0/S_1

$\sim 1 \text{ mm}$

FIGURE 15

Ortega Group vitreous quartzite along the Rio Brazos. Photograph taken from above Gavilan Creek looking west down the axis of the Jawbone Syncline.



beds. Massive 0.5-1 m-thick units of cross-bedded material are separated by 1-2 cm of micaceous material. In some places, such as the uplands above Gavilan Creek the quartzite contains large quartz pebbles up to 2 cm in diameter. All samples contain a bedding-parallel foliation and a crosscutting wide-spaced fracture cleavage (S_2). A later close-spaced cleavage (S_3) is present along Gavilan Creek (Figure 16).

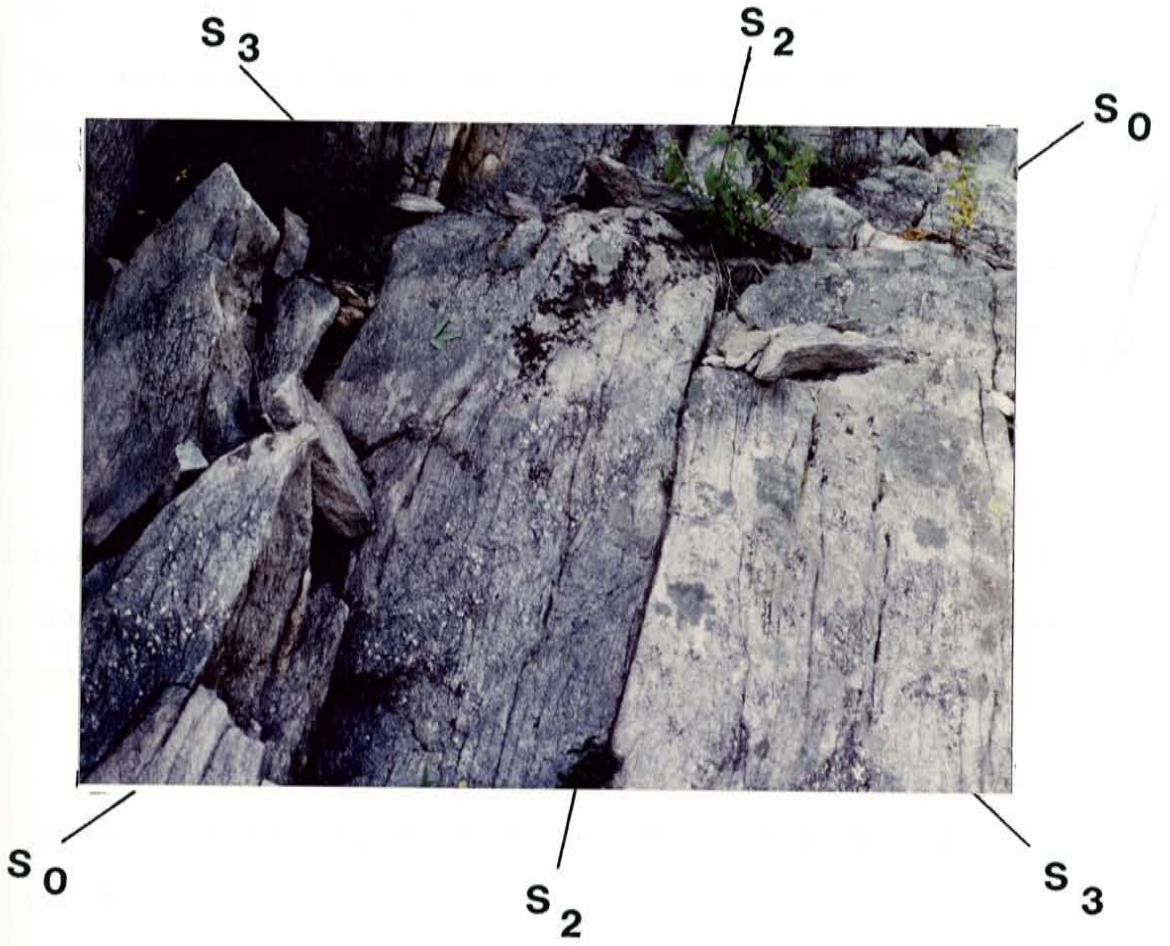
The vitreous quartzite is grey in color and contains light pink, blue, and milky quartz grains and pebbles. Rare chert clasts are present. It is a medium to coarse-grained, framework-supported meta-quartz arenite.

The vitreous quartzite contains up to 98% well-rounded to rounded quartz grains. Muscovite/sericite and hematite are accessories. The quartzite is bimodal in size, with the two populations of quartz grains averaging 0.4 and 4 mm in diameter. Many quartz grains have begun to recrystallize and their subgrains display seriate boundaries. Those that have not recrystallized are strongly undulose. Many grains contain quartz overgrowths. Rounded hematite crystals are now irregular in shape from recrystallization. Rare rounded and/or broken zircon and sphene are also present. The S_1 foliation is formed by the elongation of quartz grains, and the alignment of muscovite. The crosscutting foliations are defined by the orientation of muscovite.

On the southern slope above the confluence of the Rio Brazos and Bull Canyon, the quartzite float contains subidioblastic kyanite developed on bedding planes. It is difficult to determine if this float represents the quartzite beneath it or if it came from broken boulders in the Ritito Formation. Viridine is abundant along the Gavilan Creek in cobbles that are clearly derived from the overlying Ritito Formation.

FIGURE 16

Ortega Group vitreous quartzite along Gavilan Creek. South dipping bedding indicated by white quartz pebbles. Near-vertical fracture cleavage (S_2) is axial planar to the Jawbone syncline. S_3 foliation extends from upper left to lower right of photograph.



The brittlely deformed quartzite is slightly more micaceous than the vitreous quartzite above it. This quartzite crumbles easily to talus and is always covered with a beige clay. Red hematite stains, slickensides, and strong lineations formed by muscovite and quartz lenses are common. Layers rich in hematite and ilmenite appear blue in color and quartz-rich layers are pink. Thin dark hematite bands, thicker white mica bands, and irregular patches of pink quartzite are wavy to tightly folded and sheared creating a highly variegated appearance to the brittlely deformed rocks. Although this unit has been severely disrupted by faulting, many cross-beds show a slight overturning to the south, suggesting that this portion of the quartzite may have acted generally as a whole during deformation.

The brittlely deformed quartzite contains up to 73% rounded to well rounded quartz grains which are recrystallized to subgrains with 120° junctions and straight grain boundaries. Abundant amounts of clay (kaolinite ?) have formed within muscovite patches.

The vitreous quartzite is an upward maturing sequence in which the mica content decreases upsection. Planar cross-beds and tabular cosets with smaller trough cross-beds in the Jawbone Mountain area have been interpreted by Soegaard and Eriksson (1985) to be the result of tidal action on an inner shelf. Horizons containing larger pebbles are interpreted as winnowed lags from the tops of tidal sand bodies. Paleocurrents and facies distributions lead these authors to conclude that the Ortega Group was deposited in 3-4 m of water on a south sloping stable continental shelf. The brittle deformation was a much later event superimposed on the lower portion of the vitreous quartzite. The slightly greater mica content of the base of the vitreous quartzite is probably the result of greater amounts of clay originally deposited with the quartz in the lower part

of the section and the later addition of mica from the increased circulation of fluids through the fractured rocks.

Quartz-Muscovite Phyllite

The quartz-muscovite phyllite occurs as 1-2 cm-thick interbeds between the thick massive units of all members of the Ortega Group.

In outcrop the quartz-muscovite phyllites are dark grey, contain visible grains of pink and blue quartz, and are comprised of fine laminations 1.5 cm-thick. All rocks have a strong bedding parallel foliation and a later more east-west less steep fracture cleavage. A strong extension lineation dips towards the east and a prominent intersection lineation dips towards the west.

The quartz-muscovite phyllite is a metamorphosed matrix-supported sandy mudstone. It contains up to 20 % well-rounded quartz and hematite grains enclosed in a well foliated muscovite matrix. Both quartz and hematite grains have been deformed into "fish-shaped" grains that are elongated in the foliation direction. The "fish-shaped" grains and microfolds adjacent to the grains indicate contradicting shear senses, suggesting that these relatively incompetent micaceous interbeds have accommodated much of the shear strain from each phase of deformation and may have been sheared in different directions at different times. No overall shear direction was noticeable.

The micaceous interbeds are probably sand-rich mud layers deposited during quiet tidal times (Soegaard and Eriksson, 1985). Mud beds thicker than 1 cm require high concentrations of mud suspended in the water which would allow mud to be deposited during higher water velocities and at greater rates (McCave, 1970, in Soegaard and Erickson, 1985).

Chlorite schist

Two types of chlorite schists are present within the Ortega Group: a quartz-carbonate-chlorite schist and a quartz-plagioclase-chlorite schist; the former constitutes 95% and the latter constitutes 5% of the the chlorite schists respectively. The quartz-carbonate-chlorite schist is present in both the micaceous and vitreous quartzite, and the quartz-plagioclase schist is present only in the vitreous quartzite along Gavilan Creek.

Quartz-carbonate-chlorite schists in the micaceous quartzite is located at the top of the quartzite cliffs apparently beneath landslide material and within the quartzite apparently parallel to bedding. The schists crops out as 5-10 m-thick horizons between micaceous quartzite beds. One large outcrop of chlorite schist in the micaceous quartzite may be crosscutting the quartzite, but intense deformation has obscured the original relationships. In the vitreous quartzite along the Rio Brazos, the quartz-carbonate-chlorite schists are competent units at least 1 m-thick that are parallel to bedding. In the vitreous quartzite along Gavilan Creek both the quartz-carbonate-chlorite schist and the quartz-plagioclase-chlorite schist are present. In some outcrops along Gavilan Creek these schists are clearly bedding parallel, while in other places they form talus slopes or are not well exposed.

The quartz-carbonate-chlorite schist is dark forest green to grey green in color. Some samples contain dark green chlorite or white muscovite spots (4×1 mm) that are elongated in the foliation plane. Some chlorite schists are dark green with no mineral segregations. Along Gavilan Creek a quartz-carbonate-chlorite schist is present that contains abundant carbonate rhombohedra up to 2×1 mm in size. These rocks are foliated to intensely deformed.

The quartz-plagioclase-chlorite schist is dark green in color. Some samples contain large white plagioclase laths that reach 0.7×0.2 mm in size. In other samples the plagioclase laths are visible only in thin section. Dark green spots of chlorite and light green spots of epidote are visible in handsamples. A strong to weak foliation is present in these rocks.

The quartz-carbonate-chlorite schist is a fine-grained rock that contains subequal portions of chlorite and carbonate, and abundant quartz, magnetite, and ilmenite. Accessory amounts of plagioclase and muscovite/sericite are also present. The schists contain a prominent slightly anastomosing foliation delineated by the orientation of patches and individual crystals of chlorite and muscovite, and quartz and plagioclase.

The quartz-plagioclase-chlorite schists contain large albite laths enclosed in a fine-grained matrix of chlorite, quartz, epidote, and opaque iron oxides. The plagioclase laths are highly tectonized and saussuritized.

The chlorite schists form intermediate to mafic horizons within the Ortega Group. These horizons could either be sills or material that was contemporaneously deposited with the quartzite.

Possible Depositional Environment

The Ortega Group is interpreted as a maturing upward quartzite sequence deposited on a south sloping continental shelf (Soegaard and Eriksson, 1984) that represents the continued stabilization of a continental mass. Because depositional conditions remained constant for the time it took 1 km of quartzite to be deposited, the depositional basin must have been slowly subsiding (Smith, 1986). It is not clear if the intermediate to mafic horizons are sills or flows erupted during the deposition of the Ortega quartzite. The source of these horizons is not understood.

*INTRUSIVE ROCKS**Trondhjemite of Rio Brazos*

The trondhjemite of Rio Brazos is extensively exposed in the northern portion of the map area. Outcrops are present from south of Murphy's cow camp and north of the lower Bagwell cow camp to approximately the Carson National Forest fence line and west to the Rio Brazos. Most of the trondhjemite exposures have been strongly affected by periglacial processes as evidenced by features such as rock streams, altoplanation terraces, and stone circles. Freeze-thaw processes have fractured the rock so much that very little unbroken outcrop is present, even the tops of ridges are piles of disaggregated large blocks. The trondhjemite was classified into three groups for mapping purposes: trondhjemite outcrop, trondhjemite float overlying trondhjemite, and trondhjemite float probably overlying trondhjemite. The trondhjemite of Rio Brazos was dated at $1,654 \pm 34$ (recalculated with the new decay constants of Steiger and Jäger, 1977) Ma using Rb/Sr-whole rock methods (Barker, 1974b).

The trondhjemite is clearly intrusive into the MMS as evidenced by extremely irregular contacts between the two units, chilled margins, contaminated MMS-trondhjemite contacts, MMS xenoliths in the trondhjemite, dikes of trondhjemite within the MMS, and screens of MMS within the trondhjemite.

The irregular MMS-trondhjemite contacts are fingerlike offshoots of trondhjemite within the margin of the MMS (Figure 17). These offshots are most likely the result of trondhjemite magma injected into the MMS along their contact.

Xenoliths of MMS within the trondhjemite (Figure 18) are present in two

FIGURE 17

Trondhjemite of Rio Brazos intruding MMS amphibole schist in the lower MMS section. Note crosscutting S_2 foliation. The pencil is 15 cm long.

S₂



S₂

FIGURE 18

MMS xenoliths in the trondhjemite of Rio Brazos. The xenoliths contain two foliations, the directions of which are indicated by the knife and the pencil. The east-west foliation (S_2) is the only one visible in the trondhjemite. The pencil is 15 cm long.



S₂

S₂

areas: at the sharp western bend in the Rio Brazos where a small tributary joins it from the east and in the northwestern exposure of the trondhjemite. These MMS xenoliths are rounded in shape and range from several cm to a meter in diameter. One xenolith studied, which is representative of all other xenoliths seen, is a chlorite-quartz-plagioclase schist. The xenoliths contain two sets of foliations while the enclosing trondhjemite only displays one foliation.

At many contacts between the trondhjemite and MMS rocks both the metavolcanics and the trondhjemite have been chemically contaminated, producing a dark green silica-chlorite-actinolite schist with quartz phenocrysts.

In the lower MMS section the trondhjemite is present as 1-3 m-thick tabular dikes up to 400 m long which are subparallel to each other and the S_2 foliation in the area. Along the Rio Brazos, north of the lower Bagwell cow camp, the trondhjemite is present as screens that average 3 m in thickness and 30 m in length.

The trondhjemite is typically a light pink phaneritic inequigranular seriate rock that contains large quartz phenocrysts up to 5 mm in diameter. Potassium feldspar phenocrysts and clusters of mafic minerals are also distinctive in the trondhjemite. In places, the trondhjemite is tan in color and the quartz crystals have a brown greasy luster.

Only near the Carson National Forest gate is the trondhjemite strongly foliated. There the foliation is defined by distinct mineral segregations of felsic and mafic minerals. In most places the trondhjemite is weakly foliated. Two types of foliation are present: a mineral segregation and a fracture cleavage. In some places the trondhjemite is non-foliated. Three sets of joints are ubiquitous throughout the trondhjemite. The average direction of these joints is

N25 °W 46 °NE, N45 °W 50 °S, and N58 °E 70 °N.

In thin sections of the trondhjemite, quartz phenocrysts are as large as 5 mm in diameter, are strongly undulose and/or have begun to recrystallize. The matrix consists of intergrown equidimensional oligoclase, microcline, muscovite, and quartz. Interstitial mafic clusters include biotite, chlorite, magnetite, and epidote. Where present the foliation is delineated by elongated quartz crystals, elongated mafic clusters, and individual mica crystals both within and outside of the mafic clusters.

The timing of emplacement of the trondhjemite is difficult to constrain. The MMS xenoliths within the trondhjemite contain two foliations while the trondhjemite contains only one distinguishable foliation (S_2). The xenoliths could have been foliated before or after their incorporation into the magma. It is also possible that deformation after crystallization of the trondhjemite could have resulted in a macroscopic foliation (S_1) recorded only in the less competent fine-grained xenoliths. Four xenoliths were examined in detail. In outcrop there appears to be a similar NW and a NE trend to the foliations within the xenoliths, the NE trending foliation is present in the enclosing trondhjemite. But a stereonet plot of poles to the foliations within the xenoliths show a random distribution of all foliations. In the lower portion of the MMS section trondhjemite dikes are subparallel to the S_2 foliation while the ends of these dikes and any irregular margins along them are crosscut by the S_2 foliation. The trondhjemite probably contains one foliation in these localities, although the strongly anastomosing character of the foliation and the coarse grained nature of the trondhjemite made this determination very difficult. The MMS amphibole schists adjacent to these trondhjemite dikes contains two foliations. North of the lower Bagwell cow camp a MMS screen is apparently folded

into an open fold. The screen contains a foliation that parallels its margins. The screen and the first foliation are crosscut by a later foliation that strikes N60 °W and is probably axial planar to the fold. Macroscopic relationships indicate that there are two foliations present in the xenoliths and only one in the trondhjemite. The orientation and style of the fold is similar to another F_2 fold in the same structural domain, suggesting that this is also an F_2 fold and that the crosscutting cleavage is an S_2 foliation. Because only one foliation is distinguishable in the trondhjemite and two foliations are present in the surrounding MMS rocks, the trondhjemite of the Rio Brazos may be syntectonic. Because the dikes are subparallel to and crosscut by the S_2 foliation the orientation of the dikes may have been influenced by the D_2 phase of deformation.

Hornblendite

The hornblendite constitutes less than one percent of the intrusive Proterozoic rocks in the map area. It is present as float adjacent to the trondhjemite southwest of the Carson National Forest gate.

Subangular blocks of hornblendite float contain close-packed dark forest green amphibole crystals with an average size of 6×1.8 mm, although crystals as large as 9×4 mm are present. Interstitial to the amphibole crystals are patches of trondhjemite. These patches average 3×2 mm in size and often contain quartz crystals typical of the trondhjemite. One sample contains an 8 mm-wide vein (?) of trondhjemite, which contains smaller isolated hornblende crystals. Epidote veins 1 mm wide are common in the hornblendite.

In thin section large blue-green hornblende, and possible actinolite or actinolitic hornblende crystals are poikiloblastic and intergrown with each other. Some large amphibole crystals are replaced by mosaics of smaller amphibole.

Accessory minerals include feldspar, epidote, magnetite, and hematite. Plagioclase is intensely altered to epidote and contains many inclusions making its identification difficult. Rare myrmekite is present. Both plagioclase and quartz are interstitial to hornblende.

The hornblendite may either be a part of the MMS or it may be a cumulate related to the trondhjemite. The author agrees with Barker (1974) that the hornblendite is a cumulate rock that may possibly be related to the trondhjemite. This is supported by the ubiquitous patches of interstitial trondhjemite between close packed interlocking amphibole crystals. This texture may be the result of filter pressing and implies that this rock resulted from the mafic crystals settling out of a felsic liquid. Myrmekitic textures in plagioclase have been described in cumulates from the Bushfeld intrusion by Wagner and Brown (1967). The authors believe that the myrmekitic textures resulted from an increase in the water pressure of the magma as the melt crystallized.

Dikes

Greenstone dikes 1-2 m-thick are present in the trondhjemite. Chilled margins are present along the margins of some of the intrusions. Dike rocks are competent and strongly foliated.

Dikes are present throughout the trondhjemite. Some of the dikes intrude along fault zones. They are most often small (1 m-thick), but one exceptional 3 m-thick dike is present in the center of the map area. The dike strikes N70°E, which is similar in direction to that of the river and the tributary where they merge. The similarity in strike of both the river and the dike suggest they are fault controlled in this area.

The 3 m-thick dike in the trondhjemite is greenish brown in color. Car-

bonate patches have either weathered away leaving small holes on exposed surfaces or remain as small elongated tan spots. One strong foliation parallels the walls of the dike.

A sample of the 3 m-thick dike in the trondhjemite was examined in thin section. It is a quartz-chlorite schist which contains subequal portions of quartz and chlorite, minor amounts of carbonate and epidote, and accessory opaque iron oxides and biotite. A strong continuous foliation is delineated by chlorite and biotite laths surrounding elongated quartz grains. Larger subidioblastic epidote, magnetite and carbonate are uniformly distributed throughout the rock.

Quartz Veins

Quartz veins 2 cm to 1 m-thick occur throughout the MSMR package, the MMS, and the trondhjemite. The veins contain milky white bull quartz.

One unique quartz vein present in the lower MMS section on the hill labeled 10062-T. is granular in character and weathers into sand sized grains. Near the top of the hill this vein appears as if it has begun to form boudinage structures. In outcrop, this vein is greenish grey to milky white in color. It contains fractures 0.2 mm wide that are filled brown limonite (?) and green chlorite. Small rounded patches (0.5×1 cm) of non-granulated milky quartz are present, mostly near near the margins of the vein. In rare places flat surfaces of the vein meet in 120° angles. In thin section this vein consists of quartz crystals that meet in 120° angles and are only slightly undulatory. Fluid inclusions are abundant in this vein.

TERTIARY GEOLOGY

Tertiary units were mapped in reconnaissance style only as the emphasis of this study is the Proterozoic rocks. These units are superimposed gravels, sandstones of pyroclastic and volcanoclastic accumulations. The units are difficult to distinguish because of strong similarities in their composition and occurrence style.

EL RITO FORMATION

The El Rito formation (Smith, 1938) is the basal Phanerozoic unit in the area. It is a well-cemented conglomerate composed of Precambrian quartzite, rhyolite, greenstone, trondhjemite, and granite. Clasts are subangular to well rounded. The matrix is a fine grained arkosic sandstone and the cement is quartz. Smith believed the unit represents torrential stream deposits.

Along Gavilan Creek the El Rito forms cliffs. It contains clasts from all the Proterozoic units. Its cement is light orange to tan in color. In the central portion of the field area, the El Rito consists mostly of trondhjemite clasts with a few MMS clasts. The matrix of the El Rito conglomerate is a light tan sandstone composed of quartz, biotite, muscovite, feldspar, amphibole, epidote, and magnetite enclosed in a quartz cement. The El Rito reflects a basement source of Proterozoic rocks.

RITITO CONGLOMERATE

The Ritito conglomerate (Barker, 1958) contains pebble to boulder sized Precambrian fragments, which are unconsolidated in the field area. Barker postulated that the Ritito may be equivalent to the Conejos formation or the Biscara member of the Los Pinos formation, and that it represents an alluvial

mantle deposit. Members from all Proterozoic units are present in this gravel, although vitreous quartzite, being most resistant to weathering, is the most common clast type. No matrix was observed in the field area. This unit forms gentle slopes in the western portion of the map area.

CONEJOS FORMATION

Cross and Larson (1935) first described and named the Conejos andesite. Butler (1946) changed the name to the Conejos formation because the unit includes both andesitic to quartz latitic volcanic and fluvial material. Muehlberger (1968) refers to the unit as the Conejos quartz latite. Barker (1958) mapped the Conejos and Treasure Mountain formations together because he was unable to distinguish between them in the Cebolla quadrangle. He also stated that where the intervening welded Treasure Mountain tuff is absent, the lower Los Pinos formation and the Conejos are indistinguishable.

The Conejos formation occurs most commonly as an unconsolidated gravel consisting of sub-rounded to well rounded pebbles and cobbles of gray to greenish gray to maroon volcanics. Most of the gravel is andesitic, although some more felsic varieties are present.

A series of fluvial conglomerates and lithic rich tuffs crop out along the Rio Brazos and its tributaries north of the lower Bagwell cow camp. The conglomerates are poorly bedded and mostly framework supported. Clasts are subangular pebbles to boulders of maroon to gray intermediate volcanics, pink and white volcanics, light tan altered chalky volcanics, and subrounded MMS and trondhjemite fragments. The matrix is a light tan crystal-rich tuffaceous sandstone.

The tuffaceous material is unsorted and very friable. Lithic clasts are

subangular, range from several mm to several cm in size, and include maroon, gray, and light orange volcanic fragments. The crystal-rich matrix contains plagioclase, biotite, hornblende, and glass. White altered ash and possible feldspar are common. A few light tan tuff units are present which weather to thin slabs.

Pronounced cliffs of brownish red volcanic breccias are prominent in the northwest portion of the field area. This unit is a porous rock with olivine, iddingsite (?), pyroxene (augite) and plagioclase crystals. Calcite fills most of the pore space. This unit may be similar to the olivine quartz latite breccia described by Bingler (1968) along the Rio Tusas. Similarities to cliff-forming volcanic breccias which occur along the southwest margin of the landslide area near Bad Lands suggest that these outcrops could also be part of the Conejos formation.

On both sides of the Rio Brazos in the landslides of the Bad Lands are extensive deposits of non-sorted to poorly stratified material with angular to subrounded fragments, interpreted to be lahar deposits. The volcanics are dark grey to maroon in color and matrix-supported. The matrix is crystal rich. This material forms pinnacles, steep slopes, and hummocky slopes. These deposits seem similar to clastic tuffaceous pinnacles near the Rio de los Pinos described by Butler (1971) and are therefore assigned to the Conejos formation.

TREASURE MOUNTAIN FORMATION

The Treasure Mountain rhyolite was named by Larsen and Cross (1935) and was extended from Colorado into New Mexico by Butler (1946).

Two distinct sections of this unit are exposed in the upper Brazos Box study area. The first is directly north of the upper Bagwell cow camp. Here a basal black vitrophyre, exposed near the base of the hill is overlain by a tan to

brownish orange tuff in which the welding decreased upsection. This sequence is believed to represent an ignimbritic flow. Above this is a unit containing subangular to subrounded Precambrian fragments, mostly trondhjemite, in a tan ash matrix. Overlying this unit is an unwelded light tan tuff containing biotite, sanidine, hornblende, and abundant pumice.

The second prominent section is located due east of the upper Bagwell cow camp. The lower 4.5 m (15 ft.) of the section is a similar non-welded non-vitreous light tan tuff which contains biotite, sanidine, pyroxene, and pumice. Subangular lithic fragments include maroon to gray intermediate volcanics. In places this tuff weathers to thin slabs. Above this is 7.6 m (25 ft.) of fluvial volcanic sandstone interbedded and interlensing with framework to matrix-supported conglomerates. Cobbles and boulders include light to dark gray to maroon strongly welded lithic fragments, and light tan to orange porous volcanic material. This outcrop contains imbricated pebbles and cross-beds that suggest the local flow direction was from the north.

Several areas which contain only trondhjemite gravel are interpreted to be residual members of the ash-supported unit containing trondhjemite fragments. These units are located on the slope north of the upper Bagwell cow camp and between the 9000 ft. and 9050 ft. elevations of the two lobes that extend north from the 10,20 ft. hill west of the Murphy cow camp.

Northwest of the Thomas cow camp on the east side of the Rio Brazos is a fine-grained tan mudstone and a light beige fine-grained biotite sandstone. Both of these are interpreted to be related to the Treasure Mountain Formation.

LOS PINOS FORMATION

The Los Pinos Gravel was originally described by Atwood and Mather

(1932). Butler (1946) subdivided the unit into the Biscara member, the Esquible member, the Jarita basalt, and the Cordito member. The Jarita basalt may be correlative with the Hinsdale basalt (Butler, 1946). This study will describe only the Jarita basalt and include all conglomerates and flows in an undivided unit.

The Los Pinos formation is typically an unconsolidated gravel containing mostly dark gray to maroon intermediate volcanic pebbles to cobbles, although minor pebbles of both felsic and mafic composition are present. Variable amounts of Proterozoic pebbles to boulders are present. Many terraces, gentle slopes, and drainages contain only Precambrian members. Lithologies from all the Proterozoic units in the map area are included in this formation.

Near the eastern contact of the trondhjemite, adjacent to the periglacial terraces is a volcanic sandstone. The unit is a medium to fine-grained dense non-friable sandstone. Lithic fragments in this unit are maroon to gray to orange and subround to sub angular. The light colored matrix contains biotite and plagioclase.

Flows of the Jarita basalt are present throughout the Los Pinos formation. They are of two types. One contains olivine, iddingsite, chalcedony-filled vesicles and abundant pore space; The other contains olivine and pyroxene. All members form dark brown to gray, blocky outcrops.

AEROMAGNETIC DATA

The aeromagnetic data illustrate a magnetic low in the northern portion of the field area and a high in the southern portion of the field area (Figure 19). In some instances, magnetic lows correspond to areas of greater depth through sediments to crystalline basement rocks (Nettleton, 1971). However, aeromagnetic patterns in the upper Brazos Box area are not likely to illustrate depth to basement rocks because the low corresponds to exposed basement, in an area of possible early Eocene planation. Instead, the aeromagnetic patterns more likely result from magnetic susceptibility variations of different rock types in the Rio Brazos area.

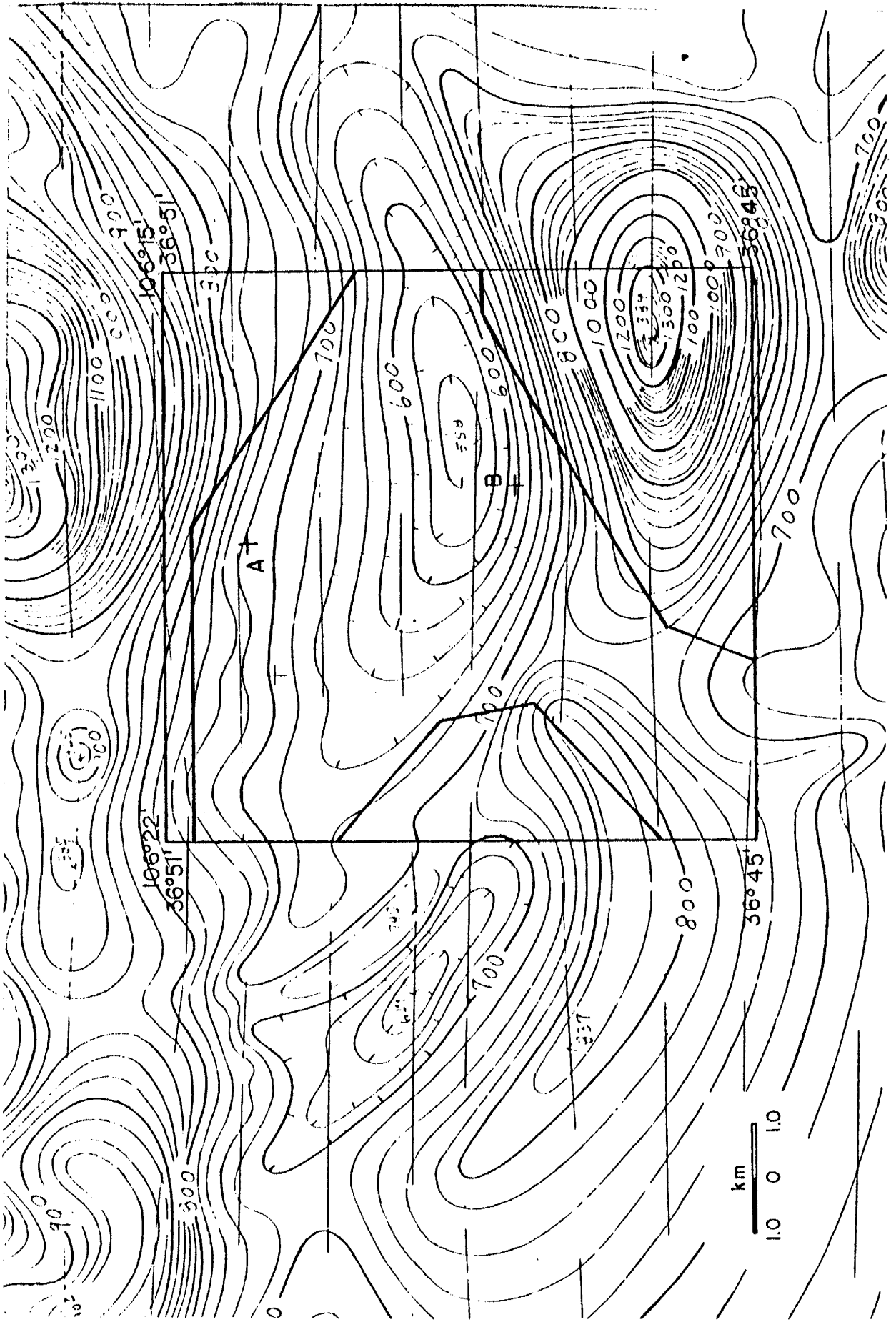
The low corresponds exceedingly well to the location of the Rio Brazos trondhjemite, which has a very low magnetic susceptibility due to the minor amount of mafic minerals present in the trondhjemite. The large size of the negative anomaly indicates that the trondhjemite is an extensive body, although the resolution of the data is such that it is impossible to determine whether the intrusion is one large body or a cluster of smaller closely spaced bodies.

The magnetic high in the south broadly corresponds geographically to the Jarita Basalt Member of the Los Pinos formation. The total magnetic positive anomaly is probably the combination of the high magnetite content of the MMS, and the high magnetic susceptibility of the andesitic and basaltic material in the Los Pinos formation.

The dipole present along the southeast margin of the field area probably contributes to the strength of negative and positive anomaly present in the field area (Lin Cordell, 1988, personal communication).

FIGURE 19

A portion of the Aeromagnetic Map of Northern New Mexico; 1976, Project 3238. Contour intervals are 20 and 100 gammas, flown at 1100', BAR, IGRF, 1965, updated removed, polyconic projection. Field area is outlined. Locality A corresponds to "Top of the World" and B corresponds to the 10,260' hill directly west of the Murphy cow camp. Map was provided courtesy of L. Cordell.



STRUCTURAL GEOLOGY
PROTEROZOIC STRUCTURES

The study area was divided into seven domains of similar structural style and lithology separated by major Tertiary faults (Figure 20 and Figure 21). Isolated fault blocks of trondhjemite were incorporated into domain 7 because structures in the blocks have orientations similar to each other and some of the blocks are too small to be considered individually. Lithology was used to discriminate between domains 2 and 3 because the orientation and style of structures are strongly influenced by rock type in these areas. The following table gives the relationship between domains and units:

DOMAIN	UNIT
Domain 1:	Ortega Group vitreous quartzite
Domain 2:	Ortega Group transitional quartzite
Domain 3:	MSMR
Domain 4:	Upper MMS
Domain 5:	Central MMS
Domain 6:	Lower MMS
Domain 7:	Trondhjemite of Rio Brazos

Subscripts refers to the sequential relationships of fabrics present in the study area, but do not imply that these fabrics were formed by separate deformational events.

FIGURE 20

Index map showing the location of structural domains in the study area. Most domains are separated by Tertiary faults.

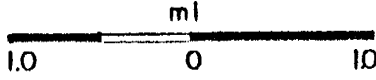
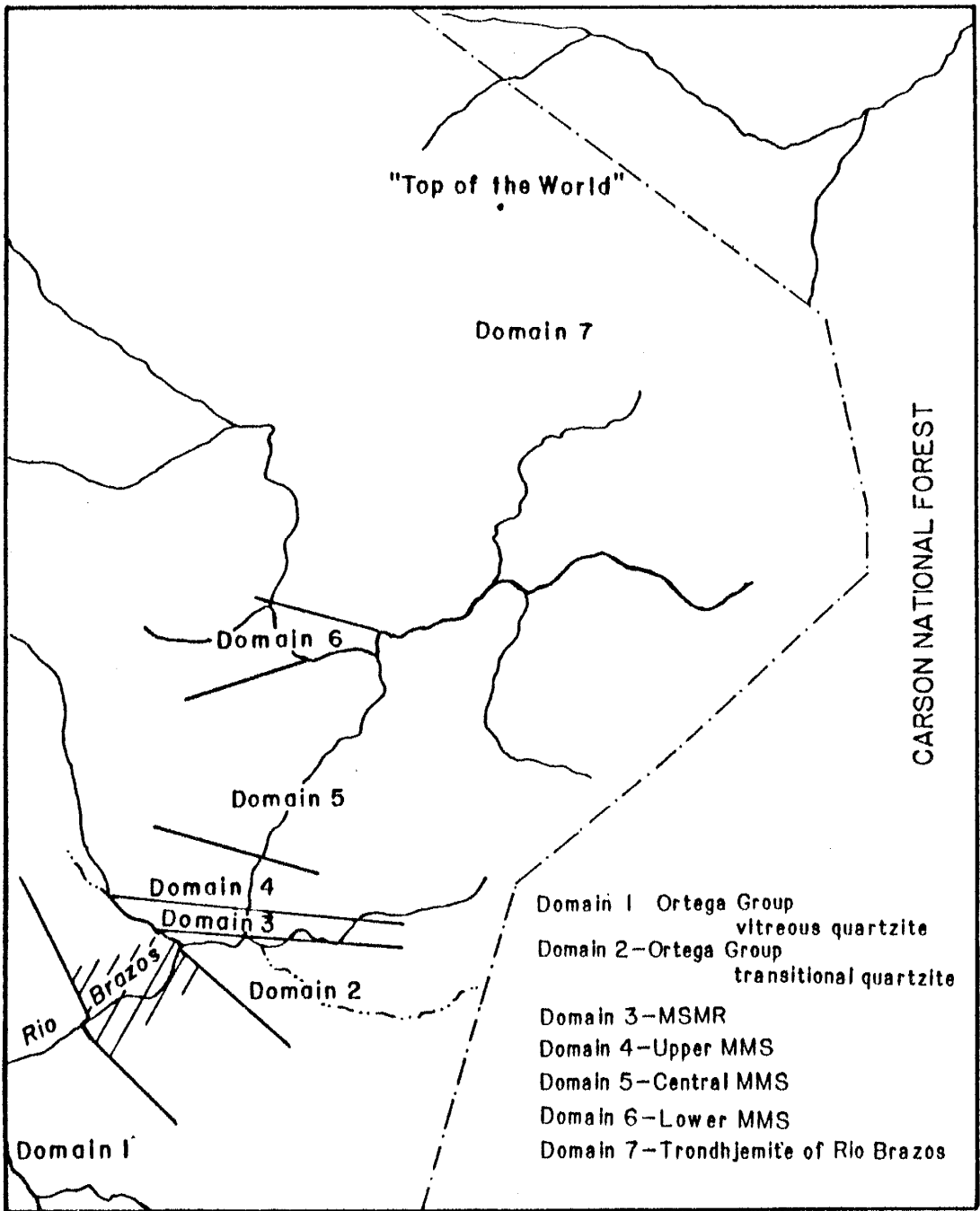
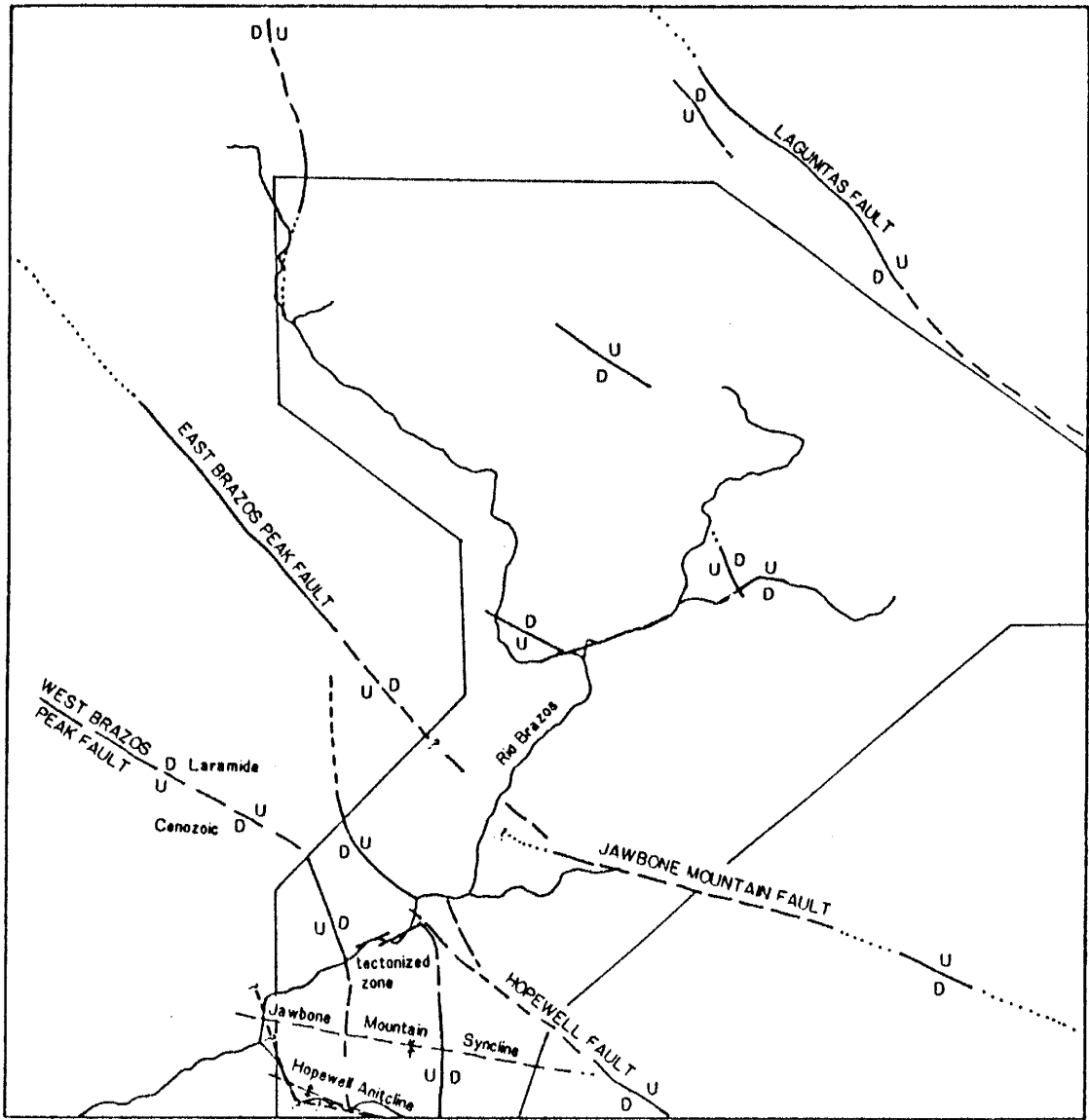


FIGURE 21

Generalized map of major structures in the upper Brazos Box field area. Map has been modified from the Structure Contour and Tectonic Map of Brazos Peak Quadrangle, Muelhberger, 1968.



FOLIATIONS

Domains 1 and 2

Rocks of domains 1 and 2 (Ortega Group- vitreous and transitional quartzite) are well bedded throughout the area. Cross-bedding and graded beds consistently indicate that all units are upright. Bedding delineates two prominent folds with nearly parallel fold hinges that pass through the southern portion of the field area- the Jawbone syncline and the Hopewell anticline (Figure 15 and 21).

A bedding-parallel, generally weak foliation (S_1) formed by the alignment of micas and elongation of quartz grains is ubiquitous throughout the Ortega Group. This foliation is typically visible only in thin section, especially in the vitreous quartzite (Figure 14).

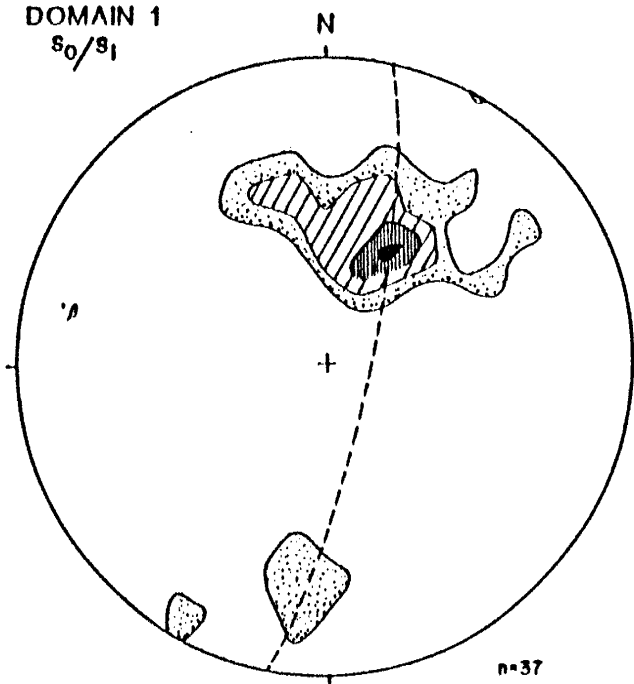
Sterographic projections of poles to S_0/S_1 are presented in Figures 22 and 23. In domain 1 structural readings from the Jawbone syncline and Hopewell anticline are plotted on the same stereonet because the folds are nearly parallel and closely spaced, and because most readings were taken from the Jawbone syncline. The average trend and plunge of both folds is 12° toward N79 °W, although the northern limb of the Jawbone syncline is the prominent structure in both domains 1 and 2. The average orientation of the northern limb of the Jawbone syncline in domain 2 is N73 °W 72 °S.

A pervasive, strong, wide- to close-spaced fracture cleavage (S_2) crosscuts S_0/S_1 and is axial planar to the Jawbone syncline and the Hopewell anticline (Figure 22). While this foliation is strongest in the vitreous and micaceous quartzite, it is also present in the transitional quartzite. The average orientation of this axial planar cleavage measured in domain 1 is N87 °W 70 °S.

FIGURE 22

Stereographic projections of poles to bedding and foliations in domain 1- the Ortega Group vitreous quartzite.

DOMAIN 1
 s_0/s_1



DOMAIN 1
 s_2

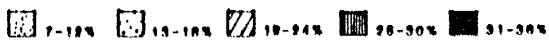
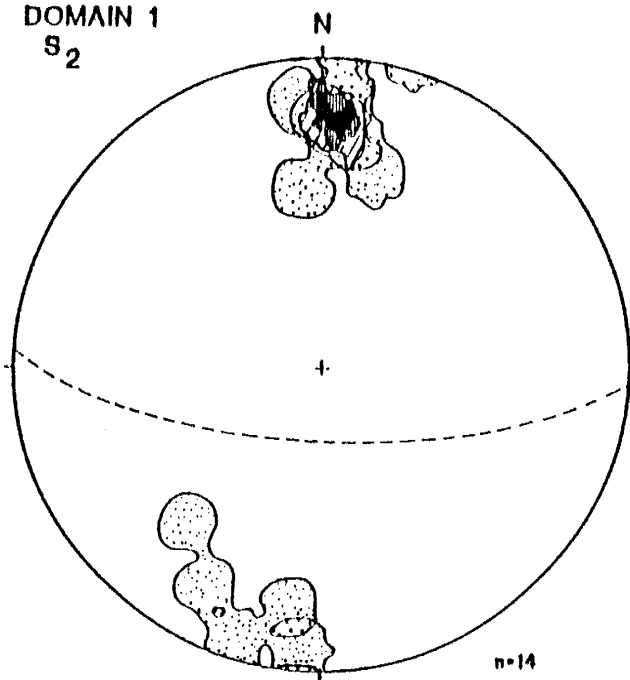
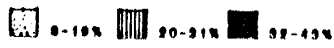
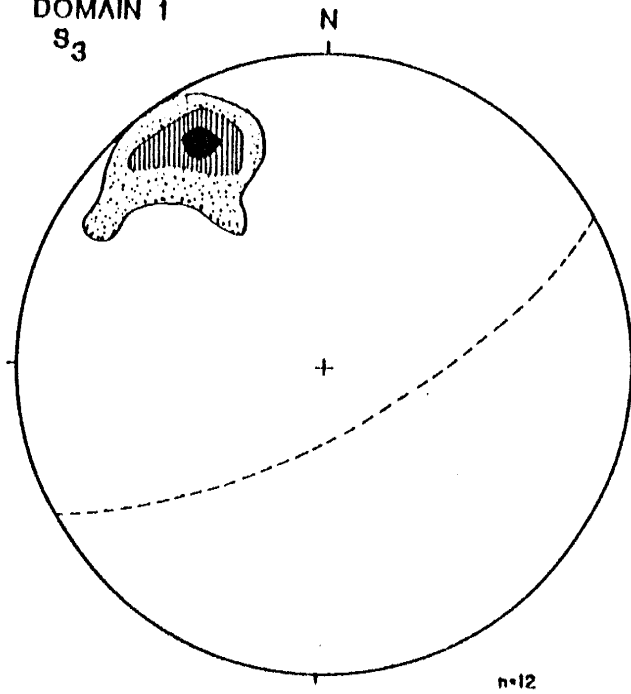


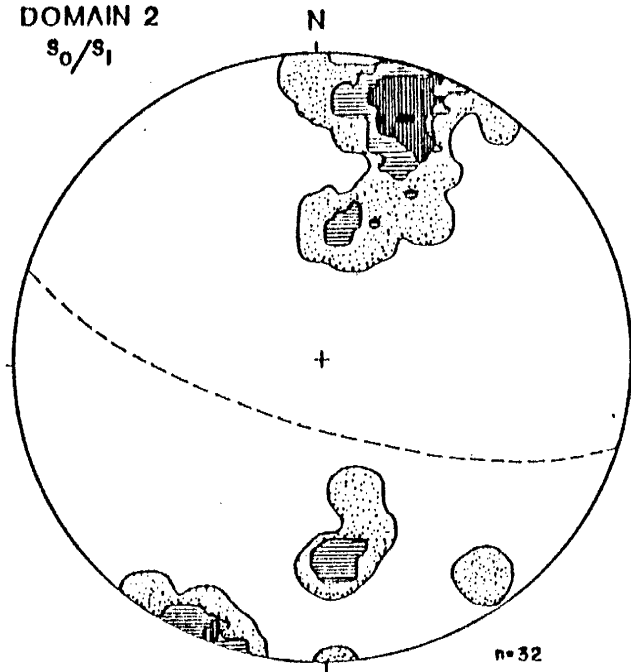
FIGURE 23

Sterographic projections of poles to the S_3 foliation in Domain 1- the Ortega Group vitreous quartzite, and to bedding and the S_1 foliation in Domain 2- the Ortega Group transitional quartzite.

DOMAIN 1
 s_3



DOMAIN 2
 s_0/s_1



A close-spaced fracture cleavage that appears to crosscut the S_2 foliation is present along Gavilan Creek in domain 1 (Figure 16, Figure 23). The granular nature of the quartzite made it difficult to determine unequivocally the relationship between these cleavages, but it appears that this is an S_3 foliation. The average orientation of this S_3 foliation is N59 E 86 °S.

Domains 3 and 4

Domains 3 and 4 (MSMR and upper MMS) are similar in structural style. The upper quartz-rich portion of the MSMR package is well-bedded, although pervasive deformation suggests that bedding has been reoriented. Bedding is delineated by 1-2 m-thick quartz-rich units separated by thin 1-2 cm-thick micaceous interbeds or in some cases phyllite pebble interbeds (Figure 11). The lower MSMR and upper MMS in domain 4 are not bedded but contain distinct compositional layering which always has an orientation similar to bedding. Compositional layering consists of mm-thick bands and lenses of more felsic material that is believed to be the result of metamorphism differentiation.

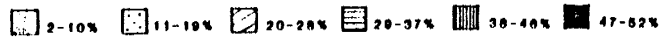
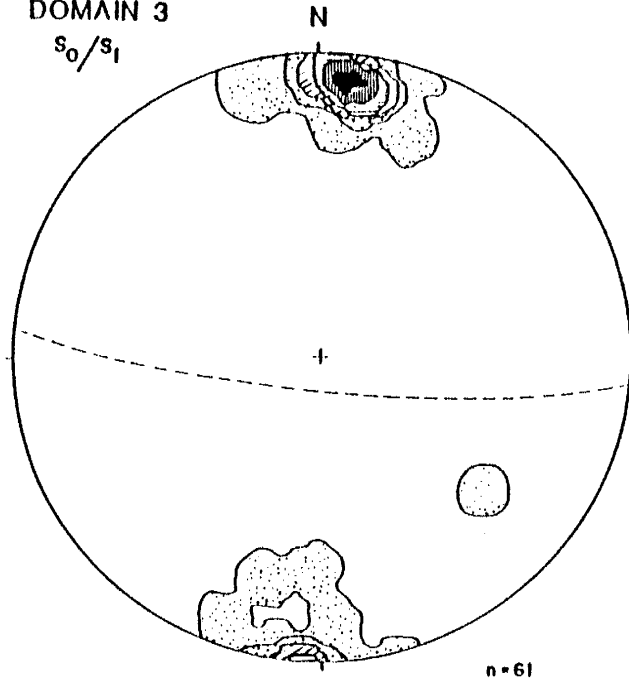
A strong, pervasive S_1 foliation is parallel to both bedding and compositional layering in these domains, as well as throughout the study area (Figure 24). This foliation is defined by many tectonite fabrics such as the truncation of early phases of the foliation by late phases of the same foliation, rotated crystals, broken and sheared crystals, and mylonitic foliations. Because the tectonite fabrics are related to the development of the prominent foliation it is regarded as an S_1 foliation, although it is a highly evolved composite fabric. Small isolated lenses and fold noses of more felsic material indicate that S_1 has transposed bedding and/or compositional layering. The average orientation of S_1 is N85 °W 81 °S in domain 3 (MSMR package) and N82 °W 87 °S in domain 4 (upper MMS). All structural features associated with this foliation, such as

FIGURE 24

Stereographic projections of poles to bedding and foliation in domain 3- the MSMR, and domain 4- the upper MMS.

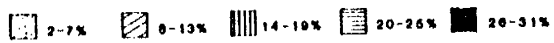
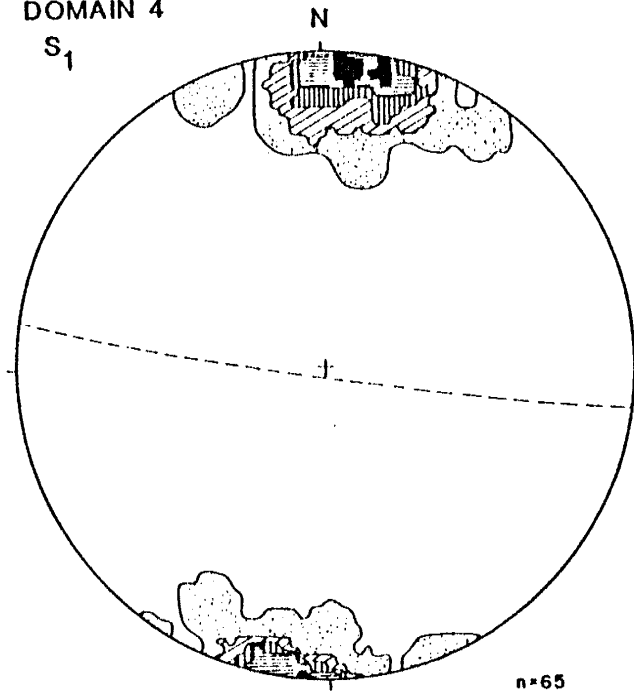
DOMAIN 3

s_0/s_1



DOMAIN 4

s_1



asymmetrical crystals and S-C fabrics, indicate that shear was north-directed.

The S_1 foliation is crosscut by one or two additional foliations. When both additional foliations are present they form what could be described as a conjugate set developed at angles of 15-30° to the S_1 foliation. These foliations may be expressed as a crenulation cleavage(s).

Domains 5 and 6

Structures in domains 5 and 6 (the central and lower MMS) are similar in style and orientation. Bedding, (S_0) which is present only in one outcrop in domain 5, (Figure 4) strikes N48°-56°E and dips 82°-90°SE. In domain 6 an outcrop of questionable bedding strikes N86°E and is overturned 57° to the south. Depositional contacts between felsic volcanics (metarhyolites) and mafic horizons are present in both domains. Along the Rio Brazos canyon in domain 5, massive biotite-amphibole schists alternate with amphibole schists. Textures reminiscent of diabases present in the amphibole schists make it difficult to ascertain if their contacts are depositional or intrusive.

Parallel to bedding and compositional layering is a subtle to strong S_1 foliation. This foliation ranges from continuous to discontinuous and is usually slightly anastomosing in thin section (Figure 25, Figure 26). Classical S-C fabrics are present, indicating that north-directed shearing was important in the formation of the S_1 foliation. Transposition of material is evidenced by isolated lenses and fold noses of more felsic material. The S_1 foliation presently strikes from N70°E to N70°W and dips steeply south in domains 5 and 6.

The S_1 foliation is crenulated into a spaced S_2 cleavage, which ranges from continuous to discontinuous in nature (Figure 25, Figure 26). This S_2 foliation is similar in strike to the S_1 foliation but has a slightly shallower dip. The S_2

FIGURE 25

Photomicrograph of a MMS amphibole schist directly adjacent to a trondhjemite dike. Note two foliations. Rock contains plagioclase, actinolite, and biotite. Plane polarized light.

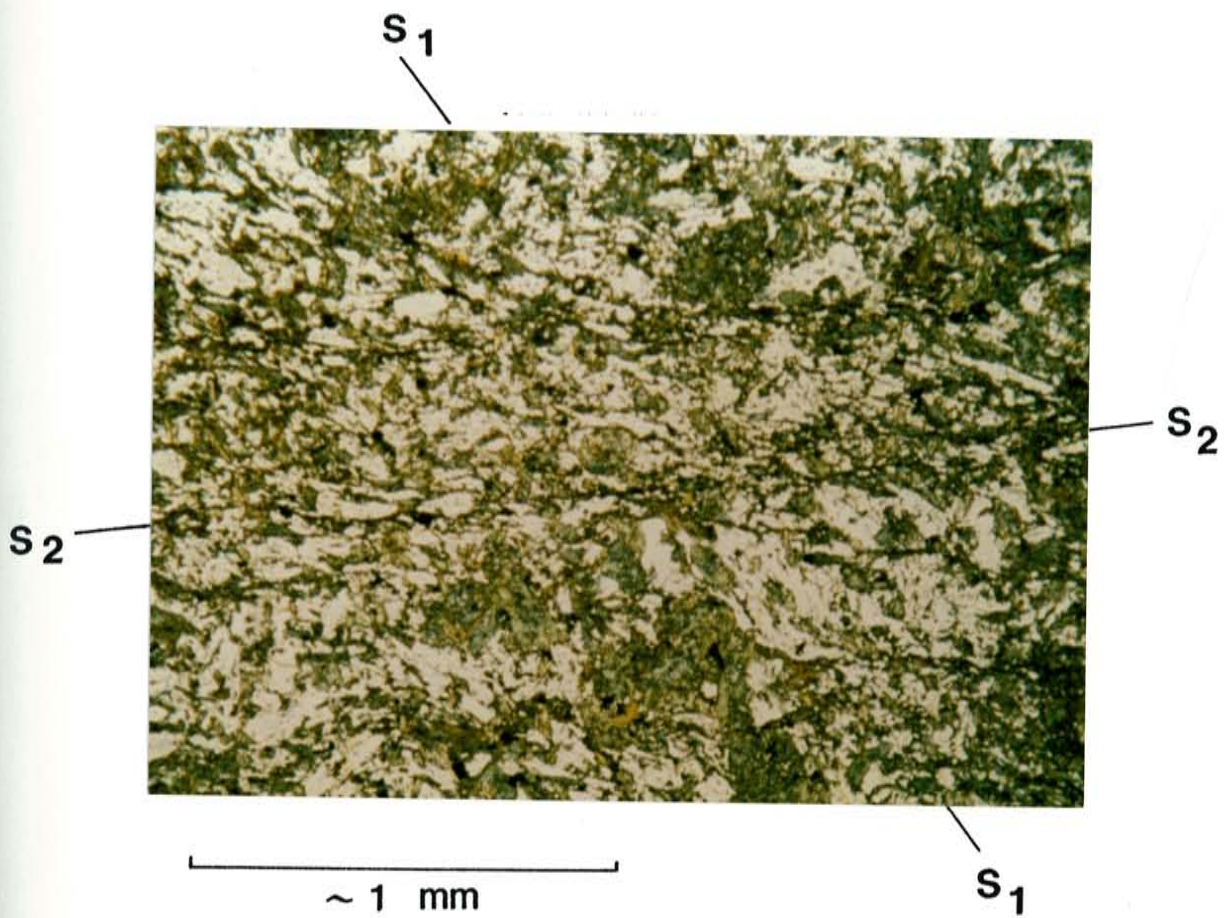
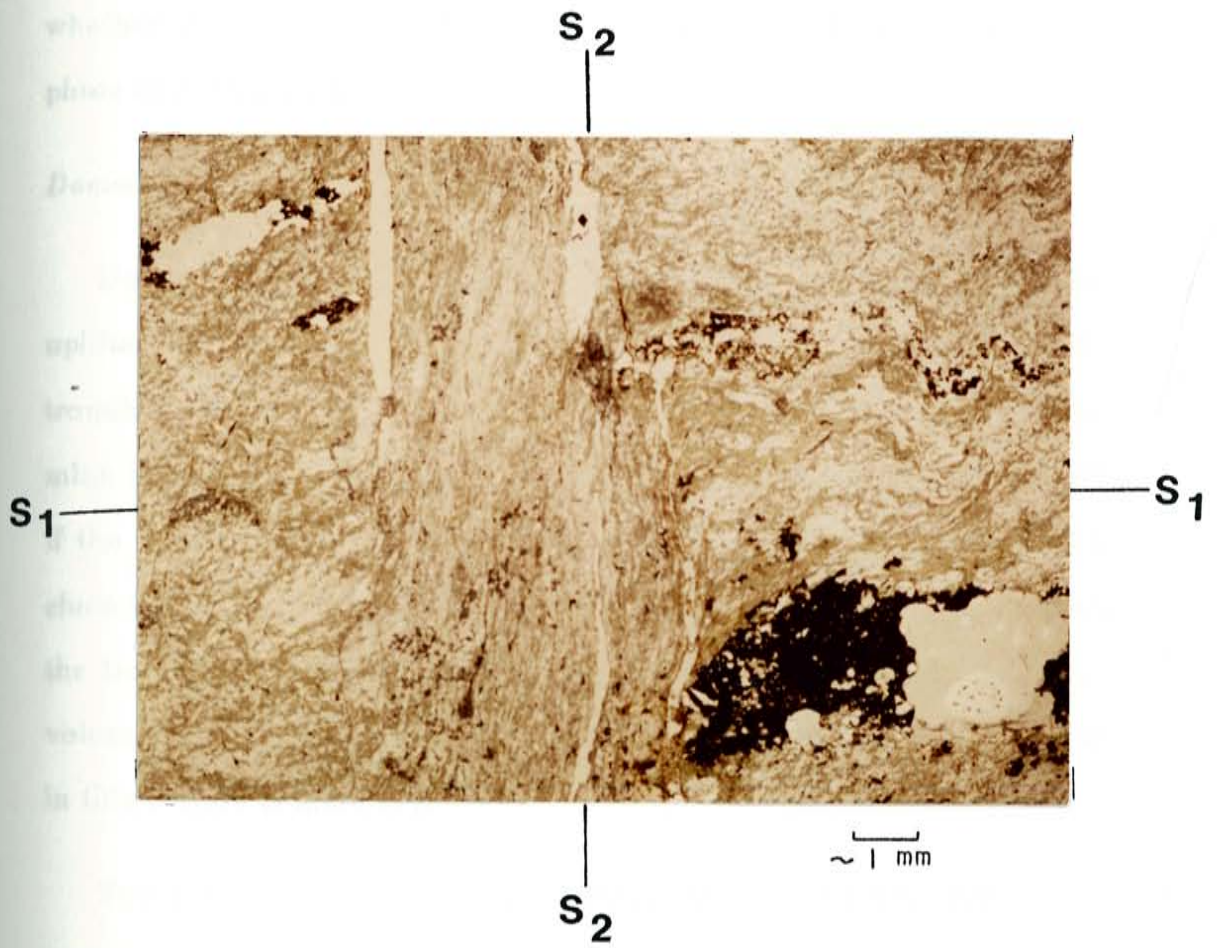


FIGURE 26

Photomicrograph of a MMS quartz-plagioclase-chlorite schist from the nose of a mesoscopic antiform. Note the S_1 is crenulated into the S_2 foliation, which is sheared in the nose of this fold. The photomicrograph is 1.7 cm in length. Plane polarized light.



foliation may or may not be the dominant outcrop foliation. In domain 5 the average orientation of S_2 is N60 °W 84 °S and in domain 6 it is N88 °W 51 °S (Figure 27).

One or two cross-cutting foliations may also be present. It is unclear whether these foliations are related to S_1 or S_2 , or if they represent a third phase of deformation.

Domain 7

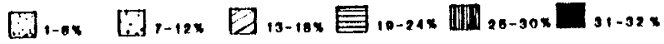
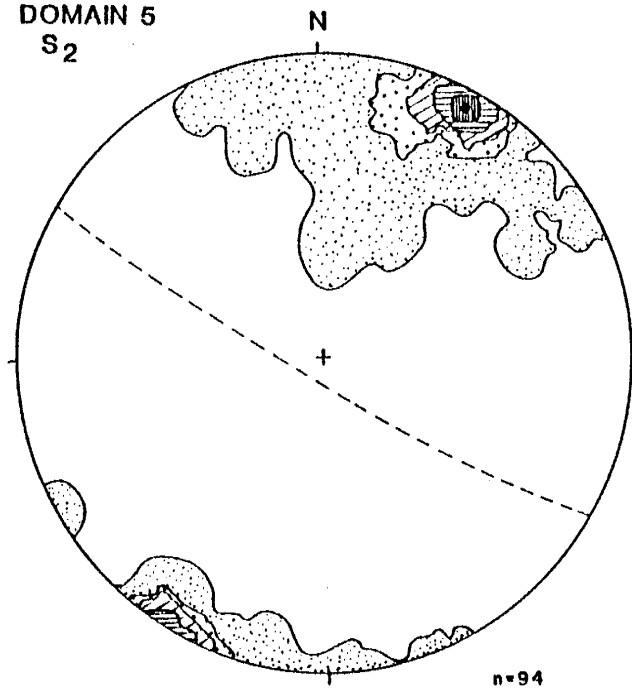
Domain 7 consists of one large trondhjemite exposure and several small uplifted fault blocks of trondhjemite. Due to the coarse grained nature of the trondhjemite and the anastomosing nature of the foliation it is difficult to determine if the trondhjemite contains one or two foliations, although it appears as if the trondhjemite contains only the S_2 fabric. Therefore it is difficult to conclude if the trondhjemite is pre- or syntectonic. Along the southern margins of the trondhjemite, intrusive contacts between the trondhjemite and mafic meta-volcanics are crosscut by a strong foliation which has been determined to be S_2 in thin section (Figure 17).

Two types of S_2 foliations are present in the trondhjemite: one is defined by segregations of quartz and feldspar alternating with biotite and minor magnetite in which the rocks approach a gneissic texture, and the other by a close-spaced fracture cleavage. Strongly foliated, nearly gneissic outcrops of trondhjemite are present only near the Carson National Forest gate; these are believed to represent one margin of the pluton. The stereographic plot (Figure 28) indicates that both types of foliations have similar orientations. The average orientation of the S_2 foliation in the trondhjemite is N88 °E 79 °NW.

FIGURE 27

Stereographic projections of poles to foliation in domain 5- the central MMS, and domain 6- the lower MMS.

DOMAIN 5
S₂



DOMAIN 6
S₂

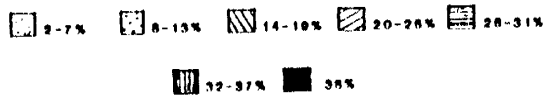
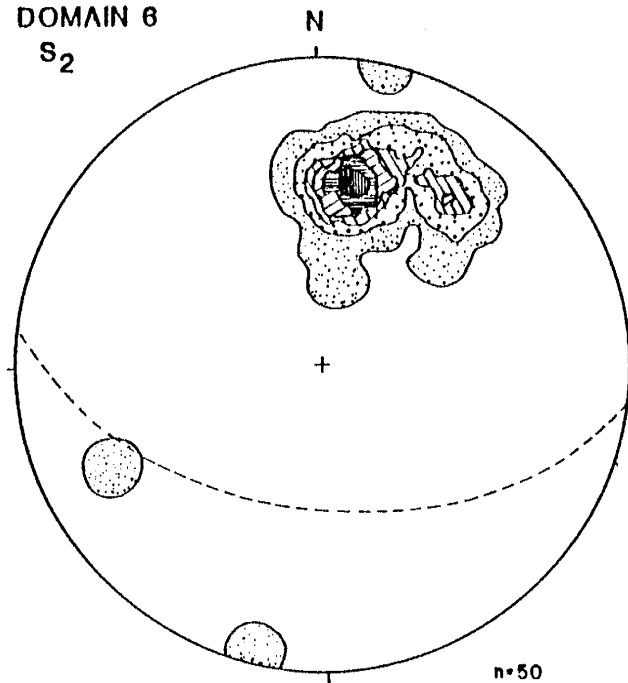
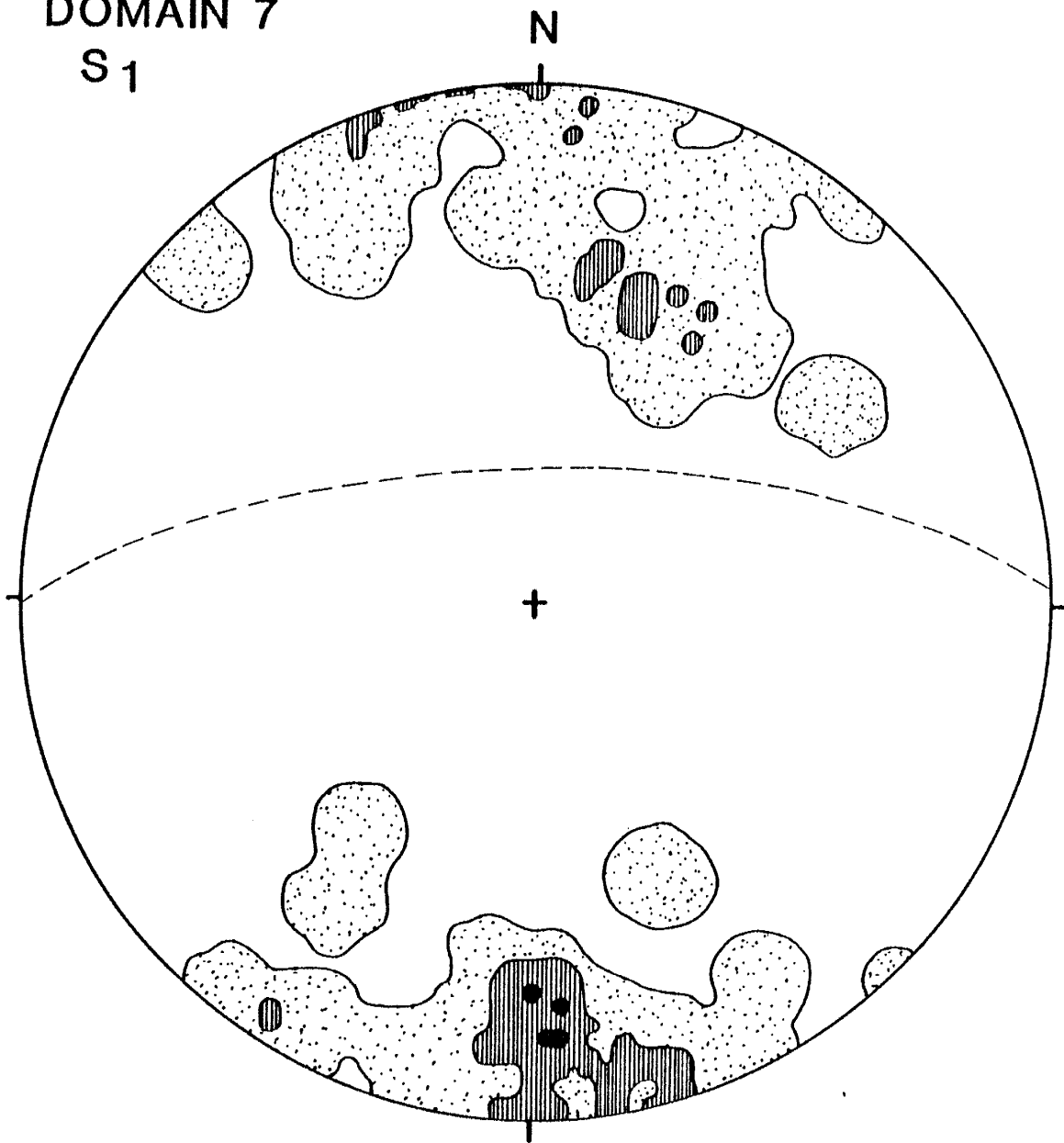


FIGURE 28

Stereographic projection of poles to the S_2 foliations from the trondhjemite of Rio Brazos in domain 7.

DOMAIN 7
S₁



n=51



FOLDS

F_1 folds are rare in the study area. Observed folds range from microscopic intrafolial folds to macroscopic folds several meters in amplitude. These folds are tight to isoclinal and are commonly associated with shear fabrics. In domain 5, a metarhyolite unit displays isoclinal F_1 folds and associated shearing, although asymmetrical porphyblasts indicate contradicting shear senses in these folds. Original flow banding in the felsic volcanics from domain 6 has been tightly to isoclinally folded into F_1 folds (Figure 9). Along the Rio Brazos, bedding-foliation relationships are complicated by conjugate foliations and a lack of identifiable primary bedding. Nevertheless, apparent vergence directions and small "M" folds suggest that the MMS has been folded into large, isoclinal F_1 folds with an average wavelength of 100 m. However, no repetition of units was found along the Rio Brazos to substantiate this.

The axial traces of the Jawbone syncline and Hopewell anticline pass through the Gavilan Creek area (Figure 15, Figure 21). These folds are interpreted as F_2 folds because their axial planar foliation cross-cuts S_0/S_1 , although their open, upright style is similar to F_3 (Williams, 1987). The average trend and plunge of these folds is 12° to $N79^\circ W$ (Figure 22), which is similar to the trace of the Jawbone syncline in the Jawbone Mountain area (Smith, 1986) and in the Cebolla quadrangle (Doney, 1968). The trend of the Hopewell anticline changes from $N30^\circ W$ to $N45^\circ W$ in the Cebolla quadrangle to "nearly west" in the Brazos Peak quadrangle (Doney, 1968).

Mesoscopic F_2 folds are rare; where exposed they are usually small, open folds. However, one small tight F_2 is recognized. On the hill labeled 1006-T in domain 6 isoclinally folded (F_1) flow bands in the felsic volcanics and the S_1 foliation in the mafic metavolcanics are refolded into open F_2 folds (Figure 9).

One small folded quartz-plagioclase-chlorite schist in the MMS appears to be the result of drag between two felsic schists.

LINEATIONS

East-dipping extension lineations are present on the S_1 surface of all domains, except the trondhjemite. They are best developed in the MSMR package and fine-grained metavolcanics. These lineations are formed by the alignment of muscovite or actinolite, streaks of such minerals as biotite, feldspar and quartz, and the elongation of pebbles. Extension lineations are illustrated for domains 3 and 4 where they are best developed (Figure 29). The average trend and plunge of the extension lineations in domain 3 is 57° to 106° and in domain 4 it is 52° to 091° .

Intersection lineations are present on all foliation surfaces and dip both east and west. They result from intersections of S_0/S_1 and S_2 , and conjugate foliations intersecting both S_0/S_1 and S_2 . Calculated lineations for the intersection of S_0/S_1 and the S_2 foliation in domain 1 are consistent with those measured in the field and roughly parallel the trend of the Jawbone syncline. Their average trend and plunge is 12° to 270° .

DISCUSSION

Three sets of foliations and folds are recognized in the upper Brazos Peak study area. Continuity between microstructures and similarity in the orientations of structures suggest that all fabrics developed as phases of one progressive deformational event (Williams, 1987; Mawer, 1988, personal communication).

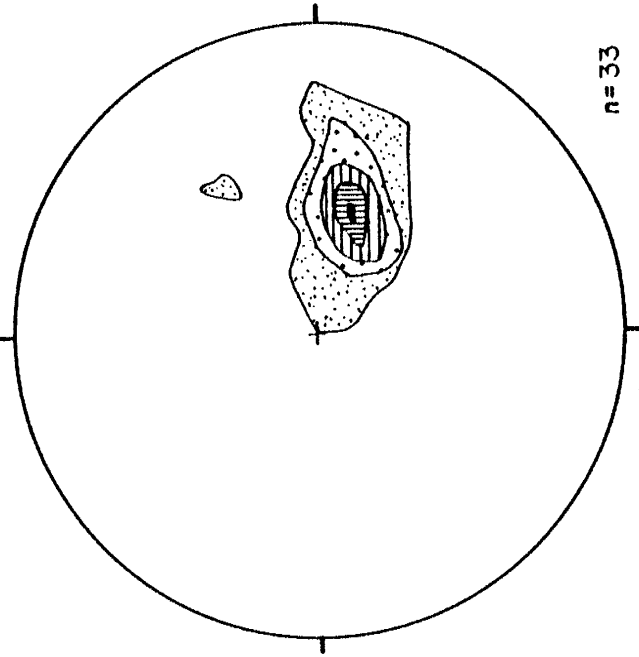
A weak to strong S_1 foliation is parallel to all bedding and compositional

FIGURE 29

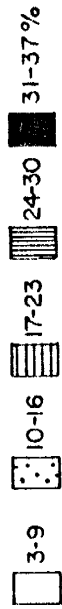
Stereographic projections of extension lineations in domain 3- the MSMR package, and domain 4- the upper MMS.

EXTENSION LINEATIONS

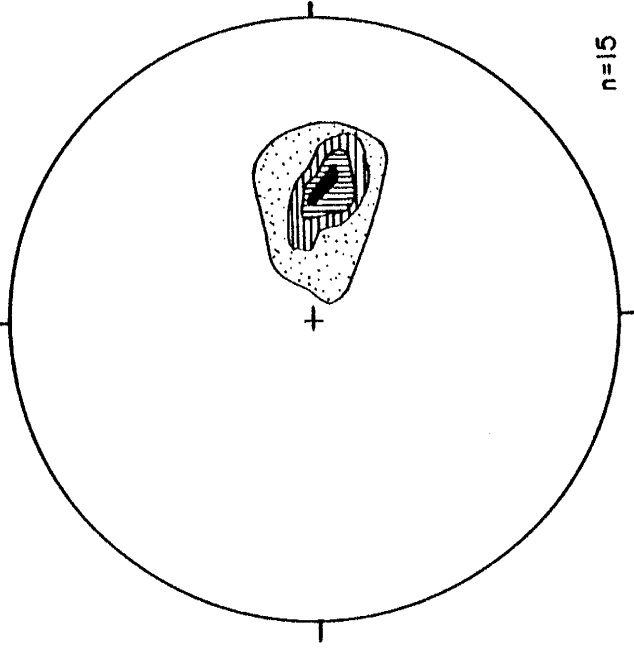
DOMAIN 3



n=33



DOMAIN 4



n=15



layering in the study area. It should be emphasized that while compositional layering may have initially been the result of primary deposition, it is now the product of metamorphism and deformation; the influence of original bedding is indeterminable.

In the MSMR package and the MMS rocks the S_1 foliation is a composite of reactivated foliations, rotated porphyroblasts, sheared crystals, and S-C mylonites. Shearing and isoclinal folding related to the development of S_1 have transposed original bedding, destroying much of the stratigraphic continuity especially in the lower MSMR package and the MMS. Original stratigraphic relationships of major lithologic packages have nevertheless remained coherent. While this composite foliation is regarded as S_1 it is possible that it is the result of processes that continued throughout the evolution of the deformation.

The Ortega Group and upper MSMR package have been disrupted by layer-parallel shearing associated with S_1 along micaceous interbeds. Opposing shear directions were seen in thin sections of these interbeds and it was difficult to determine an overall shear direction. It is possible these less resistant interbeds may have accommodated shear in different directions during several of the deformational phases.

An S_2 foliation is present throughout most of the study area. It is best developed in all lithologies of the Ortega Group, the northern MMS, and the trondhjemite of Rio Brazos. This foliation is axial planar to the Jawbone syncline, Hopewell anticline, and small mesoscopic folds in the metavolcanics. Thin sections reveal that S_1 is crenulated into a spaced S_2 foliation which is sheared northward in the noses of some F_2 folds.

It is unclear why the S_2 foliation is not well developed in the more phyllitic

material of domains 3 and 4 (the lower MSMR and upper MMS). This could be the result of sporadically developed foliation or it could indicate that the foliations related to mylonitic shearing completely overprinted previous foliations in these domains and that this foliation is a late foliation.

An S_3 close-spaced fracture cleavage is present along Gavilan Creek. The sequential relationship between S_2 and S_3 foliations is speculative. The stereographic plot of poles to S_2 from Gavilan Creek seem to form a small circle which could be the result a slight reorientation of S_2 by D_3 .

Conjugate foliations have been documented throughout the Tusas Mountains (Smith, 1986; Williams, 1987), and the Needle Mountains, Colorado (Tewksbury, 1984). These foliations are poorly understood, but may be related to late stages of shearing in which two sets of foliations form more or less simultaneously (Mawer, 1987, personal communication; Tewksbury, 1987, personal communication).

Williams (1987) believes that deformation in the Tusas Mountains was a heterogenous progressive event that involved thin-skinned tectonic processes in which the Ortega Group was sheared and thrust northward over the MSMR and MMS. In the Brazos Box study area, both the MSMR and the Ortega Group have been moved over the MMS during D_1 by north-directed shear, although it is not possible to determine the amount of movement between the two units. Micaceous interbeds within the Ortega Group are strongly deformed and sheared. Asymmetrical quartz grains in these interbeds indicate contradicting shear senses, suggesting that these incompetent layers may have accommodated movement in different directions during different phases of the deformation. It is also not possible to determine the amount of movement or direction of movement which has occurred along micaceous interbeds in the Ortega Group.

The lowermost MSMR and the uppermost MMS rocks are phyllites which form one of the least competent zones in the Proterozoic section exposed in the study area. It is possible that flexure slip related to the formation of the Jawbone syncline may have continued north-directed shear in the north limb of the syncline along this incompetent contact zone.

TERTIARY STRUCTURES

The major structural features in the study area are illustrated in Figure 21. Three major north-west-striking fault zones pass through the southern part of the field area. The first is the southern splay of the Vallecitos fault (Doney, 1968). It probably follows Gavilan Creek and therefore offsets the limb between the Jawbone syncline and Hopewell anticline, although only minor brecciation is present. Movement on the fault was most likely down to the west. It is difficult to determine the amount of movement of this fault in the study area but the quartzite does not appear severely disrupted suggesting that movement has been minimal. Barker (1958) and Doney (1986) described 213-243 m (700-800 ft.) and 243-274 m (800-900 ft.) of offset on the Vallecitos fault in the Las Tablas and Cebolla quadrangles respectively.

The second fault zone consists of the Western Brazos Peak fault and the Hopewell fault (Muehlberger, 1968). The Hopewell fault is probably a continuation of the northern splay of the Vallecitos fault. Faults in this zone are normal with dominantly down-to-the-west offset. Four separate faults have accommodated 43 m (140 ft.) to 105 m (340 ft.) of displacement.

The third major fault zone contains both the East Brazos Peak fault and the Jawbone Mountain fault (Muehlberger, 1968). Field evidence for it was found only on the eastern rim of the Rio Brazos canyon. There the MMS is brecci-

ated and the Los Pinos Gravel is offset with springs along the offsets. It is unclear why no signs of faulting are evident along the canyon. One possibility is that movement was near vertical and therefore traces of it are obscured by the near vertical foliation. This is apparently a normal fault downthrown to the west. The amount of offset is difficult to determine.

North-east to north-west cross-faults lie between the Hopewell fault and the southern splay of the Vallecitos fault. These faults are normal with down-to-the-east offset of 36 m (120 ft.) to 67 m (220 ft.). They have the same sense of displacement as the cross-faults to the south-east in the Cebolla quadrangle (Doney, 1968).

Two minor north-west-trending faults are present in the central portion of the map area. Both are normal faults with down-to-the-east displacement. One fault truncates the MMS and the other truncates a trondhjemite body. Offset on these faults is difficult to determine.

A major north-east trending tectonized zone is present in the Ortega Group near the Bad Lands (Figure 21, Figure 30). In this zone brittle deformation is superimposed on the already ductily deformed Ortega Group vitreous quartzite. Although these rocks are extremely fractured, much of the bedding in the zone is slightly overturned to the south, suggesting that this unit may have acted as a block during deformation. The tectonized zone is apparently vertical and is truncated by the major north-west faults.

The three major north-west-trending fault zones form a north-west-trending horst and graben pair along the north side of the Rio Brazos. The tectonized zone that is superimposed on the lower portion of the Ortega Group vitreous quartzite is perpendicular to the graben along the Rio Brazos. The graben

FIGURE 30

Photograph of the tectonized zone in the Ortega Group vitreous quartzite. Looking NE along Rio Brazos. Beds are near vertical. Note the fisherman in the lower left for scale.

S₀/S₁

S₀/S₁



must be at least Tertiary in age because it has been a site of preferential accumulation of Tertiary flows and lahars, all of which presently form landslides.

Small normal faults which offset the Treasure Mountain rhyolite are common in the east-central portion of the map. Up to 6 m (20 ft.) of down-to-the-west displacement is evident on these faults.

Extremely straight river segments, sharp bends in the river channel and the overall rectilinear to parallel patterns of the Rio Brazos and its tributaries suggest that the drainage is fault-controlled. However, field evidence such as brecciation or offset was not found.

Barker (1958) and Doney (1968) believe that major faults such as the Brazos fault and the Vallecitos fault have changed the orientation of the Jawbone syncline and the Hopewell anticline from northeast to east-west and therefore may have been active in the Proterozoic. Muehlberger (1968) believes that movement on the major faults in the Brazos Peak quadrangle began in the Laramide with down-to-the-east offset and that a later reversal shifted movement to down-to-the-west. Similarities in structural orientations from all domains in the study area illustrate that there has been little disruption of the Proterozoic by Tertiary faults and that movement along faults must have been near-vertical.

The tectonized zone along the Rio Brazos is truncated by the northwest fault zones, therefore it is at least early Laramide in origin. Other minor faults in the map area are pre-Treasure Mountain and pre-Los Pinos.

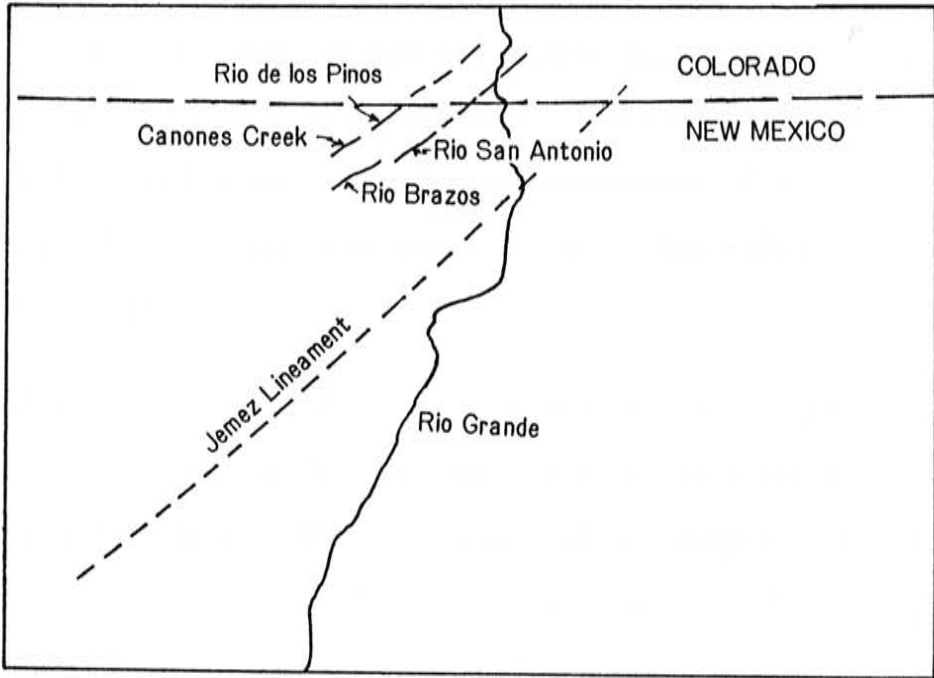
LINEAMENTS

Two major northeast trending lineaments are visible on the satellite mosaic

of New Mexico (Figure 31). They are formed by the Rio Brazos and the Rio San Antonio, and by the Canones Creek and Rio Los Pinos canyons. These lineaments extend northeast into the San Luis Valley. Because they are sub-parallel to the Jemez Lineament, they probably reflect control by major, deep basement structures.

FIGURE 31

Satellite mosaic of northern New Mexico showing the general relationships of lineaments cutting the Tusas uplift to the Jemez lineament. Dashed line in the upper portion of the photograph is the Colorado-New Mexico boundary. River names indicate the approximate location of the canyons they flow in.



METAMORPHISM

REGIONAL METAMORPHISM

Regional metamorphism present throughout the Tusas Mountains increases from greenschist facies in the northwest to amphibolite facies in the southeast (Barker, 1958; Bingler, 1968; Grambling and Williams, 1985). The only contact effects from the intrusion of the trondhjemite of Rio Brazos are thin zones of contamination; no metamorphic aureoles were found.

The MMS and the MSMR are best suited for determination of metamorphic grade because of their variable mineral composition. The limited mineralogy in the Ortega Group inhibits precise metamorphic classification. Figure 32 lists the paragenesis of each lithostratigraphic unit in the field area.

Mineral assemblages from units in the upper Brazos Box area conform to the low-grade metamorphic category as defined by Winkler (1979). Minerals diagnostic of the low-grade metamorphic category include zoisite/clinozoisite/epidote and albite, as well as prograde chlorite and actinolite. This category includes greenschist assemblages that evolved from both mafic volcanics and quartz-rich sediments. Assemblages characteristic of the quartzite and metaconglomerates have more quartz and muscovite, less chlorite, albite, and epidote, and no actinolite.

The dominant assemblage of the Ortega Group is quartz + muscovite + /- chlorite + /- sphene; and the dominant assemblage of the MMS is chlorite + zoisite/clinozoisite + /- actinolite + /- quartz. These paragenetic assemblages are indicative of both the low-grade metamorphic category defined by Winkler (1979) and the chlorite zone of the greenschist facies summarized by Turner (1980). Rock types from the MMS that fit into these metamorphic categories

FIGURE 32

Metamorphic paragenesis of lithostratigraphic units in the Upper Brazos Box study area.

METAMORPHIC PARAGENESIS FOR THE UPPER BRAZOS BOX AREA

ORTEGA GROUP

quartz-muscovite-magnetite-zircon +/- hematite +/- chlorite
+/- rutile +/- sphene (+/- almandine)

METASEDIMENTARY AND METAVOLCANIC PACKAGE

quartz-muscovite-albite/oligoclase-magnetite-chlorite +/-
carbonate +/- zircon +/- hematite +/- almandine
+/- rutile +/- sphene

MOPPIN METAVOLCANIC SERIES

MAFIC ROCKS

chlorite-quartz-albite/oligoclase-muscovite-magnetite-carbonate
+/- biotite +/- epidote/clinozoisite +/- hematite +/- rutile

actinolite-quartz-albite/oligoclase-chlorite-epidote/clinozoisite
+/- biotite +/- muscovite +/- magnetite +/- hematite +/-
ilmenite +/- sphene

FELSIC ROCKS

quartz-albite/oligoclase-chlorite-muscovite +/- K-feldspar
+/- biotite +/- epidote +/- magnetite +/- hematite +/-
rutile

TRONDHJEMITE

quartz-albite/oligoclase-k-feldspar-biotite-muscovite +/-
epidote/clinozoisite +/- magnetite +/- hematite +/- zircon
+/- carbonate

HORNBLENDITE

hornblende-oligoclase/andesine-epidote/clinozoisite-quartz +/- lucoxene

are amphibolite schists, quartz-chlorite schists, chlorite-plagioclase schists, and muscovite-quartz schists. Minerals which are characteristic of the chlorite zone, such as calcite, rutile, magnetite, and hematite are also present, although they are mostly described in pelitic rocks (Turner, 1980). Epidote pseudomorphs of chloritoid are present in the plagioclase-quartz schist (Grambling, 1988, personal communication). It is unclear why chloritoid would alter to epidote.

Several samples from the MMS quartz-chlorite schist and the plagioclase-chlorite schist contain what is interpreted to be prograde biotite. These samples fall into the biotite zone of the greenschist facies (Turner, 1980). Sphene, magnetite and calcite, which are described as related to the biotite zone also are present in some of these MMS rocks.

Albite and oligoclase co-exist in several samples from the MSMR and the MMS. Garnet thought to be almandine is present from the mylonitic zone in the MSMR to the lowermost Ortega Group. The almandine is very small (0.4×0.1 mm) and strongly deformed. Almandine is present only in the sedimentary units and is metamorphic (Williams, 1988, personal communication). These minerals indicate that the MSMR and portions of the MMS reached the greenschist-amphibolite transitional facies (Turner, 1980).

Hornblendite exposed near the Carson National Forest gate contains hornblende and probably actinolite or actinolitic hornblende. The identification of plagioclase was difficult in this sample due to the extent of alteration, but it appears as if both oligoclase and andesine are present. The presence of hornblende and andesine indicate that the hornblendite has reached at most the lower portion of the amphibolite facies (Turner, 1980).

Plagioclase compositions range from An_{3-18} with three samples having

compositions from An_{26-50} . The presence of plagioclase compositions within the peristerite gap could result from: a less than microscopic unmixing of these phases, or relatively low pressures of formation. While the peristerite solvus is poorly constrained it is known to be pressure dependent with lower pressures causing a lower solvus (Maruyama et al., 1982).

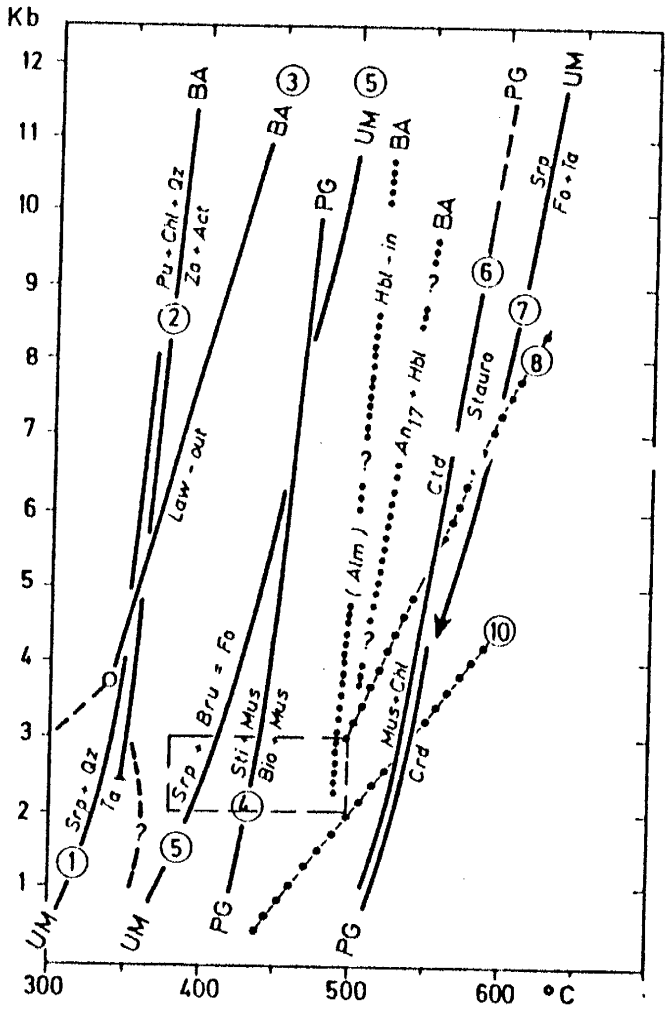
The upper conditions of metamorphism (Figure 33) can be loosely constrained by the presence of hornblende and andesine, and garnet. The poorly constrained peristerite solvus, suggests that pressures and temperatures should be less than 3-4 kb at 450 °C. The lower limit of metamorphism is defined by the presence of zoisite/clinozoisite and absence of lawsonite. Many mineral assemblages from the study area may be classified in the chlorite zone and biotite zone of the Barrovian type, which is a medium pressure metamorphism. These rocks also fit into the chlorite zone of the Abukuma type, which is a low pressure metamorphism (Miyashiro, 1975). Therefore pressures in the study area range from low to medium. Smith (1980) estimated 3 kb and 430 °C in the nearby Jawbone Mountain area. Grambling et al. (1988) report that metamorphic conditions reached 2-3 kb and 380-470 °C in the northern Tusas Mountains, and 4 kb and 480-500 °C in the central Tusas Mountains.

The distribution of metamorphic facies in the upper Brazos Box area is such that the highest grade, the amphibolite facies, is present near the Carson National Forest gate. The the greenschist-amphibolite transitional facies is present throughout the central and northern portion of the field area and includes rocks from the MMS and the trondhjemite. The chlorite zone of the greenschist facies is present in southern part of the field area and includes the Ortega Group and parts of the MMS. It is possible that the Ortega Group experienced higher metamorphic conditions, but does not contain the mineral assemblage in the

FIGURE 33

Low-grade metamorphic pressure-temperature diagram showing equilibria curves for index minerals from Winkler, 1979. Outlined area is generalized pressure-temperature range for the Upper Brazos Box study area.

Low - Grade



study area necessary to characterize it clearly. The presence of almandine may be related to the tectonized contact between the MMS and the MSMR, because almandine was only found from the mylonitic zone in the MSMR package to the lowermost Ortega Group.

A quartz-chlorite schist in the eastern portion of the field area contains nearly idioblastic actinolite that has overgrown a spaced S_2 cleavage. These relationships suggest that metamorphism peaked after the second phase of deformation. All almandine present is highly stained and sheared, suggesting that shearing related to the mylonitic zone continued after the peak of metamorphism.

Clay (kaolinite ?), present only in the brecciated vitreous quartzite of the Ortega Group, is the result of weathering in a fractured zone and is not related to the metamorphic paragenesis.

SPILLITIZATION

It is probable that rocks from the MMS were influenced by spillitization; and were keratophyers or spillites at one time. Reasons for this assumption are: the known marine origin of some of the rocks, especially the subalkaline basalts and basaltic andesites; and the association of albite-oligoclase and chlorite, which is typical of spillites. Some authors (Amstutz, 1974; Fiala, 1974; Turner, 1982) include epidote, zoisite, fibrous amphibole, sphene, and lucoxene in the spillite assemblage, as well as the association of Fe and Ti ore deposits. These minerals are typical of the Moppin Metavolcanics and iron deposits are present in MMS rocks at Iron Mountain.

Upper Brazos Box samples were evaluated for spillitization using the chemical criteria established by Fiala (1974): 1) $> 4\% \text{Na}_2\text{O}$; 2) $> 2\% \text{CaO}/\text{Na}_2\text{O} +$

K₂O; 3) 0.01-0.31% K₂O; and 4) high H₂O. Some, but not all of these criteria are met by the subalkaline basalts and basaltic andesites in the MMS. This indicates that spillitization effects have been altered by regional metamorphism. Turner (1982) suggests that fibrous actinolite replacing original pyroxenes, which is common in the MMS, indicates that "real" metamorphism has effected the rocks. Consistency in the distribution of metamorphic assemblages in different rock packages throughout the Tusas Mountains also indicate that metamorphism has overprinted any spillitization that may have occurred.

GEOCHEMISTRY

METHODS

Thirty-one samples were analyzed using an x-ray fluorescence spectrometer at the New Mexico Bureau of Mines and Mineral Resources. Samples include a representative of every member of the MMS, the Burned Mountain metarhyolite, the mylonitic zone in the MSMR package, the trondhjemite of Rio Brazos, and a dike which intrudes the trondhjemite. Most samples analyzed were also examined in thin section. Appendix 2 provides a more detailed description of the analytical techniques, precision, accuracy, and results obtained.

ALTERATION

Most Proterozoic rocks analyzed from the Brazos Box uplift have been metamorphosed to the upper greenschist facies, some rocks have reached the greenschist-amphibolite transitional facies. In addition, silicification is ubiquitous and carbonization is common. Also, spillitization probably affected the volcanic rocks during and shortly after deposition. These processes can remove and add both major and minor elements, therefore alteration effects must be considered when evaluating a protolith. High field strength elements are considered by most workers to be immobile during hydrothermal alteration and metamorphism (Pearce 1974, 1975; Winchester and Floyd, 1977). Although Pearce (1974) pointed out that slight amounts of Ti may be added during submarine alteration, and it is possible that Nb is mobilized by high fluorine fluids (Norman and Walder, 1987, personal communication). For these reasons emphasis is placed on rock classification and discrimination diagrams based on high field strength elements.

CLASSIFICATION DIAGRAMS

The classification diagrams used here are presented in Figures 34 to 36, and include the Jensen Cation, Zr/TiO₂-Nb/Y, and An-Ab-Or diagrams. Samples plotted on the Jensen Cation diagram (Jensen, 1976)(Figure 34) display a continuous series from rhyolite to tholeiitic basalt. Felsic rocks plot mostly in the calc-alkaline field, whereas intermediate to mafic rocks are uniformly distributed between calc-alkaline and tholeiitic types.

On the Zr/ TiO₂ vs Nb/Y plot (Figure 35) from Floyd and Winchester (1978) Moppin Metavolcanics samples range from sub-alkaline basalt to rhyolites. The Burned Mountain metarhyolite plots in the rhyolite field. Because Zr, Ti, Nb, and Y are considered to be immobile trace elements the Zr/TiO₂ vs Nb/Y diagram will be used to identify protoliths of the rocks in this study.

The trondhjemite of Rio Brazos plots in the trondhjemite field of the An-Ab-Or diagram (Figure 36) revised by Barker (1979). The results of analyses of the trondhjemite are consistent with those analyzed by Barker (1976).

TECTONIC DISCRIMINATION DIAGRAMS

Mafic samples from the MMS are plotted on tectonic discrimination diagrams in Figures 37 to 39. On the Ti-Cr diagram (Pearce, 1975) most samples fall within or near the island arc tholeiite field (Figure 37). Two anomalous amphibole schists plot in the ocean floor basalt field near the island arc tholeiite field.

Samples plotted on the Ti-Zr-Y diagram (Pearce and Cann, 1973) fall mostly within fields B and C, although there is considerable scatter in the analyses (Figure 38). A problem with this plot is that fields B and C do not distinguish

FIGURE 34

Jensen cation plot (1976) showing samples from the MMS and Burned Mountain metarhyolite. Symbols presented here are used throughout the geochemistry section. Open symbols represent samples with $>4\%$ LOI.

FeO + Fe₂O₃ + TiO₂

MgO

Al₂O₃

PROTOLITH

- ◆ Metasedimentary (volcanic origin)
- ▲ Metavolcaniclastic
- Plutonic - Hypabyssal
- Dike
- Unknown
- > 4% LOI

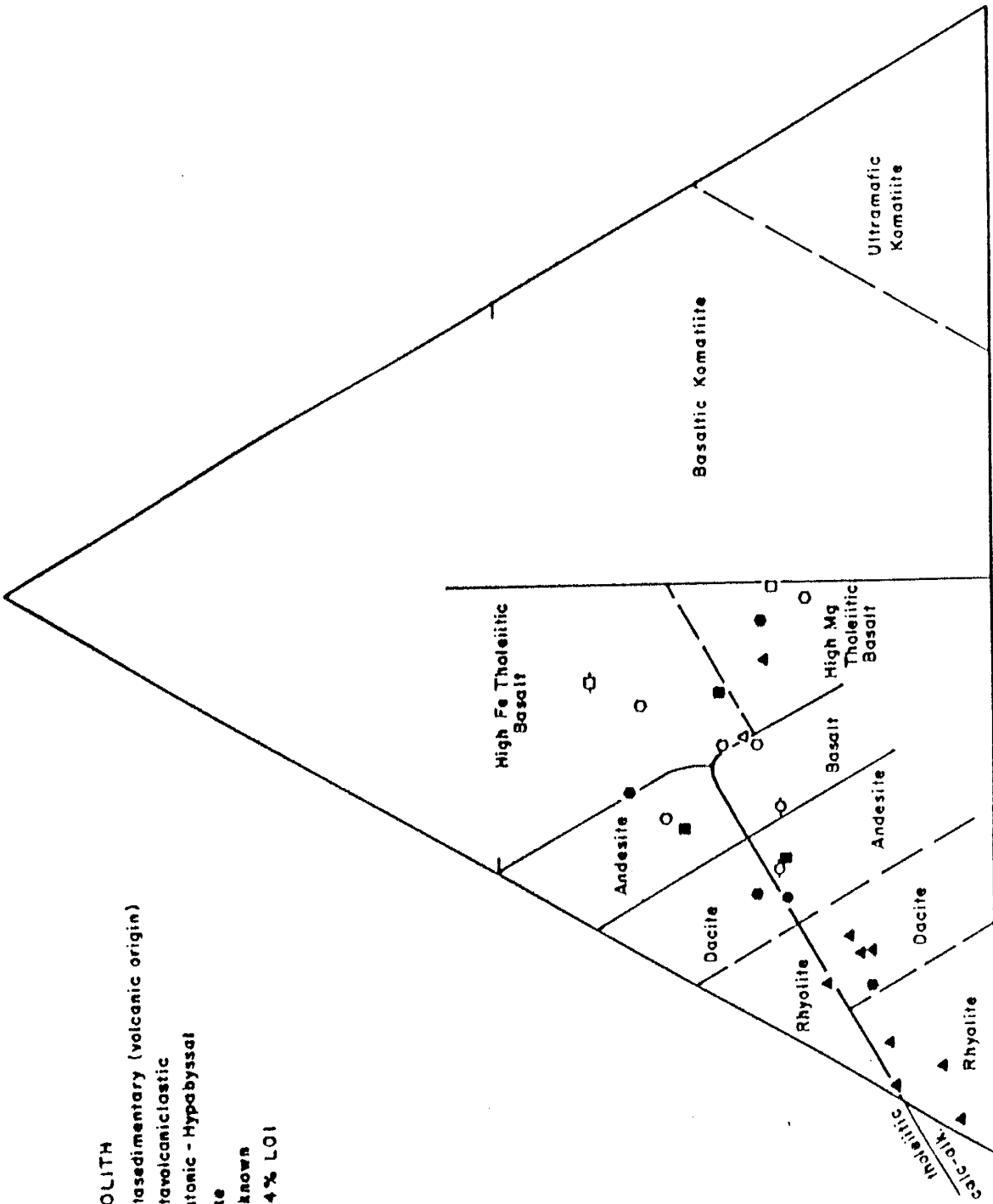


FIGURE 35

Zr/TiO₂ vs Nb/Y plot of samples from the MMS and Burned Mountain metarhyolite (Floyd and Winchester, 1978). Triangles with bars under them represent the Burned Mountain metarhyolite.

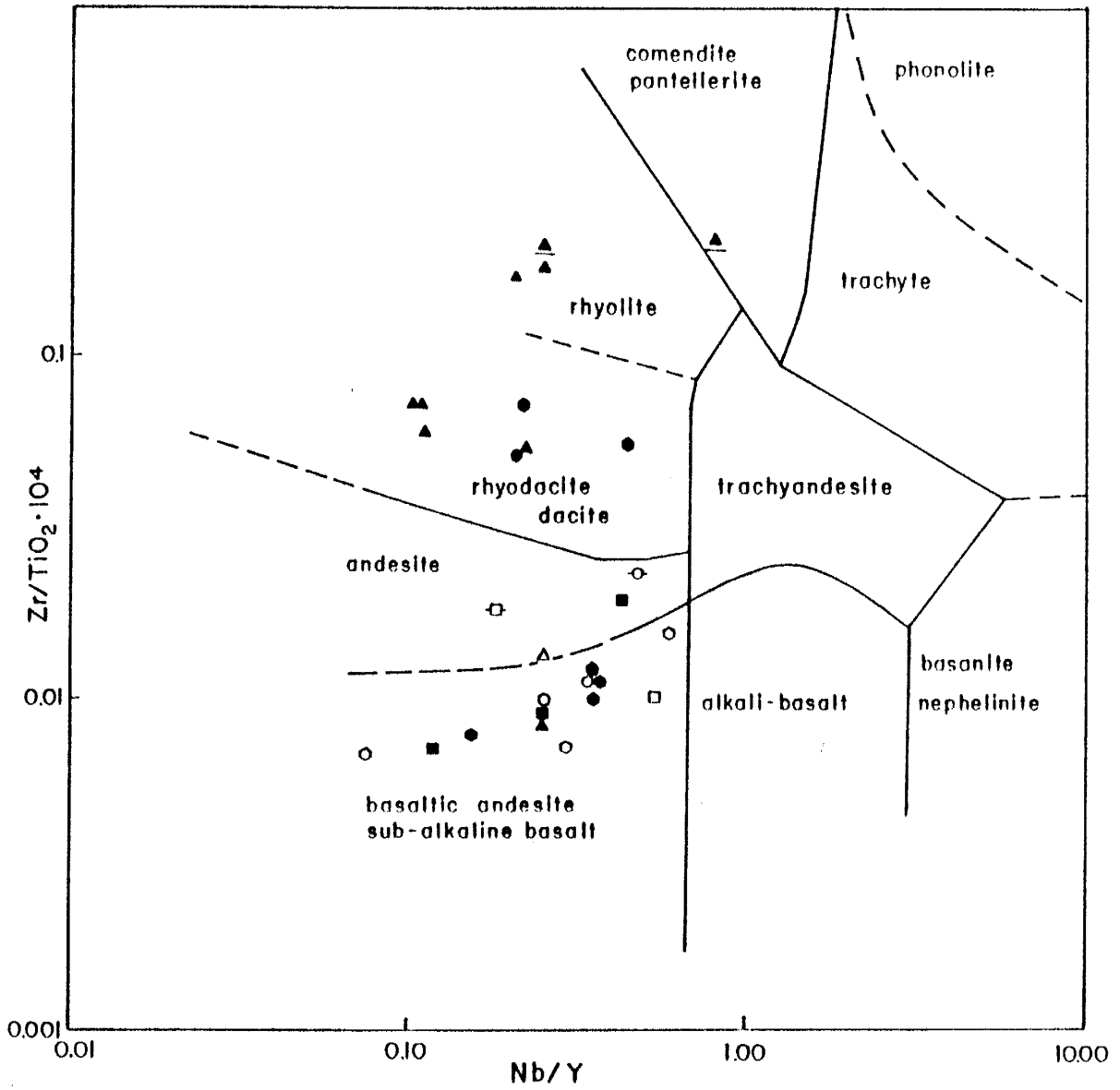


FIGURE 36

Samples of the trondhjemite of Rio Brazos plotted on the An-Ab-Or diagram (Barker, 1979). Black squares are samples from this study, squares with a diagonal through them are from Barker, 1979.

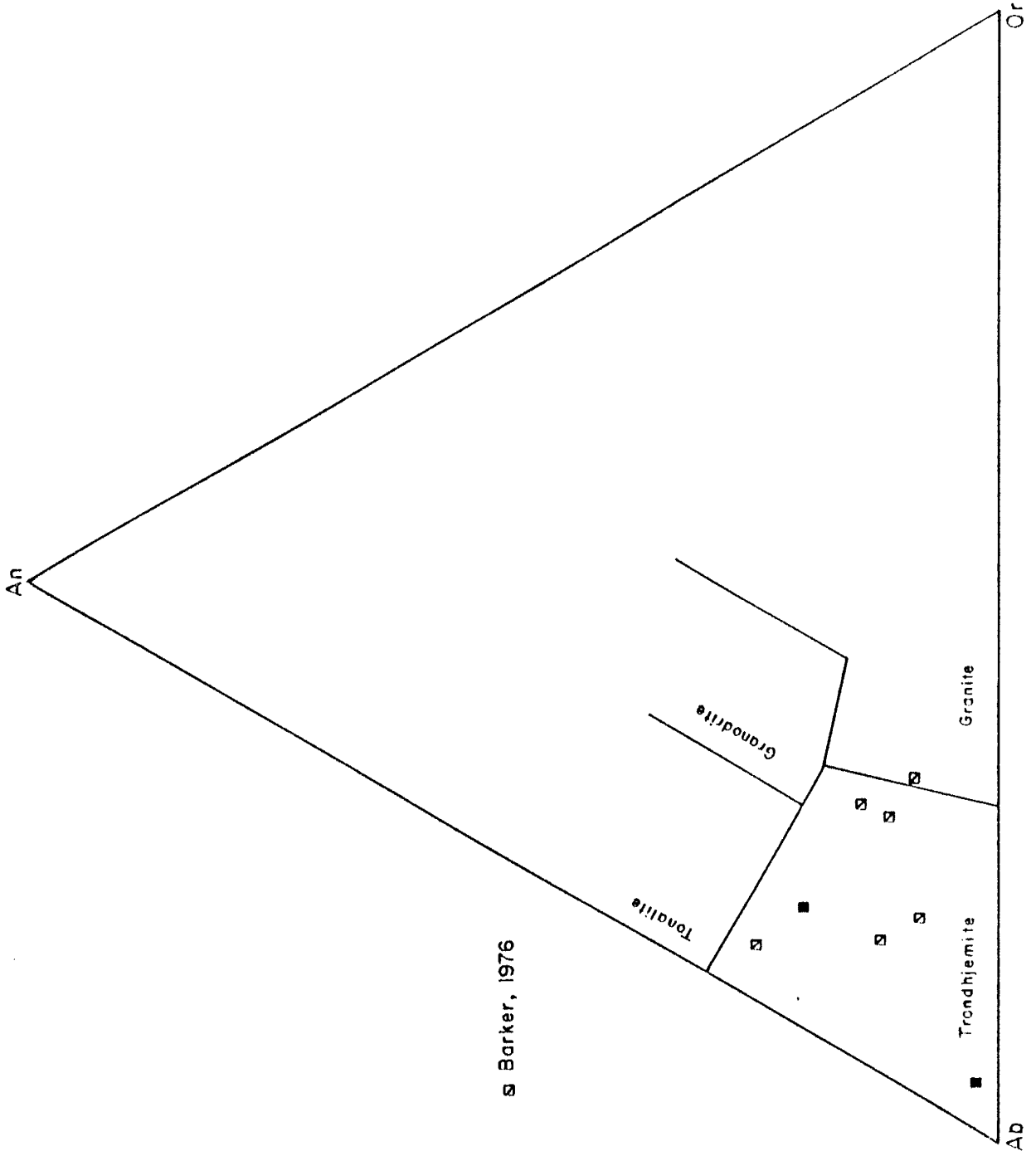


FIGURE 37

Mafic samples from the MMS are plotted on the Ti vs Cr diagram from Pearce, 1975. IAT indicates the island arc tholeiite field and OFB indicates the ocean floor basalt field.

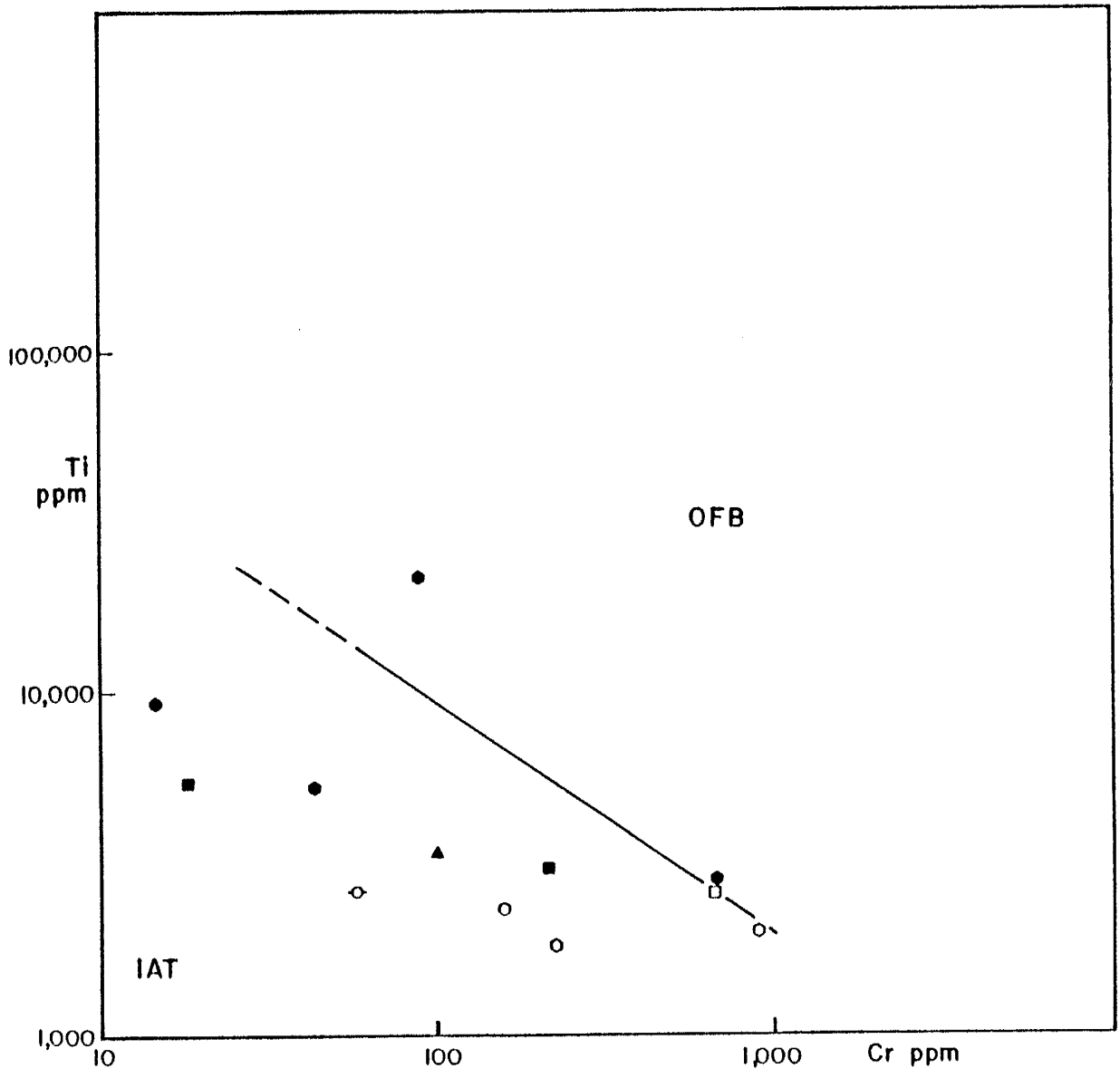


FIGURE 38

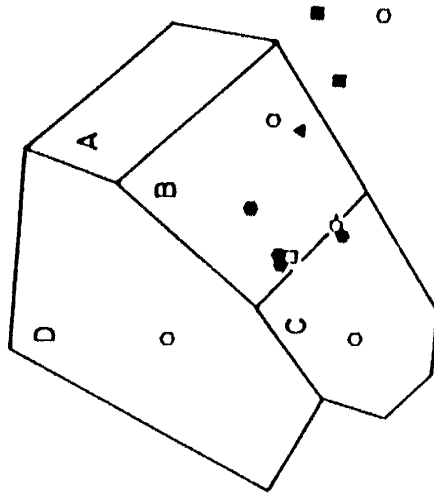
Mafic samples from the MMS plotted on the Ti-Zr-Y diagram from Pearce and Cann, 1973.

Ti/100

Y x 3

Zr

- A low K tholeiites
- B low K tholeiites
ocean floor basalts
- C calc-alkali basalts
- D within plate basalts



between low K-tholeiites, ocean floor basalts, or calc-alkali basalts.

On the Ti-Zr plot from Pearce and Cann (1973) mafic MMS samples plot in or near the low K-tholeiite field and on the Ti/1000 vs Zr diagram from Garcia (1978) the majority of samples plot as island arc tholeiites (Figure 39). An amphibole schist and an epidote-plagioclase schist plot in or near the ocean floor basalt field in both diagrams. Mafic samples from the Hopewell Lake area (Boadi, 1986) and the Jawbone Mountain area (Smith, 1986) plot in the calc-alkali basalt field and near the boundary between the calc-alkali basalt-low-K tholeiite field. This discrepancy between chemical analyses could be the result of sampling, or alteration of the rocks, or it could represent increased fractionation of material in the arc. The data from all three study areas falls on the volcanic arc trend described by Garcia (1978), suggesting that it may represent the evolution of an arc. Ti and Zr do not discriminate between island arcs or a continental margin arcs.

The anomalous samples in field D on the Ti-Zr-Y diagram (Figure 38) and in the ocean floor basalt fields on the Ti-Zr diagrams (Figure 39) contain high amounts of sphene and magnetite which accounts for their high Ti content.

Rocks of granitic composition are plotted on the Nb vs Y discrimination diagram (Pearce et al., 1984) in Figure 40. Rhyolites from the MMS and the trondhjemite of Rio Brazos plot in the volcanic arc and syn-collisional field. Whereas, Burned Mountain metarhyolite samples from this study, as well as from Boadi (1976) and Smith (1976), plot in the within-plate field. An exception is the metarhyolite sample that plots in the ocean ridge field near the within-plate field.

FIGURE 39

Mafic samples from the MMS plotted on: A) the Ti vs Zr diagram from Pearce and Cann, 1973 and B) the Ti vs Zr diagram from Garcia 1978. Samples indicated by crosses are from Boadi (1986) and those indicated by the asterisk are from Smith (1986). OFB indicates the ocean floor basalt field, CAB indicates the calc-alkaline basalt field, and IAT indicates the island arc field.

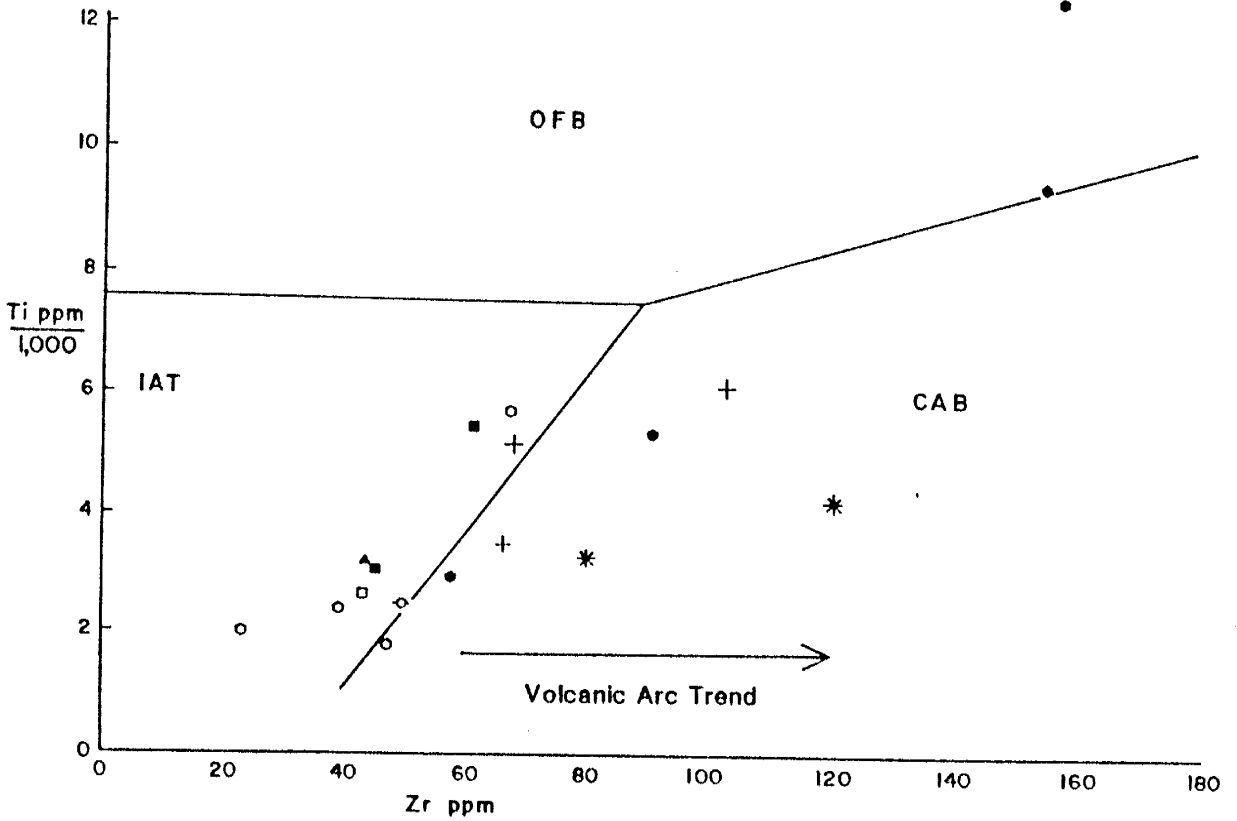
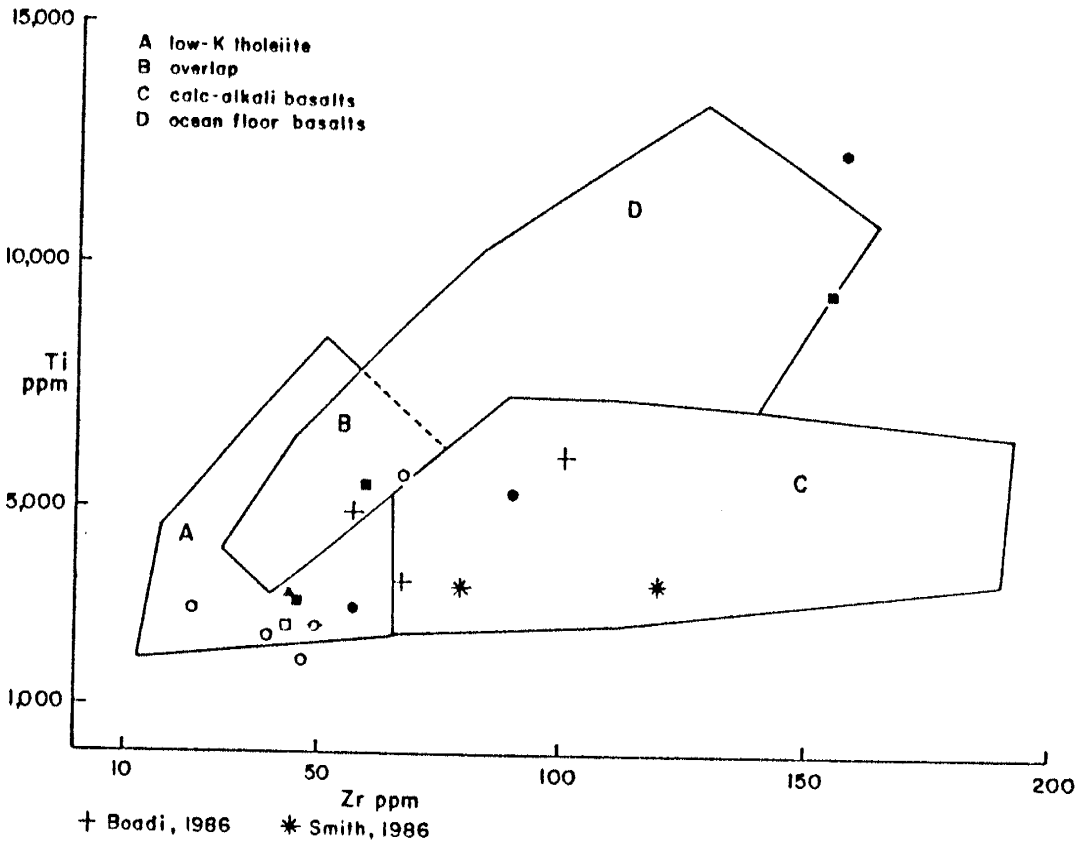
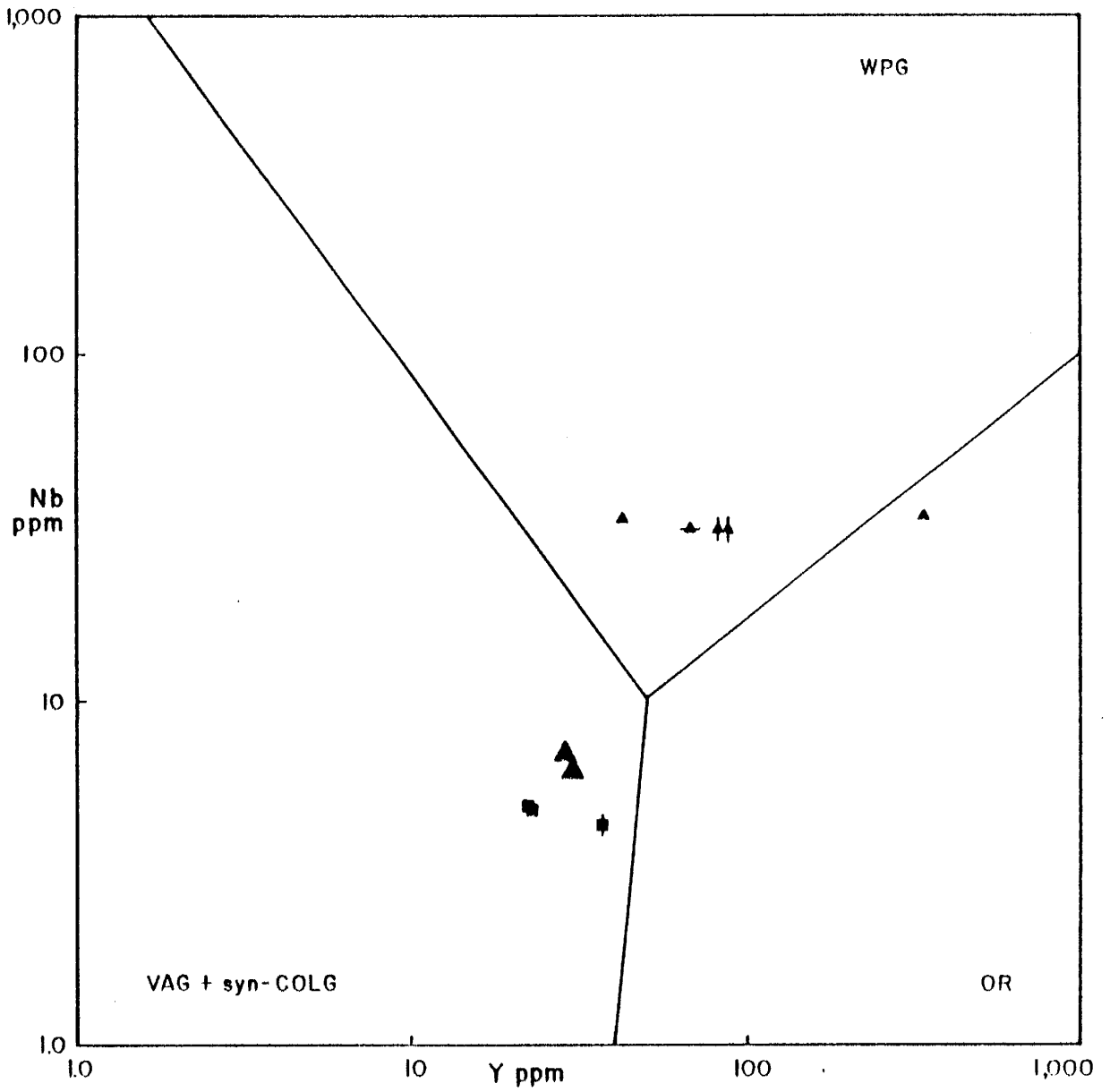


FIGURE 40

Felsic samples plotted on the Nb vs Y diagram from Pearce et al., 1984. Large triangles represent felsic volcanics (metarhyolites) from the MMS, small triangles represent the Burned Mountain metarhyolite, and boxes represent the trondhjemite of Rio Brazos. VAG + Syn COLG indicates the volcanic arc granite and syn-collisional field, WPG indicates the within plate field, ORG indicates the ocean ridge granite.



▲ BMR - Boadi, 1986 ♣ BMR - Smith, 1986 ◆ Barker, 1976

DISCUSSION

DEPOSITIONAL AND TECTONIC SETTING(S) OF THE NORTH TUSAS PRECAMBRIAN

Proterozoic supracrustal rocks in the Tusas Mountains make up distinctive lithostratigraphic packages that are significantly different from one another in terms of lithology, age, and chemistry. For this reason, possible depositional and tectonic environments are considered separately for each package.

Moppin Metavolcanics

Relict textures common in the MMS mafic units include: pillows, amygdules, brecciated flow tops, and graded beds. The proximity of graded beds to pillowed and vesiculated units suggest that volcanism and sedimentation (turbidites ?) were contemporaneous processes, and were for the most part subaqueous.

Relict flow bands and primary volcanic breccias are common in felsic MMS rocks. Rhyolites and rhyodacites are present in the exposed lower portion of the MMS section.

Geochemically the MMS ranges from rhyolite to basalt. Andesites also have been described elsewhere in the Tusas Mountains (Gibson, 1980; Kent, 1981; Boadi, 1986; Smith, 1986). Mafic rocks from the upper Brazos Box study area plot mostly as island arc tholeiites on the Ti vs. Zr diagram from Garcia (1978) and as low-K tholeiites on the Ti vs. Zr diagram from Pearce and Cann (1973) (Figure 39) suggesting that the MMS may have been deposited in an arc setting. However, mafic Moppin Metavolcanic samples from the Jawbone Mountain area (Smith, 1986) and the Hopewell Lake area (Boadi, 1986) plot

mostly as calc-alkaline basalts. At present, it is not known why mafic samples from the adjacent study areas have different geochemical signatures. Differences may be due in part to variably alteration, or may reflect geochemical variation in the original rocks. The MMS mafic samples fall on the volcanic arc trend indicated on the Ti vs Zr plot from Garcia (1978), so it is possible that the MMS arc may have evolved in time and/or space from tholeiitic to calc-alkaline. Felsic volcanic rocks from the MMS plot in the arc syn-collision field of the tectonic discrimination diagram of Pearce et al. (1984), supporting an arc model for the deposition of the MMS.

The MMS may have been deposited in an island arc, or continental margin arc. Characteristics of each arc environment outlined by Carey and Sigurdsson (1984), Pearce (1986), and Wessel (1986) were evaluated to determine which arc setting the MMS was most likely deposited in. The lack of continentally derived sediments suggests that the arc was not located on a continental margin. Pillows, pyroclastics, turbidites, basalts, andesites, and felsic plutons are found in both island and continental margin arcs, although tholeiitic basalts and pillows are more common in island arcs. Continental margin arcs ideally have a greater compositional range of volcanic material (alkali basalt to andesite to rhyodacite to rhyolite) than island arcs. Although the MMS section contains rhyodacites and rhyolites, there is at least one modern example of an island arc (Fiji) with a full compositional range of volcanics (Gill, 1988) Therefore, the wide compositional range of volcanic material present in the MMS section does not rule out an island arc environment. Barker (1976) states that trondhjemite of Rio Brazos is similar chemically to a tonalite at Fiji and a dacite at Saipan, which are both modern island arcs. On a chondrite-normalized rare-earth element diagram the trondhjemite of Rio Brazos has a mildly-fractionated, relatively-flat pattern with a strong negative Eu anomaly, which Barker (1979)

suggests is broadly similar to island arc plutons.

The MMS arc was probably not a continental or subaqueous back arc because there are no recognized pelagic, fresh water, and/or continentally derived sediments. Garcia (1978) and Carey and Sigurdsson (1984) describe oceanic back arcs as containing <10% fragmental volcanic material. The MMS section contains approximately 50% fragmental material further suggesting that it was not deposited in an evolved oceanic back arc. Although turbidites may be present in the field area, other gravity flows such as slumps and debris flows, which would be associated with an incipient rift (Carey and Sigurdsson, 1984), are not recognized, also suggesting that the MMS was not an intra-arc basin or a back arc basin in the initial stages of formation.

In summary, the Moppin Metavolcanics was deposited as felsic to mafic volcanics intercalated with volcanoclastics in an arc environment, most likely an island arc because: 1) mafic rocks in the MMS are mostly sub-alkaline tholeiites with an arc geochemical signature; 2) textures such as pillows and pyroclastics are present which are associated with subaqueous island arcs; 3) there are no known continentally derived sediments in the MMS section which would argue against a continental margin arc; 4) the MMS section does not contain any pelagic sediments which would argue against an evolved oceanic back arc basin; 5) the geochemistry of the trondjemite of Rio Brazos is broadly similar geochemically to plutons in modern island arcs.

Metasedimentary and Metarhyolite Package

Silver (in Reed et al., 1987) obtained a U-Pb zircon date of 1,700 Ma for the Burned Mountain metarhyolite.

The Burned Mountain metarhyolite was most likely erupted as an ash flow

tuff. Evidence for this origin includes relict eutaxitic textures and related features reminiscent of welding, the great areal extent of exposures, zones of unsorted broken crystals, and lithic fragments. Metarhyolite outcrops range from 30-100 m thick and extend up to 20 km in length (Barker, 1958; Doney, 1978; Gibson, 1981; Smith, 1986).

The exact depositional setting for the Burned Mountain metarhyolite in the north Tusas Mountains is not clear. Kent (1980) and Smith (1986) concluded that the Burned Mountain metarhyolite was erupted subaerially because there are no marine sediments immediately adjacent to the Burned Mountain metarhyolite in either of their study areas in the Tusas Mountains. Boadi (1986) states that a marine incursion may have been responsible for the immature sediments intercalated with the metarhyolite in the Hopewell Lake area. In the upper Brazos Box study area it cannot be determined conclusively whether the Burned Mountain metarhyolite was deposited subaerially or subaqueously. The poorly sorted metaconglomerate beneath and above the metarhyolite was deposited in a fluvial or near-shore marine environment. Gradation upsection into marine sediments over a very short interval indicates that the depositional environment was near shore, regardless of whether it was marine or subaerial. Subaqueous deposition of the Burned Mountain metarhyolite is the favored model due to the close proximity of the marine sediments to the metarhyolite. The poorly sorted, immature nature of the metaconglomerate surrounding the metarhyolite is consistent with deposition in an extensional setting.

Trace element geochemistry from the Burned Mountain metarhyolite is similar to that of modern felsic volcanics from continental rift systems or back arc basins in or near continents (Condie, 1986; Robertson, 1988, personal com-

munication). The Burned Mountain metarhyolite plots in the within-plate fields on the Nd vs. Y (Figure 40) and the Ta vs. Yb diagrams of Pearce et al. (1984), and in the extensional fields on the La/Yb vs. Yb and the Hf vs. Zr discrimination diagrams from Condie (1986) (Robertson, 1988, personal communication). The Burned Mountain metarhyolite is also chemically similar to the Skaergaard granite which is associated with attenuated crust (Pearce et al., 1984).

In summary, the geochemical signature of the Burned Mountain metarhyolite and the poorly sorted metaconglomerates associated with it suggest that the tectonic environment may have been extensional during the deposition of the lower MSMR package. Gradation of the poorly sorted metaconglomerate at the base of the MSMR package into marine quartzites in the upper portion of the unit reflects the subsequent stabilization of this setting and onset of a marine transgression.

Ortega Group

The Ortega Group exposed in the study area is a maturing-upward quartzite sequence that begins with a basal transitional quartzite and evolves upsection into a clean vitreous quartzite. Soegaard and Eriksson (1985) examined sedimentary features in the Ortega Group of the Jawbone Mountain area and concluded that these features were formed by tide, wave, and storm processes on a shallow shelf, under about 3-4 m of water. They recognized pebble beds as lag deposits winnowed by storms. Using paleocurrent indicators Soegaard and Eriksson were able to determine that the shallow shelf on which the Ortega was deposited sloped southward and received sediments from the north.

A significant amount of felsic continental mass must have existed to supply

the quartz necessary for an approximately 1 km thick section of quartzite to have been deposited. Also, basin subsidence must have kept pace with sedimentation to maintain the same depositional environment during time it took the quartzite to be deposited (Smith, 1986).

In summary, the Ortega Group was deposited on a relatively stable, but slowly subsiding shallow continental shelf.

Trondhjemite of Rio Brazos

The trondhjemite of Rio Brazos is clearly intrusive into the MMS and may possibly be syntectonic. Barker (1974) obtained a Rb-Sr whole-rock isochron of $1,654 \pm 23$ Ma from the trondhjemite, although it is unclear whether this is a crystallization age or a metamorphic age. Low $^{87}\text{Sr}/^{86}\text{Sr}$ ratios of 0.7032 suggest that the trondhjemite evolved by fractional crystallization or partial melting of a mafic to ultramafic source. Barker (1976) prefers a fractional crystallization model because $\delta^{18}\text{O}$ values of 2.9 and 4.0 from an adjacent hornblendite are similar to the trondhjemite and therefore suggest that the hornblendite could be a cumulate derived from the trondhjemite. Boadi (1988, personal communication) indicates that the granite of Hopewell Lake may be a trondhjemite which could be related to the trondhjemite of Rio Brazos. The $^{87}\text{Sr}/^{86}\text{Sr}$ ratio of 0.7026 from the granite of Hopewell Lake is similar to that of the trondhjemite of Rio Brazos.

On a tectonic discrimination diagram from Pearce et al. (1984), the trondhjemite plots in the volcanic arc and syn-collision field. Barker (1976, 1979) summarizes the occurrences of trondhjemites relevant to the Proterozoic, but also in the Phanerozoic; trondhjemites are found along active continental margins and in subvolcanic portions of island arcs, where they form as a result of

subduction or back-arc spreading. Because the MMS which the trondhjemite intrudes is dominantly a low-K tholeiite, the trondhjemite in the Rio Brazos area is most likely related to the subvolcanic region of an arc. Barker (1976) compares the trondhjemite of Rio Brazos to similar low- Al_2O_3 types of felsic plutons such as the dacite of Saipan and the tonalite of Fiji which are located in island arc settings. On a chondrite-normalized rare-earth element diagram the trondhjemite of Rio Brazos has a mildly fractionated, relatively flat signature with a large negative Eu anomaly which is similar to an island arc signature (Barker, 1979). Lack of ophiolites, melanges, and other rocks related to subduction imply that subduction may not have taken place in the immediate area and that the trondhjemite formed as a melt at the base of a thick pile of volcanic material (Barker, 1976).

The trondhjemite probably intruded the subvolcanic region of an arc as it is present only in the lower exposed portion of the MMS section. The trondhjemite may be syntectonic because it contains only one identifiable foliation while the surrounding MMS rocks contain two foliations, and it is geochemically similar to plutons from arcs and syn-collisional tectonic settings. If the trondhjemite intruded after the formation of the MMS arc, it could have inherited the syn-collisional and island arc signature from the MMS.

EVOLUTION OF SETTINGS IN THE NORTH TUSAS MOUNTAINS

Moppin Metavolcanic rocks formed in an arc, probably an island arc, independent of continental crust, while both the MSMR and Ortega Group required continental crust to form. There are at least three ways to explain the relationship of the MMS to the MSMR and the Ortega Group in the north Tusas Mountains: 1) the MMS arc was an island arc that was accreted to a continental mass before ca. 1,700 Ma, the time of the Burned Mountain metarhy-

olite eruption, subsequent extensional and then stable shelf settings prevailed, both upon an MMS basement; 2) the MMS arc was a continental margin arc, whose tectonic regime changed from compressional to extensional during the time interval in which the Burned Mountain metarhyolite and associated immature conglomerates were accumulated; Ortega Group rocks were then deposited on the MSMR; 3) the MMS and the combined MSMR- Ortega Groups formed in geographically separate tectonic (and depositional) settings and were later tectonically assembled, probably during the D_1 deformational phase.

Contact relationships between the MMS and the MSMR have been obscured by deformation, therefore it is difficult to determine the exact nature of the relationship between these units. The MSMR was probably deposited directly on the MMS because the former contains pebbles that are lithologically similar to the underlying MMS (Gibson, 1981; Boadi, 1986; Smith, 1986). The poorly sorted MSMR conglomerate was most likely deposited in an extensional environment because the metaconglomerate is poorly sorted and relatively immature, and the chemical signature of the Burned Mountain metarhyolite is extensional. The gradation from immature, poorly sorted sediments of the MSMR package into vitreous quartzite of the Ortega Group suggests the tectonic environment changed from an extensional to a relatively stable continental shelf undergoing a marine transgression.

The exact timing and mechanics of terrane assemblage or change of tectonic and depositional settings required by the various scenarios discussed is poorly understood. The youngest supracrustal unit present, the Ortega Group, contains the oldest tectonite fabric recognized in the north Tusas. Therefore, if any earlier fabrics developed during the accretion of the MMS to an older, pre-existing continental mass or the rifting of the arc, they have been completely

obliterated, or developed in discrete zones not currently exposed. Fabrics present in the mylonitic zone at the base of the MSMR package are associated with the earliest recognized deformational event and record north-directed transport of the MSMR and the Ortega Group over the MMS. It is impossible to determine the extent of movement along this ductile fault zone or how much section, if any, has been removed. If the trondhjemite of Rio Brazos intruded syntectonically at about 1,654 Ma the deformation may have been related to the Mazatzal orogeny, which occurred about 1,670 Ma (Conway, 1984) in central and northern Arizona. Because the date on the trondhjemite is a Rb-Sr date, and because an S_1 fabric has not been recognized in the trondhjemite, the pluton may have intruded at any time before the D_2 deformational phase.

Whatever terrane evolution and/or assemblage scenario one favors, the Proterozoic rocks in the study area record three phases of a progressive deformation. The first phase resulted in a complex composite fabric that produced rotated porphyroblasts, reactivated foliations, and mylonitic foliations. A major mylonite zone is developed slightly above the MMS-MSMR contact, although all rocks surrounding the contact are strongly deformed and thinner mylonite zones are present throughout the Proterozoic section. The S_1 foliation is developed parallel to bedding and compositional layering throughout the area in all rock types. Shear fabrics indicate that material was transported northward parallel to the S_1 foliation. Folds of this generation are isoclinal. The second phase of deformation resulted in open folds and a prominent axial planar cleavage. Major folds formed during this episode are the Jawbone syncline and the Hopewell anticline. The lowermost MSMR rocks and uppermost MMS rocks are some of the least competent rocks in the field area. The formation of the Jawbone syncline could have caused flexure slip within this incompetent contact zone which may have continued north-directed shear along the north-

ern limb of the syncline. The third phase of deformation produced a fracture cleavage recorded along Gavilan Creek. Metamorphism from the upper greenschist to the lower amphibolite facies was synchronous with deformation and peaked near the end of the second phase of deformation.

The favored model calls for the MMS to form in an island arc that was subsequently accreted to a landmass before ca. 1,700 Ma. First the MSMR and then the Ortega Group were deposited on the MMS. This model is favored because both the MMS lithologies and the chemical signatures of those lithologies are consistent with formation in an island arc. The phyllite clasts in the MSMR are believed to have been derived from the underlying MMS because this is the simplest, most direct source for the clasts. It is believed that later shear strongly influenced the contact between the MMS and the MSMR.

RELATIONSHIP OF THE NORTH TUSAS PROTEROZOIC ROCKS TO REGIONAL PROTEROZOIC ROCKS

Proterozoic assemblages similar to that exposed in the north Tusas Mountains are common in the cores of a number of uplifts in southern Colorado and northern New Mexico. In general these are mafic-dominated volcanic and volcanoclastic supracrustal assemblages which are intruded by felsic plutons and overlain by immature metasediments and/or mature quartzite-dominated sequences. These include assemblages in the Salida-Gunnison area (Bickford and Boardman, 1984; Knoper and Condie, 1988) and the Needle Mountains of Colorado (Barker, 1969; Tewksbury, 1983, 1985); and the Gold Hill-Wheeler Peak area (Condie and McCrink, 1982) of New Mexico.

All these assemblages have been metamorphosed to greenschist or amphibolite facies, and have undergone two to three periods of deformation. An ex-

tensive shear zone delineated by mylonites occurs at the Uncompahgre-Irving contact in the Needle Mountains. Here the Uncompahgre Formation was thrust south over the Irving Formation (Tewksbury, 1985).

The ages of these assemblages are constrained by dates from felsic volcanics within the supracrustal successions and plutons that intrude the supracrustals. U-Pb dates from supracrustal rocks in the Dubois greenstone belt of the Gunnison area record two periods of volcanism: one from 1,770-1,760 Ma and a second from 1,745-1,730 Ma (Bickford and Boardman, 1984). The Twilight Gneiss in the Needle Mountains has been dated at 1,734 Ma (Silver and Barker in Reed et al., 1987). Syntectonic tonalites and diorites from the Gold Hill area have U-Pb dates of 1,750 Ma (Bowring and Van Schmus in Condie and McCrink, 1982). A metagabbro from near Gold Hill has a U-Pb date of 1,741 Ma (Bowring in Reed et al., 1987). Stacey et al. (1976) report model lead ages of 1,720 Ma and 1,710 Ma from massive sulfide deposits in the Pecos greenstone belt.

SUMMARY

GEOLOGIC HISTORY

The following geologic history of the upper Brazos Box study area assumes that the MMS formed in an island arc, that the MSMR was deposited directly on the MMS, and that later shear strongly influenced the contact between the two units. Figure 41 is an idealized illustration of the evolution of the study area.

>1,755 Ma : Deposition of the MMS as mafic through felsic volcanics and volcanoclastics and intrusion of the Maquinita granodiorite (southeast of the study area) in an arc, probably an island arc.

Accretion of the MMS arc to a continental mass.

>1,700 Ma: Exposure and erosion of the MMS, deposition of the MSMR basal metaconglomerates.

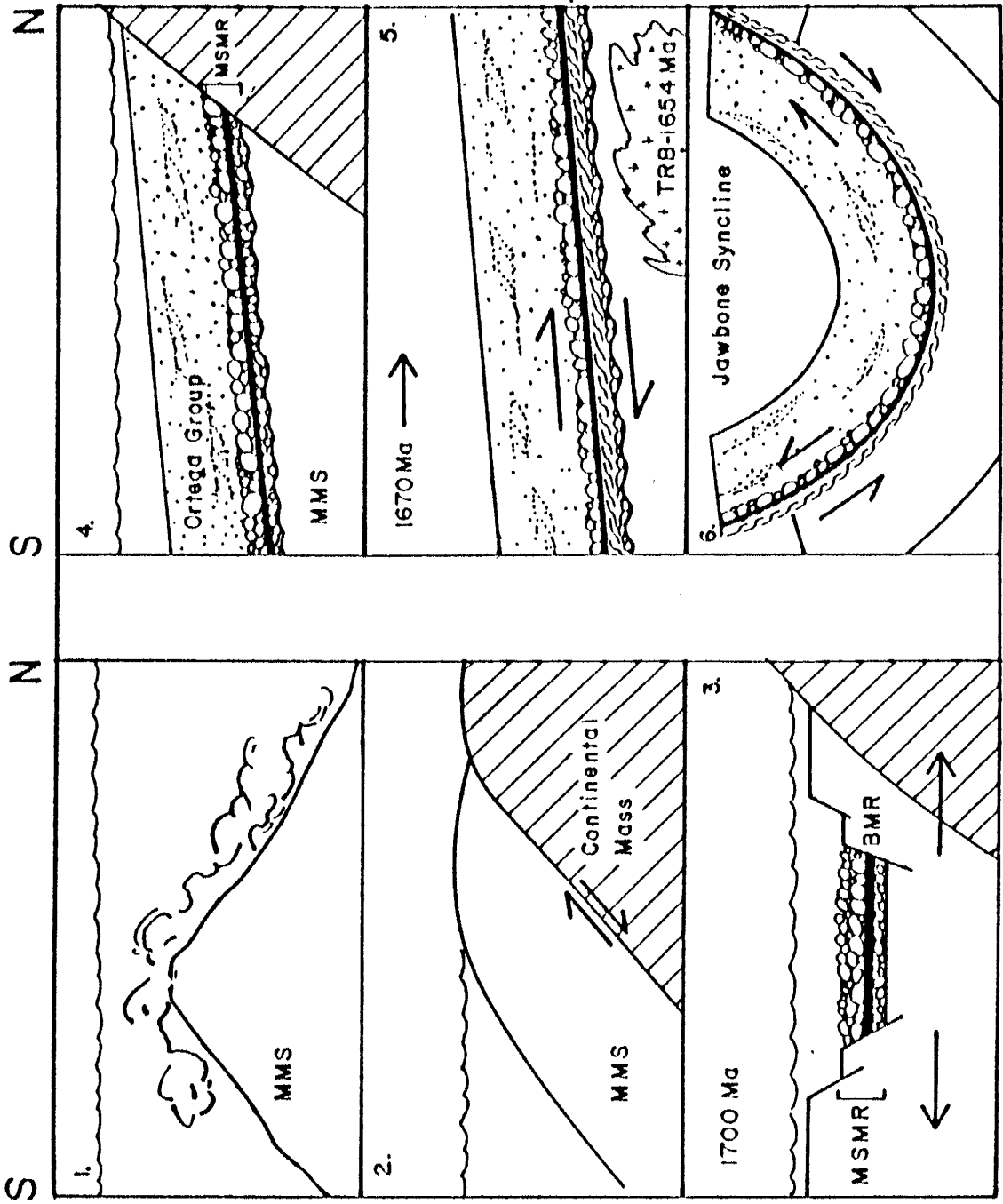
ca. 1,700: Eruption of the Burned Mountain metarhyolite as an ash-flow tuff in a nearshore, probably submarine, extensional continental environment.

1,700-?: Continued deposition of the MSMR poorly sorted metaconglomerate in an extensional setting. Clasts from the MMS and Burned Mountain metarhyolite are incorporated into the MSMR.

The upward maturing of sediments caused by the stabilization of a landmass and a marine transgression results in deposition of the Ortega Group quartzites in 3-4 m of water on a continental shelf. Deposition of the quartzite must have kept pace with slow basinal subsidence to keep environmental characteristics the same during the time it took 1 km of quartzite to be

FIGURE 41

Generalized sequence of probable Proterozoic geologic events in the upper Brazos Box area: 1) development of the MMS arc; 2) accretion of the MMS arc to a continental mass; 3) eruption of the Burned Mountain metarhyolite at ca. 1,700 Ma in an extensional environment, and deposition of the MSMR poorly sorted conglomerates; 4) deposition of the upper MSMR and Ortega Group on a relatively stable shallow continental shelf; 5) recorded deformation begins, possibly related to the Matazal orogeny at ca. 1670 Ma, and intrusion of the trondhjemite of Rio Brazos ca. 1,654 Ma; 6) possible north-directed shear along the northern limb of the Jawbone syncline generated by flexure slip during the folding of the syncline.



deposited (Smith, 1986).

~ 1,670: Deformation begins, possibly related to the Mazatzal orogeny (Conway, 1984). The MSMR package and the Ortega Group are thrust northward over the MMS along the MMS-MSMR contact. Although a thin section of metaconglomerate lies beneath the mylonite zone, the contact itself has been deformed.

ca. 1,654 Ma: Possible syntectonic intrusion of trondhjemite of the Rio Brazos and continued deformation of Proterozoic rocks.

?: The formation of the Jawbone Syncline (F_2) may have involved flexure slip causing continued northward shearing along the mylonite zone, which is the least competent zone between the Ortega Group-MSMR and the MMS.

?: Formation of the S_3 foliation.

1,654-1,300 Ma ?: Burial of the Proterozoic rocks to depths of 2-3 km. Continued deformation and metamorphism from the greenschist to the lower amphibolite facies.

RECOMMENDATIONS FOR FUTURE WORK

- 1). Detailed study of the contact relations and the tectonic fabrics of the trondhjemite of the Rio Brazos is needed to determine if it is pre- or syntectonic.
- 2). Detailed study of the S_2 and the S_3 foliation in the vitreous quartzite of the Ortega Group is needed to verify the sequential relationship between these deformational phases.
- 3). Detailed study of the mylonite zone between the MMS and the MSMR is needed to determine: a) presence or absence of a metamorphic grade jump; b) kinematics of the displacement history; c) amount of displacement.

REFERENCES CITED

- Atwood, W. W., and Mather, K. F., 1932, Physiography and Quaternary Geology of the San Juan Mountains, Colorado: U.S. Geological Survey Professional Paper 166, 176 p.
- Amstutz G. C., 1974, Spilites and Spilitic Rocks: International Union of Geological Sciences, Series A, No. 4, Springer-Verlag, 482 p.
- Baltz, E. H., 1976, Resume of Rio Grande Depression in North-Central New Mexico: New Mexico Bureau of Mines and Mineral Resources, Circular 163, p. 210-228.
- Barker, F., 1958, Precambrian and Tertiary Geology of the Las Tables Quadrangle, New Mexico: New Mexico Bureau of Mines and Mineral Resources, Bulletin 45, 104 p.
- Barker, F., 1969, Precambrian Geology of the Needle Mountains, Southwestern Colorado: United States Geological Survey Professional Paper 644-A, 35 p.
- Barker, F., and Friedman, I., 1974, Precambrian Metavolcanic Rocks of the Tusas Mountains, New Mexico: Major Elements and Oxygen Isotopes: New Mexico Geological Society Guidebook, 25th Field Conference, Ghost Ranch, p.115-117.
- Barker, F., Peterman, Z.E., and Henderson, R.E., 1974, Rubidium-Strontium dating of the Trondhjemite of Rio Brazos, New Mexico, and of the Kroenke Granodiorite, Colorado: U.S. Geological Survey Journal of Research, v. 2, no. 6, p. 705-709.
- Barker, F., Arth, J. G., Peterman, Z. E., and Friedman, I., 1976, The 1.7- to 1.8-b.y.-Old Trondhjemites of Southwestern Colorado and Northern New Mexico: Geochemistry and Depths of Genesis: Geological Society of America Bulletin, v. 87, p. 189-198.
- Barker, F., 1979, Trondhjemite: Definition, Environment and Hypotheses of Origin, in Barker, F., ed., Trondhjemites, Dacites, and Related Rocks: Elsevier, New York, p. 1-12.
- Bickford, E. C., and Boardman, S. J., A Proterozoic Volcano-Plutonic Terrane, Gunnison and Salida Areas, Colorado: Journal of Geology, v. 92, p. 657-666.
- Bingler, E. C., 1965, Precambrian Geology of La Madera Quadrangle, Rio Arriba County, New Mexico: New Mexico Bureau of Mines and Mineral Resources, Bulletin 80, 132 p.
- Bingler, E.C., 1968, Geology and Mineral Resources of Rio Arriba County, New Mexico: New Mexico Bureau of Mines and Mineral Resources, Bulletin 91, 158 p.

- Boadi, I. O., 1986, Gold Mineralization and Precambrian Geology of the Hopewell Lake Area, Rio Arriba County, New Mexico: M.S. Thesis, New Mexico Institute of Mining and Technology, 107 p.
- Butler, A.P., Jr., 1946, Tertiary and Quaternary Geology of the Tusas-Tres Piedras Area, New Mexico: Harvard Univ., Cambridge, Mass., Ph.D. dissert., 188 p.
- Butler, A. P., Jr., 1971, Tertiary Volcanic Stratigraphy of the Eastern Tusas Mountains, Southwest of the San Luis Valley, Colorado-New Mexico: New Mexico Geological Society Guidebook 22, p. 289-300.
- Carey, S., and Sigurdsson, H., 1984, A Model of Volcanogenic Sedimentation in Marginal Basins, in Kokelaar, B. P., and Howells, M. F., ed., Marginal Basin Geology Volcanic and Associated Sedimentary and Tectonic Processes in Modern and Ancient Marginal Basins: Blackwell Scientific Publications, 322 p.
- Condie K. C., 1986, Geochemistry and Tectonic Setting of Early Proterozoic Supracrustal Rocks in the Southwestern United States: *Journal of Geology*, v. 94, p. 845-864.
- Condie, K. C., and McCrink, 1982, Geochemistry of Proterozoic Volcanic and Granitic Rocks from the Gold Hill-Wheeler Peak Area, Northern New Mexico: *Precambrian Research*, v. 19, p. 114-166.
- Condie, K. C., and Nuter, J. A., 1981, Geochemistry of the Dubois Greenstone Succession: An Early Proterozoic Bimodal Volcanic Association in West-Central Colorado: *Precambrian Research*, v. 15, p. 131-156.
- Conway, C. M., 1984, Extent and Implications of Silicic Alkalic Magmatism and Quartz Arenite Sedimentation in the Proterozoic of Central Arizona: *Geological Society of America Abstracts with Programs*, v 16, P. 216.
- Cross W. and Larsen, E. S., 1935, A Brief Review of the Geology of the San Juan Region of Southwestern Colorado: United States Geological Survey, Bulletin 843, 138 p.
- Doney, H. G., Geology of the Cebolla Quadrangle, Rio Arriba County, New Mexico: New Mexico Bureau of Mines and Mineral Resources, Bulletin 92, 114 p.
- Epis, R. C., and Chapin, C. E., Geomorphic and Tectonic Implications of the Post-Laramide, Late Eocene Erosion Surface in the Southern Rocky Mountains: *Geological Society of America Memoir* 144, p. 45-75.
- Fiala, F., 1974, Some Notes on the Problem of Spilites, in Amstutz, G. C., (ed) Spilites and Spilitic Rocks: International Union of Geological Sciences, Series A, No. 4, 482 p.
- Floyd, P. A., and Winchester, J. A., 1978, Identification and Discrimination of

Altered and Metamorphosed Volcanic Rocks Using Immobile Elements, *Chemical Geology*, v.21, p. 281-306.

Garcia, M. O., 1978, Criteria for the Identification of Ancient Volcanic Arcs: *Earth-Science Reviews*, v. 14, p. 147-165.

Gibson, T. R., 1981, Precambrian Geology of the Burned Mountain-Hopewell Lake Area, Rio Arriba County, New Mexico: M.S. Thesis, New Mexico Institute of Mining and Technology, 105 p.

Gill, J. B., 1987, Early Geochemical Evolution of an Oceanic Island Arc and Backarc: Fiji and the South Fiji Basin: *Journal of Geology*, v. 95, p. 598-615.

Grambling J. A. and Williams, M. L., 1984, The Effects of Fe^{3+} and Mn^{3+} on Aluminum Silicate Phase Relations in North-Central New Mexico, U.S.A.: *Journal of Petrology*, v. 26, p. 324-354.

Grambling, J. A., 1986, Crustal Thickening During Proterozoic Metamorphism and Deformation in New Mexico: *Geology*, v. 14, p. 149-152.

Grambling, J. A., Williams, M. L., and Mawer, C. K., 1988a, The Proterozoic Tectonic Assemblage of New Mexico: *Geology*, in press.

Grambling, J. A., Williams, M. L., Mawer, C. K., and Smith, R. F., 1988b, Metamorphic Evolution of Proterozoic Rocks in New Mexico: *Journal of the Geological Society of London: Special Volume on Metamorphic Belts*, in press.

Gresens, R. L., and Stensrud, H. L., 1974, Recognition of More Metarhyolite Occurrences in Northern New Mexico and a Possible Precambrian Stratigraphy: *The Mountain Geologist*, v. 11, no. 3, p. 109-124.

Jensen, L. S., 1976, A New Cation Plot for Classifying Subalkalic Volcanic Rocks: Ontario Division of Mines, Miscellaneous Paper 66, 22 p.

Just, E., 1937, Geology and Economic Features in the Pegmatites of Taos and Rio Arriba Counties, New Mexico: New Mexico Bureau of Mines and Mineral Resources, Bulletin 13, 73 p.

Kent, S. C., 1880, Precambrian Geology of the Tusas Mountain Area, Rio Arriba County, New Mexico: M.S. Thesis, New Mexico Institute of Mining and Technology, 150 p.

Knoper, M., and Condie, K. C., 1988, Geochemistry and Petrogenesis of Early Proterozoic Amphibolites, West-Central Colorado, U.S.A.: *Chemical Geology*, v. 67, p. 209-225.

Larsen, E. S., Jr., and Cross, W., 1956, Geology and Petrology of the San Juan Region, Southwestern Colorado: U.S. Geological Society Professional Paper 258, 303 p.

- Lucas, S. G., Ingersoll, R. V., 1981, Cenozoic Continental Deposits of New Mexico: An Overview: Geological Society of America Bulletin, Part 1, v. 92, p. 917-932.
- Manley, K., and Wobus, R., 1982a, Reconnaissance Geologic Map of the Mule Canyon Quadrangle, Rio Arriba County, New Mexico: United States Geological Survey, Map MF-1407.
- Manley K., and Wobus, R., 1982b, Reconnaissance Geologic Map of the Las Tablas Quadrangle, Rio Arriba County, New Mexico: United States Geological Survey, Map MF-1408.
- Maruyama S., Liou, J. G., Suzuki, K., 1982, The Peristerite Gap in Low-Grade Metamorphic Rocks: Contributions to Mineral Petrology, v 81, p. 268-276.
- Miyashiro, A., 1975, Metamorphism and Metamorphic Belts: George Allan & Unwin Ltd., 492 p.
- Montgomery, A. P., 1953, Precambrian Geology of the Picuris Range, New Mexico Institute of Mining and Technology, State Bureau of Mines and Mineral Resources, Bulletin 30.
- Muehlberger, W. P., 1968, Brazos Peak, New Mexico Institute of Mining and Technology, State Bureau of Mines and Mineral Resources, Geologic Map 22.
- Muehlberger, W. R., and Muehlberger, S., 1982, Espanola-Chama-Taos, A Climb Through Time: New Mexico Bureau of Mines and Mineral Resources, Scenic Trips to the Geologic Past No. 13, 97 p.
- Nettleton, L. L., 1971, Elementary Gravity and Magnetism for Geologists and Seismologists: Society of Economic Geologists, Monograph Series Number 1, 121 p.
- Pearce, J. A., 1974, Statistical Analysis of Major Element Patterns in Basalts: Journal of Petrology, v. 17, p. 15-43.
- Pearce, J. A., 1975, Basalt Geochemistry Used to Investigate Past Tectonic Environments on Cyprus: Tectonophysics, v. 25, p. 41-67.
- Pearce J. A., 1987, An Expert System for the Tectonic Characterization of Ancient Volcanic Rocks: Journal of Volcanology and Geothermal Research, v. 32, p. 51-65.
- Pearce, J. A., and Cann, J. R., 1973, Tectonic Setting of Basic Volcanic Rocks Determined Using Trace Element Analyses: Earth and Planetary Science Letters, v. 19, p. 290-300.
- Pearce, J. A., Harris, N. B. W., and Tindle, A. G., 1984, Trace Element Discrimination Diagrams for the Tectonic Interpretation of Granitic Rocks: Journal of Petrology, v. 25, p. 956-983.

- Reed, J. C., Bickford, M. E., Premo, W.R., Aleinkoff, J. N., and Pallister, J. S., 1987, Evolution of the Early Proterozoic Colorado Province: Constraints from U-Pb Geochronology: *Geology* no. 9, p. 861-865.
- Robertson, J. M., Bowring, S., Williams, M., and Grambling, J., in prep. Precambrian of New Mexico, part of the chapter Precambrian of the Conterminous U.S., in a future GSA DNAG volume.
- Robertson, J. M., and Moench, R. H., 1979, The Pecos Greenstone Belt: A Proterozoic Volcano-Sedimentary Sequence in the Southern Sangre de Cristo Mountains, New Mexico, *New Mexico Geological Society Guidebook* 30, p. 165-173.
- Smith, H. T. U., 1938, Tertiary Geology of the Abiquiu Quadrangle: *Journal of Geology*, v. 48, 933-965.
- Smith, S. S., 1986, Precambrian geology of the Jawbone Mountain Area, Rio Arriba County, New Mexico: M.S. Thesis, New Mexico Tech, 99 p.
- Soegaard, K., and Eriksson, K. A., 1985, Evidence of Tide, Storm, and Wave Interaction on a Precambrian Siliciclastic Shelf: the 1700 m.y. Ortega Group, New Mexico: *Journal of Sedimentary Petrology*, v.55, p.672-684.
- Stacey, J. S., Doe, B. R., Silver, L. T., and Zartman, R. E., 1976, Plumbtectonics II A, Precambrian Massive Sulfide Deposits: *United States Geological Survey Open-File Report* 76-476, 26 p.
- Steiger R. H. and Jäger, E., 1977, Subcommittee of Geochronology: Convention on the Usage of Decay Constants in Geo- and Cosmochronology: *Earth and Planetary Science Letters*, v. 36, p. 359-362.
- Tewksbury, B.J., 1985, Revised Interpretation of the Age of Allochthonous Rocks of the Uncompahgre Formation, Needle Mountains, Colorado: *Geological Society of America Bulletin*, v. 96, p. 224-232.
- Tewksbury, B. J., 1986, Conjugate Crenulation Cleavages in the Uncompahgre Formation, Needle Mountains, Colorado: *Journal of Structural Geology*, v. 8, p. 145-155.
- Troger, W. E., 1979, *Optical Determination of Rock Forming Minerals*: translated by; Bambauer, H. U., Taborszdy, F., and Trochim, H. D., E. Schweizerbartsche Verlagsbuchhandlung, Stuttgart, 187 p.
- Vernon, R. H., 1986, A Microstructural Indicator of Shear Sense in Volcanic Rocks and its Relationship to Porphyblast Rotation in Metamorphic Rocks: *Journal of Geology*, v. 95, p. 127-133.
- Wager, R. L. and Brown, G. M., 1967, *Layered Ingeous Rocks*: W. H. Freeman and Company, San Francisco, 588 p.
- Wessel, G., R., 1986, *The Geology of Plate Margins*: Geological Society of

America, Map and Chart Series MC-59.

- Williams, M.L., Grambling, J.A., and Bowring, S.A., 1986, Redefinition of the Vadito Group, an Extensive Felsic Volcanic-Sedimentary Sequence in the Proterozoic of N.M.: Geological Society of America Abstracts with Programs, v.18, p. 422.
- Williams, M.L., 1987, Stratigraphic, Structural, and Metamorphic Relationships in Proterozoic Rocks from Northern New Mexico: P.H.D. Dissertation, University of New Mexico, 138 p.
- Winchester, J. A., and Floyd, P. A., 1977, Geochemical Discrimination of Different Magma Series and their Differentiation Products Using Immobile Elements: Chemical Geology, v. 20, p. 325-343.
- Winkler, H. G. F., 1976, Petrogenesis of Metamorphic Rocks, 5th Edition: Springer-Verlag, 347 p.
- Wobus, R., and Manley, K., 1982, Reconnaissance Map of the Burned Mountain Quadrangle, Rio Arriba County, New Mexico: United States Geological Survey, Map MF-1409.
- Wobus, R., 1985, Changes in the nomenclature and stratigraphy of Proterozoic metamorphic rocks, Tusas Mountains, north-central New Mexico: U.S. Geological Survey Bulletin 1571, 19 p.

APPENDIX A

THIN SECTION DESCRIPTIONS

*SUPRACRUSTAL ROCKS**MOPPIN METAVOLCANICS**Mafic to Intermediate Rocks**Amphibole Schist*

Two types of amphibole schists are present in the field area, a fine-grained uniformly-textured type and a dark green type with darker spots of actinolitic hornblende clusters. Both types contain a weak foliation.

Amphibole schists contain 40-88% actinolite or actinolitic hornblende, 8-44% plagioclase, < 1-5% epidote, 0-20% quartz, 0-9% biotite, 0-2% chlorite, 0-8% carbonate, and accessory clinozoisite, zoisite, magnetite and ilmenite. One spotted sample contains 5% sphene. Plagioclase, which ranges from albite (An_{2-12}) to oligoclase (An_{27-28}) in composition, is partially to completely altered to sericite, and epidote, with minor clinozoisite and zoisite.

Blue-green to yellow-green pleochroic actinolite or actinolitic hornblende occurs in four forms; 1) as subidoblastic fibrous intergrowths (0.06×0.06 mm to 0.1×0.3 mm); 2) as subidoblastic crystals poikilitically enclosing quartz and feldspar (0.3×0.4 mm); 3) as fine idioblastic needles (0.006×0.02 mm); and 4) as large masses with rectangular to prismatic shapes (0.2×0.2 mm) that may contain relict twins. In most thin sections amphiboles occur as felted mats containing larger actinolite crystals and/or clusters of crystals. The nearly square shapes of some of the larger actinolite crystals suggest that they are

forming pseudomorphs after pyroxene crystals. Several samples have been deformed to the point where actinolitic hornblende crystals are bent back on themselves. Interstitial to the amphibole, in the groundmass are: xenoblastic quartz and plagioclase (0.03×0.03), granular to subidioblastic epidote, xenoblastic clinozoisite (0.03×0.03 mm), and idioblastic to subidioblastic biotite (0.15×0.06 mm). In some samples larger subidioblastic plagioclase (0.9×0.3 mm) laths that are intergrown and enclose smaller actinolite crystals are reminiscent of diabasic textures. Some samples contain broken to subidioblastic plagioclase and actinolite (0.1×0.2 mm) randomly distributed in a poorly sorted matrix.

In thin section the foliation is formed by discontinuous cleavage bands composed of oriented chlorite and actinolite crystals, which alternate with microlithons of xenoblastic quartz and feldspar. Carbonate occurs as xenoblastic masses commonly elongated in the cleavage direction, as fine flecks in the matrix, and as small veins. The carbonate veins, which average 1 mm in width, have been both isoclinally folded and sheared.

Relict vesicles (1.0×1.0 to 2.0×3.0 mm) are filled with patchy to radiating plagioclase and/or epidote, +/- chlorite, +/- biotite (Figure 6). The amygdules show little to no flattening. Associated with these amygdules are large (1.5×0.6 mm) individual and clustered plagioclase crystals. Bedding in the amphibole schists is the result of variation of plagioclase and amphibole content.

Amphibole schists sample numbers are: 89-A, 132-A, 144, 224, 226, 226-G, and 7-49.

Plagioclase-Chlorite Schist

Both plagioclase-chlorite schists and chlorite-plagioclase schists are present in the study area. The transition from chlorite-schist to plagioclase-chlorite schist is reflected in a wide compositional variation as seen in the mineral percentages: 25-59% plagioclase, 8-37% chlorite, 8-24% quartz, and <1-15% muscovite. Epidote and carbonate vary from 0 to 15% and 10% respectively. Biotite, clinozoisite, magnetite, and ilmenite are present as accessories. Plagioclase composition ranges from albite to oligoclase (An_{2-11} and An_{27-29}), with albite as the most common type. Plagioclase has been altered to sericite and epidote and, in some cases, alteration has advanced to the point where only patches of granular epidote, + /- sericite, + /- clinozoisite remain.

The plagioclase-chlorite schists are foliated, on a scale of 1.2 to 0.04 mm in thickness. In mica-rich samples, the microlithons are formed by bands of idioblastic muscovite (0.02×0.001 mm), polygonal quartz (0.03×0.03 mm), and minor idioblastic to subidioblastic chlorite (0.2×0.06 mm). In mica poor samples, microlithons consist of xenoblastic to polygonal quartz (0.06×0.06 mm) and subidioblastic plagioclase (0.4×0.3 mm). Cleavage bands are defined by idioblastic to subidioblastic chlorite and muscovite. Calcite is common as irregular lenses elongated in the foliation plane. S-C fabrics related to formation of the S_1 and the S_2 foliations are present. In some samples the S_1 foliation, which is delineated by cleavage bands and microlithons of muscovite and chlorite, are crenulated into a later S_2 foliation.

A sample taken from a F_2 fold nose on the hill labeled 10062-T, contains a microscopic S_1 foliation that has been crenulated into the axial planar cleavage of a F_2 fold. This later S_2 foliation also forms several isolated mm-thick shear bands, across which material has been transported in a northern direction (Fig-

ure 26).

Some samples contain whole to broken plagioclase crystals, which are erratically distributed in a fine groundmass of idioblastic to subidioblastic epidote and muscovite and xenoblastic quartz and feldspar. Other samples contain intergrown plagioclase laths (0.3×0.12 mm) with interstitial xenoblastic epidote, chlorite, and carbonate.

The crystal-rich chlorite-plagioclase schist contains up to 45% equant plagioclase crystals (2.0×2.0 mm) that have been partly to completely saussuritized and are rimmed by chlorite. The groundmass in these samples is comprised of fine-grained subidioblastic to xenoblastic chlorite, epidote, albite, quartz, and minor biotite.

The equant nature of the larger isolated plagioclase crystals, the extent of their alteration, and the fine grained groundmass that contains them, suggests that the crystals are relict phenocrysts in an intrusive rock.

Plagioclase-chlorite schist sample numbers are 107, and 224. Chlorite-plagioclase schists sample numbers are 27, 128-A, 138-A, and 164-B.

Muscovite-Chlorite Phyllite

Muscovite-chlorite phyllites to schists contain 21-50% chlorite, 16-39% muscovite/sericite, 7-14% quartz, 0-16% plagioclase, 4-7% opaques, as well as accessory epidote, rutile and hematite. Carbonate rhombohedra (siderite) may comprise up to 20% of the rock. Plagioclase composition ranges from albite to oligoclase (An_{2-5} and An_{27}). Minor alteration of plagioclase to sericite and/or epidote is present in these samples.

In the fine-grained phyllites, the foliation is continuous and laminar in char-

acter. As the quartz and feldspar content increase the foliation becomes discontinuous and wide-spaced, and microlithons become an important element of the foliation. Foliation is defined by a fine-grained (0.14×0.03 mm) mixture of idioblastic chlorite and muscovite, which alternates with coarser grained (0.1×0.04 mm) idioblastic to subidioblastic chlorite. In finer grained samples the phyllosilicates are disrupted only by randomly dispersed quartz lenses (0.15×0.06 mm), which have recrystallized to smaller polygonal quartz crystals (0.02×0.02 mm). Idioblastic to xenoblastic opaque magnetite (0.09×0.09 mm), hematite, and opaque dust are prominent in some samples along foliation planes.

A variety of the muscovite-chlorite schists contains abundant siderite crystals that weather leaving limonite filled rhombohedral cavities. In thin section these siderite rhombohedra are subidioblastic to xenoblastic, contain abundant deformation lamella, and range from 1.5×2.0 mm to 1.2×0.77 mm in size. The carbonates contain abundant patches of plagioclase, indicating that they are partially the alteration products of feldspar, yet they are generally idioblastic indicating that the carbonates are also places where growth could nucleate (Grambling, 1988, personal communication). Trains of opaque minerals contained in the carbonates are at a high angle to those in the foliation and trains of opaque minerals in the margins of the crystals are transitional between the two orientations indicating that the crystals have rotated synkinematically in a northerly direction as a result of shearing (Figure 7)

Muscovite-chlorite schists samples include: Adit and 253.

Biotite-Amphibole Schist

Biotite-amphibole schists are very distinct in that they contain up to 20%

large (7×5 mm) blackish green megacrysts in a dark green matrix. In thin section it can be seen that the megacrysts are subidioblastic to xenoblastic, pleochroic green to yellowish green actinolite or actinolitic hornblende that are strongly poikiloblastic with greenish brown biotite. Rectangular outlines of single actinolite crystals and crystal masses, as well as relict twinning indicate that this amphibole has formed pseudomorphs after pyroxene. Carbonate lenses have formed in pressure shadows around many porphyblasts. Idioblastic to subidioblastic biotite and large amphibole pseudomorphs are fringed by idioblastic to subidioblastic chlorite (0.15×0.08 mm), which is usually oriented in the foliation plane. The groundmass is comprised of chlorite, biotite (0.15×0.06 mm), subidioblastic to granular epidote (0.34×0.15 mm), and xenoblastic to polygonal quartz (0.08×0.06 mm). Xenoblastic carbonate (0.15×0.17 mm) occurs in patches. Chlorite forms an anastomosing foliation.

The biotite-amphibole schist sample number is 314.

Chlorite-Quartz Schist

Both chlorite-quartz schists and quartz-chlorite schists are present in the Upper Brazos Box area. This wide compositional variation is reflected in the mineral percents; 23-61% quartz and 22-42% chlorite. Muscovite and carbonate vary from 0-20%, feldspar from 0-12%, and opaque minerals from <1 to 24%. Clinzoisite, rutile, and hematite are minor accessories that may or may not be present. Plagioclase, when present is albite to oligoclase (Λn_{2-8} and Λn_{30}) in composition. Alteration of plagioclase to sericite ranges from minor to nearly complete. Most large plagioclase crystals contain carbonate blebs.

All samples contain a strong continuous to discontinuous foliation defined by cleavage bands of idioblastic to subidioblastic chlorite (0.06×0.01 mm) and

muscovite (0.02×0.004 mm), and microlithons of polygonal to xenoblastic quartz (0.12×0.08 mm) and minor plagioclase (0.2×0.12 mm). Elongate discontinuous lenses of carbonate may be associated with the microlithons. Banding thickness varies from 1.2 to 0.02 mm. Some thin sections reveal dispersed larger broken to rounded plagioclase crystals (0.15×0.15 mm). It is impossible to distinguish if the rounded character of these crystals is primary or tectonic. One sample contains broken feldspar crystals that have been sheared in a southeast direction.

A unit present in a saddle northeast of the Thomas cow camp contains 16% actinolitic hornblende. These large (3.1×0.12 mm) idioblastic to subidioblastic crystals have overgrown the S_2 foliation at the expense of chlorite leaving the quartz poikilitically enclosed in the amphibole. These relationships indicate that the amphibole, which probably represents the peak of metamorphism formed after the D_2 event.

Quartz-chlorite schist sample numbers are 114 and 171.

Chlorite-Quartz-Muscovite Phyllite

The chlorite-quartz-muscovite phyllites contain 32% muscovite, 26% quartz, 19% chlorite, 10% feldspar, 10% opaque minerals, and 3% epidote. Plagioclase composition ranges from albite (An_{2-8}) to oligoclase (An_{27-28}).

Idioblastic muscovite forms a strong lineation along which subidioblastic broken opaque iron oxide crystals (0.18×0.18 mm) and opaque dust are distributed. Lenses of quartz that have recrystallized to equant polygons (0.09×0.09 mm) help delineate the foliation. Larger subidioblastic to rounded quartz and feldspar (1.2×2.1 mm) now form asymmetrical elongated forms that parallel the foliation direction. Quartz has also recrystallized as tails around

these asymmetrical crystals. The fine lamination and tectonized, highly strained crystals indicate that these samples are mylonitic. But, the direction of shear is unknown because no oriented samples were taken.

Chlorite-quartz-muscovite schist sample number is 263-B. Chlorite-quartz schist sample number is 38.

Felsic Metavolcanics

Chlorite-Plagioclase-Quartz Schist

This unit contains three distinct textural types of rocks: a light and dark green flow banded type, a brecciated type, and a strongly foliated spotted type.

The chlorite-plagioclase-quartz schists contain; 30-51% quartz, 35-43% plagioclase, 5-15% chlorite, 1-5% biotite, along with accessory muscovite/sericite, epidote, clinozoisite, carbonate, opaque iron oxides and rutile. Plagioclase composition ranges from albite (An_{2-12}) to oligoclase (An_{21-30}), and the banded rock type contains rare andesine (An_{32}). Most plagioclase contains only minor sericite, although some samples contain rectangular masses of idioblastic to subidioblastic epidote and/or muscovite which could represent completely altered plagioclase.

The most distinct aspect of this unit in thin section are bands and lenses of xenoblastic quartz and plagioclase (0.02×0.02 mm) with indistinct grain boundaries, alternating with coarser grained bands of subidioblastic plagioclase (0.5×0.24 mm) and polygonal quartz (0.06×0.06 mm). These bands may or may not be separated by thinner bands and lenses of chlorite (0.09×0.06 mm) + /- muscovite (0.07×0.02 mm). In some samples lenses of subidioblastic to xenoblastic epidote and/or xenoblastic carbonate are oriented along this major fol-

iation plane. Individual carbonate rhombohedra (0.07×0.03 mm) may have their long axes aligned in the foliation plane. Large (1×2 mm) idioblastic to slightly subidioblastic plagioclase crystals and broken plagioclase crystals occur as clusters and isolated crystals. Plagioclase crystals also may have their long axes aligned in the foliation direction. Biotite, chlorite, and magnetite occur commonly together as clusters. Large nearly idioblastic biotite crystals (0.2×0.1 mm) are superimposed on fine-grained chlorite masses suggesting that the biotite is prograde. Idioblastic magnetite is abundant and large enough (0.5×0.5 mm) to be seen in hand sample. In thin section these iron oxides are rimmed by biotite.

Bands in the "banded type" of schist are interpreted to represent original flow bands, which may have been accentuated by metamorphic differentiation. These bands have been deformed into open to isoclinal F_1 folds. In thin section it can be seen that these early folds are refolded into open folds. The S_2 axial planar cleavage is formed by the orientation of micas and thin lenses of recrystallized quartz and feldspar.

Plagioclase-quartz schists sample numbers are 137-A and 149-B. Chlorite-plagioclase schist sample number are 91 and 92.

Muscovite-Quartz Schist

Muscovite-quartz schists contain up to 9% quartz and 6% feldspar phenocrysts. The groundmass consists of: 40-49% quartz, 30-36% muscovite, 1-4% chlorite. Accessories include: biotite, epidote, carbonate, magnetite and hematite. The composition of plagioclase ranges from albite (An_{2-5}) to oligoclase (An_{28-30}). Plagioclase has altered to sericite and/or epidote.

These rocks are characterized by large quartz and feldspar crystals enclosed

in a fine grained matrix of quartz, feldspar, and muscovite. The quartz crystals are rounded and strongly embayed, and are interpreted to represent relict phenocrysts. Some quartz crystals are partially or wholly recrystallized to smaller polygonal crystals (0.09×0.09 mm), while in other crystals there has been no recrystallization and the quartz displays strong undulatory extinction. Medium-sized quartz and sericite, with minor carbonate have crystallized adjacent to the larger porphyblasts in the direction of the foliation.

A discontinuous spaced anastomosing foliation is defined by irregular bands and lenses (2.5×0.2 mm wide) of cryptocrystalline (0.008×0.008 mm) quartz and feldspar with indistinct grain boundaries, which alternate with bands of polygonal quartz and subidioblastic to xenoblastic feldspar (0.4×0.4 mm). Muscovite orientation helps to delineate the foliation. Muscovite ranges from individual idioblastic crystals (0.07×0.02 mm) between polygonal quartz, to thin anastomosing bands which, coalesce to form muscovite cleavage bands as wide 3.0 mm. The thick ribbon-like bands of muscovite are strongly crenulated. Large strained idioblastic to subidioblastic chlorite crystals (1.0×0.15 mm) are also oriented parallel to the foliation and are commonly associated with epidote. Subidioblastic biotite (0.09×0.06 mm) is usually oriented at a high angle to the foliation. Biotite appears to be altering to chlorite. Xenoblastic carbonates (0.4×0.3 mm) form lenses with no particular orientation. Idioblastic to subidioblastic magnetite are rimmed by chlorite.

Medium-sized crystals are present adjacent to phenocrysts and in irregular lenses. Plagioclase is located only in the lenses. These groups of crystals could be the result of primary crystallization from vapor phase in void areas (Chamberlin, 1988, personal communication), and/or the result of metamorphic and deformational processes. Because the rocks are strongly deformed in

outcrop and shear fabrics are present in the general area, it is assumed that metamorphic and deformational processes have formed the dominant portion of these fabrics. In these samples, the asymmetry of pressure shadows adjacent to phenocrysts indicate that significant shear has occurred, although conflicting directions are recorded.

Muscovite-quartz and quartz-muscovite schist sample numbers are 162 and 165.

METASEDIMENT AND METARHYOLITE PACKAGE

Phyllite Pebble Metaconglomerate

The phyllite pebble metaconglomerate contains: green and pink phyllite pebbles, red and black chert pebbles, and quartz pebbles, in a poorly sorted matrix of quartz and muscovite. In thin section the average composition of this unit is: 35% quartz, 25% muscovite, 15% plagioclase, 2% epidote, 2% opaque iron oxides, and accessory chlorite, carbonate, zircon, and sphene. Plagioclase, which is albite to oligoclase in composition (An_{28} and An_{24-26}), has been partially altered to sericite + /- epidote.

Quartz pebbles and grains either exhibit undulatory extinction or have been recrystallized to polygonal grains with smooth grain boundaries and 120° between grains. Rare quartz grains have seriate boundaries. Overgrowths are common on quartz pebbles and grains.

Quartz grains in the matrix range from 3.0 mm to 0.03 mm in diameter. Idioblastic muscovite (0.02×0.003 mm) is also an important constituent of the matrix. In thin section, the major foliation (S_1) is defined by individual muscovite crystals between polygonal quartz grains, bands of muscovite, and

strongly flattened phyllite pebbles. Epidote is present as granular patches (0.1×0.1 mm) and subidioblastic crystals (0.03×0.03 mm). Chlorite forms irregularly shaped patches (0.2×0.15 mm) in the matrix. Rare rhombohedral carbonate (siderite) crystals average 0.2×0.07 mm in size. Detrital magnetite (0.2×0.2 mm) is present as subrounded crystals that presently have seriate recrystallized boundaries. Rounded and sometimes broken zircon (0.015×0.015 mm), and sphene (0.1×0.1 mm) are present as minor accessories.

The sample number from the lower metaconglomerate unit 250-B. Samples from the MSMR upper micaceous quartzite with isolated phyllite pebbles are 192 and 256.

Chlorite-Muscovite-Quartz Phyllonite

The chlorite-muscovite-quartz phyllonite contains: 40-42% quartz, 30-32% muscovite, 10-18% chlorite, 6-9% carbonate, 4-8% plagioclase, 2-8% opaque iron oxides, and accessory epidote and garnet (almandine?). Plagioclase is oligoclase ($A_{n_{13-19}}$) in composition.

The foliation in these samples is lamellar and pervasive. It is defined by lenses of xenoblastic quartz-rich material alternating with lenses of idioblastic to subidioblastic muscovite and subidioblastic to xenoblastic chlorite-rich material (1.5×1.0 mm). Microlithons and cleavage bands average 0.2 mm thick. "Fish-shaped" lenses rich of both opaque dust and phyllitic material reach 15×2 mm in size. Quartz crystals (0.4×0.2 mm) have recrystallized to smaller polygonal material which are also elongated as "fish-shapes" in the direction of foliation. The asymmetry of the "fish-shaped" grains indicate that north-directed shear has strongly influenced this phyllonite.

Subidioblastic to xenoblastic plagioclase is present both as individual crystals

(0.5 × 0.5 mm) and clusters, which have been highly sheared. Small rare garnets (0.4 × 0.1 mm), thought to be almandine, have been strongly tectonized and their fragments are distributed along the shear direction. Carbonate rhombohedra (0.8 × 0.5 mm) are unstrained and contain trains of opaque minerals that parallel similar mineral trains in the foliation. These relationships indicate that the carbonate formed after the deformation. Magnetite crystals (1.0 × 0.05 mm) are both broken and sheared as well as idioblastic, indicating that magnetite formed both during and after shearing.

Phyllonite sample numbers are 288-A and 7-122-G.

Burned Mountain Metarhyolite

The Burned Mountain Metarhyolite is a muscovite-quartz schist that contains 5-10% quartz phenocrysts, 0-5% microcline phenocrysts, 42-46% matrix quartz, 38-40% muscovite, 2-6% carbonate, 3-4% plagioclase and 1-2% opaque iron oxides. Plagioclase is albite (An₅₋₈) in composition.

Quartz crystals are strongly embayed implying that they are relict phenocrysts. Rare quartz crystals are near hexagonal in shape. Most quartz and all microcline phenocrysts have been well round and subsequently tectonized. Phenocrysts range in size from 3 × 3 mm to 1.5 × 1.5 mm. Near the base of the unit, samples contain no feldspar phenocrysts.

The groundmass contains a strong discontinuous anastomosing foliation that averages 1-5 mm-thick and is deflected around phenocrysts. This fabric is composed of microlithons of polygonal quartz (0.02 × 0.02 mm) and idioblastic to subidioblastic muscovite (0.01 × 0.002 mm) and cleavage bands of muscovite. Magnetite occurs as large rounded crystals (0.3 × 0.3 mm) and as small grains and dust (0.015 × 0.015 mm) distributed along the foliation planes. Carbonate

forms subidioblastic to xenoblastic crystals (0.2×0.2 mm) within or adjacent to feldspar, in pressure shadows around larger crystals, and in lenses elongated in the foliation plane. In some samples the carbonate is calcite, but near the base of the section siderite is present.

Medium-sized crystals of polygonal quartz and xenoblastic carbonate are adjacent to phenocrysts in the plane of the foliation, and in lenses, which also include plagioclase. These crystals may represent vapor phase crystallization in primary voids (Chamberlin, 1988, personal communication) and/or metamorphic and deformational phenomena. Since deformation has been so severe, it is assumed that the crystals next to phenocrysts are pressure shadows, possibly overprinting a primary fabric. The asymmetry of pressure shadows and broken crystals (which can also be primary features) were used to determine that this unit experienced north-directed shear.

Burned Mountain metarhyolite sample numbers are 9-1, 9-2, and 7-117.

Chlorite schist

The chlorite schist forms intermediate to mafic horizons between beds in the MSMR. The schist contains 38% chlorite, 20% plagioclase, 15% quartz, 10% epidote, 10% carbonate, 5% sphene, 2% clinozoisite, and 1% opaque iron oxides. Plagioclase is oligoclase ($A_{n_{10-12}}$) in composition.

Subidioblastic to xenoblastic plagioclase laths average 0.6×0.3 mm in size and are slightly altered to muscovite and epidote. Idioblastic to subidioblastic chlorite (0.04×0.02 mm) occurs as irregular patches and individual laths elongated in the plane of the foliation. Rhombohedral to xenoblastic carbonate (0.2×0.2 mm) contains rare irregularly shaped patches of feldspar. Xenoblastic epidote (0.2×0.2 mm) is dispersed evenly throughout the rock. Subidiob-

lastic sphene (0.45×0.25 mm) has its long axis oriented in the plane of the foliation. Xenoblastic opaque iron oxide is present in the center of some sphene crystals. The foliation is defined by discontinuous patches of both chlorite, and quartz and feldspar.

The chlorite schist is represented by sample 7-1.

ORTEGA GROUP

Transitional Package

The transitional quartzite contains: 42-67% quartz, 20-25% muscovite, 5-38% opaque iron oxides, 0-7% feldspar, and accessory chert, chlorite, hematite, rutile, and, zircon. Plagioclase is albite to oligoclase in composition (Λ_{n7-19}). Isolated phyllite and chert pebbles are present throughout the transitional quartzite.

Larger quartz and feldspar grains (0.6×0.6 mm) are contained in a matrix of fined-grained quartz (0.1×0.1 mm) and idioblastic muscovite (0.03×0.02 mm). Quartz grains (4×2 mm to 0.4×0.2 mm) are well-rounded and either display undulatory extinction or have at least partially recrystallized to polygonal subgrains (0.06×0.06 mm). Quartz overgrowths parallel to the foliation are common. Hematite is present as rounded (0.3×0.3 mm) grains that now have irregular grain boundaries, indicating they have recrystallized. Idioblastic to subidioblastic chlorite (0.2×0.1 mm) is always associated with hematite. Rounded and sometimes broken, rutile (0.5×0.4 mm) and zircon (0.2×0.05 mm) are present in the lower portions of the beds. Bedding is defined by the presence of heavy minerals at the base of beds and cross-beds, and a decrease in grain size towards the top of the beds. In thin section a strong anastomosing bedding-parallel foliation is defined by flattened quartz grains and aligned mica

crystals. This unit is a bimodal micaceous sandstone that is usually framework supported.

The transitional quartzite sample number is 50.

Vitreous Quartzite

The vitreous quartzite contains 87-98% quartz, 2-12% muscovite, 1-4% opaque iron oxides, sphene, and zircon. Rare samples contain accessory chlorite which is associated with magnetite. Near the base of the vitreous quartzite the rocks contain more mica. A brittlely deformed zone is superimposed on this more micaceous base of the vitreous quartzite.

All samples are framework supported and many are bimodal in character. Larger quartz grains in these samples average 1-3 mm in diameter, while smaller quartz grains range from 0.3-1 mm in diameter. Quartz grains are well rounded to rounded in shape. Many quartz grains have begun to recrystallize and their subgrains display seriate boundaries, those that have not recrystallized are strongly undulose. Many crystals contain quartz overgrowths. Between larger grains, is fine-grained quartz and muscovite. Rounded hematite crystals (0.1×0.1 mm) are irregular in shape from recrystallization. Hematite crystals are most abundant at the base of beds and their abundance decreases upward in each bed. Opaque iron oxides also occur as small grains and dust between quartz and muscovite, and outlining cleavage in muscovite. Idioblastic muscovite (0.23×0.03 mm) occurs between quartz and magnetite crystals. Rare rounded and/or broken zircon (0.2×0.2 mm) and sphene (0.02×0.02 mm) are associated with hematite in the base of the beds.

The bedding parallel foliation (S_1) delineated by the elongation of quartz grains and the alignment of muscovite crystals. The crosscutting foliation (S_2)

is defined by the orientation of muscovite and the truncation of quartz grains.

The more micaceous base of the vitreous quartzite contains: 48-73% quartz, 20-40% muscovite and sericite, 5-10% clay (kaolinite ?), 6-7% opaque iron oxides, and accessory rutile and zircon. In thin section it can be seen that what were large rounded quartz grains with an average size of 1×1 mm have been recrystallized to small (0.2×0.2 mm) polygonal grains with straight boundaries and 120° junctions.

A strong foliation in the micaceous base of the vitreous quartzite is formed by uniform bands of polygonal quartz separated by lamellar bands (0.2 mm to 2 cm thick) of muscovite and sericite. Patches kaolinite (?) have formed in the center of muscovite + sericite masses. Hematite grains (0.2×0.2 mm) are rounded in overall shape, but their edges now seriate from recrystallization. Ilmenite needles (0.4×0.04 mm) are common in the muscovite + sericite lenses, and the long axes of the needles parallel the foliation. Hematite and ilmenite crystals occur in layers that probably represent original bedding, but are now strongly deformed into open to isoclinal folds as well as strongly sheared. In some samples the foliation is disrupted while in others it appears not to have been. Rounded rutile needles (0.14×0.06 mm) and zircon crystals (0.03×0.006 mm) are also present.

Vitreous quartzite sample numbers are: OF, 313-B, 315, 317-B, and 321. Tectonized quartzite sample numbers are 67-B and 7-144. Sample 128 is probably float from the Ritito Formation.

Quartz-Muscovite Phyllite

Quartz-muscovite phyllites form thin interbeds between quartzite beds in the Ortega Group. These phyllites contain: 75% muscovite, 18% quartz, and

7% opaque iron oxides. Well-rounded detrital quartz grains (0.3×0.15 mm) and hematite crystals are enclosed in a well-foliated muscovite matrix. Quartz grain are strongly undulatory and are usually not recrystallized. The quartz and hematite grains are deformed into "fish-shapes" which are elongated in the foliation plane. Fine laminations (1.5 cm-thick) are delineated by the normal grading of hematite crystals. Idioblastic muscovite (0.08×0.008 mm) forms a discontinuous anastomosing foliation. Contradicting shear senses indicated by "fish-shaped" grains and microfolds adjacent to these grains are present in this unit, suggesting that these incompetent micaceous interbeds have accommodated stress from each phase of deformation and may have been sheared in different directions at different times. No overall shear direction was determined from the asymmetry of the quartz and hematite grains.

Sample 7-119-A is a micaceous interbed.

Chlorite schist

The quartz-chlorite schists form intermediate to mafic horizons that are apparently parallel to bedding in the Ortega Group. The chlorite schists contain 25% chlorite, 25% carbonate, 20% quartz, 15% opaque iron oxides, 10% muscovite/sericite, and 6% plagioclase. Idioblastic to subidioblastic chlorite and muscovite crystals average 0.03×0.006 mm in size. Carbonate is xenoblastic and contains abundant strain lamella. Quartz (0.04×0.04 mm) is xenoblastic to polygonal in shape and usually displays undulatory extinction. Plagioclase (0.04×0.03 mm) is subidioblastic to xenoblastic in shape. Two types of iron oxides are present: subidioblastic equidimensional magnetite (0.4×0.3 mm) and subidioblastic ilmenite needles (0.3×0.1 mm). A prominent foliation is delineated by the orientation of chlorite and muscovite crystals and patches, the elongation of carbonates, and the orientation of ilmenite needles.

The quartz-plagioclase-chlorite schists contain 33% chlorite, 25% plagioclase, 16% quartz, 13% epidote, 13% opaque iron oxides, and <1% carbonate. Plagioclase is albite (An_{5-8}) in composition. It is slightly saussuritized. Large plagioclase laths (3.4×1 mm) are inclosed in a fine-grained matrix of chlorite, quartz, epidote, and opaque iron oxides. The laths are greatly deformed. Chlorite is idioblastic to subidioblastic in shape and averages 0.05×0.02 mm in size. Nearly polygonal quartz (0.06×0.06 mm) is contained in patches of chlorite. Large xenoblastic to subidioblastic epidote reaches 0.7×0.7 mm in size. Xenoblastic magnetite (0.4×0.4 mm) is always associated with chlorite.

The chlorite schists are represented by samples 7-75-C and 7-79.

INTRUSIVE UNITS

Trondhjemite of the Rio Brazos

The trondhjemite of Rio Brazos contains: 35-66% quartz, 3-33% plagioclase, 6-8% microcline, 12-15% muscovite, 0-10% biotite, 0-5% chlorite, and accessory carbonate, opaque iron oxides, epidote, clinozoisite, zircon, and hematite. Plagioclase is albite (An_8) to oligoclase (An_{26-28}) in composition. It is usually only slightly altered to sericite with minor epidote and clinozoisite. Plagioclase twins are a combination of albite and pericline. Microcline displays characteristic gridiron twins.

Quartz occurs as large (5×4 mm) highly strained anhedral crystals that are strongly undulose and/or have recrystallized to smaller polygonal subgrains (1×0.5 mm) with lobate to seriate boundaries. These large quartz crystals are set in a matrix consisting of equidimensional (1×1 mm) strongly intergrown anhedral quartz, subhedral to anhedral feldspar, and intensely poikilitic muscovite (1×0.3 mm to 0.2×0.1 mm). Mafic minerals occur in clusters in-

terstitial to quartz and feldspar. The clusters of mafic minerals contain subhedral to anhedral, dark brown biotite (0.2×0.1 mm), subhedral to anhedral chlorite (0.2×0.1 mm), subhedral muscovite (0.2×0.1 mm), and euhedral to anhedral magnetite (0.5×0.3 mm). Granular masses (1×1 mm to 0.2×0.2 mm) of subidioblastic to xenoblastic epidote may be present within the mafic clusters as well as within plagioclase crystals.

In samples that are strongly foliated, the foliation is defined by elongated quartz crystals, which have been subsequently recrystallized, and elongated mafic clusters containing preferentially oriented biotite crystals. Biotite and muscovite are also preferentially oriented throughout the matrix. In most samples the foliation is defined by a weak alignment of micas.

Trondhjemite samples include TROND, 89-II, 116, and 282.

Contaminated Trondhjemite

The contaminated trondhjemite present as xenoliths and at some contacts with the MMS. Contaminated trondhjemite samples examined contain: 15-52% quartz, 33-60% feldspar, 0-30% actinolitic hornblende, 6-10% biotite, 0-15% chlorite, and accessory muscovite, epidote, clinozoisite, and opaque iron oxides. Plagioclase, which is albite (An_{8-10}) in composition, is partially altered to sericite + /- epidote + /- clinozoisite.

Quartz is present as large (3×1.5 mm) rounded relict phenocrysts with undulatory extinction, that have partly recrystallized to polygonal subgrains (0.1×0.1 mm). Highly saussuritized feldspar is present both as large (2×1 mm) isolated and clustered crystals. The matrix contains xenoblastic to polygonal quartz (0.06×0.06 mm) and subidioblastic to xenoblastic feldspar (0.6×0.4 mm). Idioblastic to subidioblastic blue-green actinolite or actinolitic-

hornblende (1×0.2 mm) and /or subidioblastic biotite (0.08×0.05 mm) form a strong anastomosing foliation in some samples. Subidioblastic to xenoblastic chlorite (0.1×0.02 mm) and idioblastic to xenoblastic magnetite are common in mafic clusters associated with biotite.

Xenoliths examined contain no amphibole. The xenoliths contain idioblastic biotite superimposed on xenoblastic interstitial patches of chlorite. The idioblastic, superimposed nature of the biotite suggest that the biotite is prograde. The large quartz and feldspar crystals in these samples are assumed to represent relict phenocrysts contributed from the intruding trondhjemite.

Samples from contaminated trondhjemite contacts are 46-A and 89-B. A xenolith is represented by sample 197.

Hornblendite

The hornblendite contains 87% hornblende, 3% plagioclase, 5% epidote, 3% quartz, 2% clinozoisite, and accessory myrmekite. Plagioclase is highly saussuritized, but it appears to be andesine (An_{49}) in composition. Accessory minerals include opaque iron oxides and hematite. Lucoxene is present in the trondhjemite adjacent to the hornblendite. Minerals other than hornblende are present in interstitial patches of trondhjemite.

Thin section study reveals that what appears to be euhedral hornblende crystals in hand sample (6×2 mm) are instead intergrown subhedral to anhedral crystals. Rare, nearly euhedral hornblende crystals are present. Quartz is present as anhedral crystals (0.12×0.12 mm) between amphiboles and as small (0.02×0.02 mm) poikilitic inclusions in hornblende. Anhedral plagioclase (0.7×0.5 mm) is associated with the interstitial quartz. Myrmekitic textures are rare. Epidote is present in granular patches (0.17×0.13 mm) within horn-

blende and plagioclase, and as patches (0.7×0.5 mm) between crystals. Rare clinozoisite (0.4×0.2 mm) is associated with the epidote.

The hornblende-trondhjemite contact is represented by sample 284.

Dikes

The large 3 m-wide dike in the trondhjemite is a calcite-quartz-chlorite schist. It contains 32% chlorite, 30% quartz, 16% carbonate, 8% opaque iron oxides, 8% epidote, 4% biotite, and 2% clinozoisite. A strong nearly lamellar cleavage, which averages 0.1 mm-thick, is delineated by oriented laths of subidioblastic chlorite (0.2×0.03 mm) and biotite (0.1×0.02 mm), and elongated quartz grains (0.06×0.03 mm). Quartz displays undulatory extinction. Subidioblastic epidote (0.2×0.2 mm), magnetite (0.15×0.15 mm), and idioblastic to subidioblastic ilmenite are uniformly distributed throughout the sample. Calcite is present as xenoblastic crystals (0.4×0.3 mm) and patches (2.5×1.0 mm).

Sample 84-B is a dike.

Quartz Veins

The unique granular quartz vein on the hill labeled 10062-T contains 95% quartz, and accessory muscovite, chlorite, carbonate and opaque iron oxides. Polygonal quartz grains (0.25×0.25 mm) meet at 120° and have straight grain boundaries. The extinction in the quartz grains is slightly undulatory. Abundant fluid inclusion trails which cut across quartz grains are seen in thin section. Chlorite is present as isolated crystals (0.03×0.01 mm) and as xenoblastic masses (0.12×0.06 mm) between quartz. Idioblastic muscovite (0.1×0.02 mm) and chlorite occur as fracture fillings forming thin lines across the sample.

Carbonate occurs as xenoblastic patches (0.07×0.02 mm) interstitial to quartz crystals. Opaque iron oxides is present as dust within carbonates and as idioblastic isolated magnetite crystals (0.04×0.04 mm).

Sample 106-B is a quartz vein.

APPENDIX B

GEOCHEMICAL METHODS

Samples were analyzed on the Rigaku 3064 x-ray Fluorescence Spectrometer at the New Mexico Bureau of Mines and Mineral Resources in Socorro. Major element concentrations were determined using fused disks, which were made with .5 g sample, approximately 2.7 g spectroflux (#95173A), and several beads of ammonia nitrate. Trace element concentrations were measured on pressed pellets, which were made with 8.0 g of sample and 8 drops of polyvinyl alcohol as a binder.

C.I.P.W. norms and Jensen cation percentages were calculated using PETDAT (Knoper, 1988, unpublished programs).

Table B1 contains the sample analyses, table B2 contains the accuracy of the analyses, table B3 contains the precision of the analyses, and table B4 contains the determination limits of some of the trace elements.

The following equations were used to calculate the mean (\bar{X}), standard deviation (S.D.), coefficient of variation (C.V.), and error (ERR.):

Mean	$\bar{X} = \frac{1}{n} \sum X$
Standard Deviation	$S.D. = \frac{1}{n} \sum (X - \bar{X})^2$
Coefficient of Variation	$C.V. = \frac{S.D.}{\bar{X}} \times 100$
Error	$ERR. = \frac{ (A.V. - R.V.) }{R.V.} \times 100$

Table B1: Sample Analyses (164)

SAMPLE	314	132A	89A	224	144	226
SiO2	46.98	50.00	58.23	51.91	50.19	52.09
TiO2	0.44	2.07	0.91	0.51	0.48	0.54
Al2O3	12.31	13.35	14.59	14.39	13.05	15.23
Fe2O3-T	10.76	15.34	11.91	13.27	10.99	11.72
MgO	9.45	5.45	2.66	6.69	8.65	8.47
CaO	11.86	9.55	6.84	10.11	9.12	6.59
Na2O	2.11	2.67	4.48	3.63	4.52	4.58
K2O	1.76	0.31	0.69	0.53	0.11	0.14
MnO	0.19	0.27	0.20	0.23	0.19	0.19
P2O5	0.14	0.24	0.56	0.16	0.20	0.16
LOI	5.23	1.20	0.23	0.80	2.76	1.78
TOTAL	101.23	100.45	101.30	102.23	100.26	101.49
Rb	37	7	10	8	1	2
Ba	533	98	320	281	51	108
Sr	427	197	89	226	291	121
Pb	8	6	5	6	4	4
Th	4	2	3	1	2	2
U	5	2	3	4	3	2
V	310	390	89	250	275	245
Cr	658	87	18	213	666	100
Ni	120	38	3	51	88	29
Cu	109	51	8	5	67	5
Zn	75	123	33	67	84	87
Ga	8	23	12	12	13	13
Y	10	46	38	21	17	15
Zr	43	158	62	45	13	44
Nb	5	7	5	5	5	4
LITHOLOGY	b-a sh	a sh	a sh	a sh	a-sh	a sh
K2O/Na2O	0.83	0.12	0.15	0.15	0.02	0.03
Na2O+K2O	3.87	2.98	5.17	4.16	4.63	4.72
Al2O3/TiO2	28.0	6.4	16.0	28.2	27.2	28.2
CaO/TiO2	27.0	4.6	7.5	19.8	19.0	12.2
Zr/TiO2	0.010	0.008	0.007	0.009	0.003	0.008
K/Rb	391.6	363.4	553.3	524.3	981.7	564.1
Ba/Sr	1.25	0.50	3.61	1.24	0.17	0.89
Rb/Sr	0.087	0.036	0.117	0.037	0.003	0.017
Ti/Zr	60.9	78.7	88.3	67.8	222.7	73.8
Zr/Nb	8.1	22.3	13.6	8.4	2.4	10.1
Nb/Y	0.51	0.15	0.12	0.25	0.31	0.28
Zr/Y	4.2	3.4	1.6	2.1	0.7	2.9
FeO-T/MgO	1.02	2.53	4.03	1.79	1.14	1.25

KEY: sh=schist; b=biotite; a=amphibole; p=plagioclase; c=chlorite; e=epidote; m=muscovite; q=quartz;
cc=carbonate; s=sericite; ND=not detected; NA=not analyzed; major elements=wt.%; trace
elements=ppm

Table B1: Sample Analyses (165)

SAMPLE	107	224-24	138A	128A	164	27
SiO2	48.56	51.49	56.47	42.71	60.39	62.37
TiO2	0.42	0.46	1.56	0.40	0.74	0.82
Al2O3	19.59	19.90	14.57	21.46	13.37	14.53
Fe2O3-T	10.89	9.78	15.46	17.97	9.81	7.33
MgO	5.28	3.83	3.15	7.51	5.08	1.80
CaO	4.70	6.97	1.76	1.63	2.60	5.96
Na2O	3.63	4.44	3.68	2.74	3.19	4.33
K2O	0.42	1.15	0.14	1.07	0.12	0.25
MnO	0.13	0.15	0.17	0.16	0.21	0.13
P2O5	0.11	0.31	0.30	0.11	0.32	0.20
LOI	5.73	2.79	2.49	5.18	4.40	1.78
TOTAL	99.46	101.27	99.74	100.94	100.23	99.50
Rb	187	20	3	22	3	5
Ba	183	484	98	500	122	199
Sr	580	566	225	250	63	494
Pb	51	7	11	8	4	11
Th	46	3	3	2	2	2
U	11	5	4	4	4	4
V	310	200	318	214	217	172
Cr	58	96	14	156	232	43
Ni	66	24	4	92	43	22
Cu	68	80	56	10	27	74
Zn	91	80	128	148	106	71
Ga	20	16	17	22	15	14
Y	17	17	37	23	19	19
Zr	213	88	155	39	99	91
Nb	24	7	13	9	5	7
LITHOLOGY	p-c sh	p-c sh	c-p sh	c-p sh	c-p sh	e-p sh
K2O/Na2O	0.12	0.26	0.04	0.39	0.04	0.06
Na2O+K2O	4.05	5.59	3.82	3.81	3.31	4.58
Al2O3/TiO2	46.6	43.3	9.3	53.7	18.2	17.7
CaO/TiO2	11.2	15.2	1.1	4.1	3.5	7.3
Zr/TiO2	0.051	0.019	0.010	0.010	0.013	0.011
K/Rb	18.6	489.0	353.2	411.0	292.1	440.6
Ba/Sr	0.32	0.85	0.44	1.99	1.92	0.40
Rb/Sr	0.323	0.034	0.015	0.086	0.054	0.010
Ti/Zr	11.8	31.3	60.4	61.4	44.7	54.2
Zr/Nb	9.0	12.0	12.0	4.4	20.5	13.0
Nb/Y	1.42	0.43	0.35	0.38	0.25	0.37
Zr/Y	12.7	5.2	4.2	1.7	5.1	4.8
FeO-T/MgO	1.86	2.30	4.42	2.15	1.74	3.67

KEY: sh=schist; b=biotite; a=amphibole; p=plagioclase; c=chlorite; e=epidote; m=muscovite; q=quartz;
 cc=carbonate; s=sericite; ND=not detected; NA=not analyzed; major elements=wt.% trace
 elements=ppm

Table B1: Sample Analyses (166)

SAMPLE	253	171	114	263B	38	149B
SiO ₂	49.01	53.66	52.62	43.43	76.64	73.19
TiO ₂	0.31	0.39	0.34	0.94	0.25	0.21
Al ₂ O ₃	13.53	15.68	15.62	21.53	10.77	13.89
Fe ₂ O ₃ -T	9.43	8.05	10.16	19.78	4.99	4.64
MgO	4.95	2.81	11.59	4.09	1.47	0.96
CaO	7.01	6.32	2.93	1.11	0.83	0.83
Na ₂ O	4.49	4.11	2.60	2.84	5.30	4.49
K ₂ O	0.76	1.68	0.28	2.26	0.10	1.49
MnO	0.20	0.18	0.16	0.11	0.07	0.07
P ₂ O ₅	0.11	0.24	0.04	0.29	0.08	0.08
LOI	11.47	7.11	5.00	4.64	1.15	0.90
TOTAL	101.26	100.22	101.34	101.02	101.63	100.73
Rb	15	30	5	45	2	19
Ba	774	750	129	880	29	1203
Sr	192	294	147	610	79	74
Pb	16	9	6	11	5	4
Th	2	5	0	5	5	5
U	4	7	3	1	6	5
V	192	145	214	229	15	12
Cr	228	105	890	130	13	11
Ni	33	17	320	44	13	3
Cu	9	48	73	40	ND	23
Zn	100	86	67	80	34	88
Ga	14	15	11	18	7	16
Y	8	17	10	10	28	29
Zr	47	91	24	63	125	113
Nb	5	8	3	7	6	6
LITHOLOGY	m-cc sh	q-c sh	q-c sh	q-m sh	c-q sh	p-q sh
K ₂ O/Na ₂ O	0.17	0.41	0.11	0.80	0.02	0.33
Na ₂ O+K ₂ O	5.25	5.79	2.88	5.10	5.39	5.98
Al ₂ O ₃ /TiO ₂	44.2	40.2	45.9	22.9	43.1	66.8
CaO/TiO ₂	22.9	16.2	8.6	1.2	3.3	4.0
Zr/TiO ₂	0.015	0.023	0.007	0.007	0.050	0.054
K/Rb	412.3	456.7	437.0	419.4	370.2	652.3
Ba/Sr	4.04	2.55	0.88	1.44	0.36	16.26
Rb/Sr	0.080	0.104	0.036	0.073	0.027	0.256
Ti/Zr	39.4	25.8	86.7	90.1	12.0	11.1
Zr/Nb	9.5	11.4	8.4	8.5	21.3	17.5
Nb/Y	0.59	0.47	0.29	0.72	0.21	0.22
Zr/Y	5.6	5.4	2.4	6.1	4.5	3.9
FeO-T/MgO	1.71	2.58	0.79	4.35	3.05	4.35

KEY: sh=schist; b=biotite; a=amphibole; p=plagioclase; c=chlorite; e=epidote; m=muscovite; q=quartz;
cc=carbonate; s=sericite; ND=not detected; NA=not analyzed; major elements=wt.%, trace
elements=ppm

Table B1: Sample Analyses (167)

SAMPLE	91B	93	137	127	RHY1	RHY2
SiO2	76.84	74.36	75.52	77.46	78.68	78.96
TiO2	0.20	0.23	0.24	0.17	0.05	0.05
Al2O3	11.39	13.24	12.24	12.01	12.04	12.35
Fe2O3-T	3.40	3.52	2.89	2.83	1.07	0.74
MgO	1.38	1.51	1.50	1.02	0.51	0.13
CaO	0.58	0.68	0.78	0.29	0.34	0.27
Na2O	5.37	5.02	5.21	3.12	4.73	6.88
K2O	0.26	0.77	0.31	2.20	1.28	0.74
MnO	0.06	0.05	0.42	0.06	0.03	0.03
P2O5	0.04	0.04	0.04	0.06	0.02	0.03
LOI	0.56	0.99	0.97	1.28	0.75	0.39
TOTAL	100.08	100.40	100.12	100.50	99.50	100.56
Rb	4	15	6	47	23	11
Ba	68	517	85	755	600	365
Sr	58	57	61	103	51	87
Pb	2	1	0	8	3	1
Th	3	3	2	4	7	5
U	4	5	4	6	6	5
V	1	8	ND	18	4	3
Cr	12	44	11	13	8	16
Ni	1	5	2	5	2	6
Cu	9	7	4	8	7	ND
Zn	25	19	26	37	12	17
Ga	12	17	14	11	11	8
Y	52	52	45	20	30	28
Zr	142	170	141	121	90	97
Nb	5	6	5	5	6	7
LITHOLOGY	c-p sh	p-q sh	p-q sh	m-q sh	q-s sh	q-s sh
K2O/Na2O	0.05	0.15	0.06	0.70	0.27	0.11
Na2O+K2O	5.63	5.79	5.53	5.32	6.01	7.62
Al2O3/TiO2	57.0	56.6	51.4	70.6	240.8	274.4
CaO/TiO2	2.9	2.9	3.3	1.7	6.8	6.0
Zr/TiO2	0.071	0.073	0.059	0.060	0.179	0.216
K/Rb	516.3	421.3	432.3	2708.3	452.3	572.4
Ba/Sr	1.17	9.11	1.39	1.26	11.68	4.20
Rb/Sr	0.072	0.267	0.099	0.167	0.458	0.124
Ti/Zr	8.4	8.3	10.2	10.1	3.3	2.8
Zr/Nb	26.4	27.0	28.1	20.8	14.7	14.6
Nb/Y	0.10	0.12	0.11	0.22	0.20	0.24
Zr/Y	2.7	3.3	3.1	4.5	3.0	3.5
FeO-T/MgO	2.22	2.10	1.73	2.49	1.90	5.08

KEY: sh=schist; b=biotite; a=amphibole; p=plagioclase; c=chlorite; e=epidote; m=muscovite; q=quartz;
cc=carbonate; s=sericite; ND=not detected; NA=not analyzed; major elements=wt.%; trace
elements=ppm

Table B1: Sample Analyses (168)

SAMPLE	BMR	BMR-B	GG	RBT	151	84B
SiO ₂	78.94	80.47	69.55	73.10	78.20	48.07
TiO ₂	0.11	0.11	0.26	0.20	0.08	3.21
Al ₂ O ₃	11.87	10.65	15.06	13.49	12.34	11.89
Fe ₂ O ₃ -T	2.03	1.97	4.77	3.22	1.22	16.79
MgO	0.12	0.42	1.24	1.17	1.26	5.24
CaO	0.44	0.65	0.81	2.22	0.21	8.23
Na ₂ O	3.73	0.72	0.78	4.09	6.28	1.73
K ₂ O	1.99	2.95	3.89	0.91	0.44	0.64
MnO	0.06	0.09	0.11	0.49	0.03	0.32
P ₂ O ₅	0.03	0.04	0.09	0.06	0.03	1.71
LOI	1.09	1.70	3.18	0.53	0.60	5.31
TOTAL	100.41	99.76	99.73	99.48	100.68	103.14
Rb	54	63	92	17	7	12
Ba	700	NA	NA	437	51	625
Sr	90	38	46	166	40	398
Pb	14	18	18	5	1	15
Th	16	14	7	4	9	2
U	9	7	6	5	6	3
V	0	NA	NA	13	275	103
Cr	6	NA	NA	26	666	22
Ni	3	NA	NA	3	6	5
Cu	6	NA	NA	8	9	13
Zn	182	NA	NA	25	14	237
Ga	24	NA	NA	11	12	20
Y	42	134	24	37	22	104
Zr	240	192	142	114	101	573
Nb	33	33	10	4	5	19
LITHOLOGY	m-q sh	m-q sh	m-q sh	trond	trond	q-c sh
K ₂ O/Na ₂ O	0.53	4.07	5.00	0.22	0.07	0.37
Na ₂ O+K ₂ O	5.72	3.67	4.67	5.01	6.72	2.37
Al ₂ O ₃ /TiO ₂	107.9	96.8	58.6	67.4	154.3	3.7
CaO/TiO ₂	4.0	5.9	3.1	11.1	2.6	2.6
Zr/TiO ₂	0.219	0.175	0.055	0.057	0.127	0.018
K/Rb	307.0	388.5	350.6	439.6	542.6	426.7
Ba/Sr	7.77	NA	NA	2.62	1.26	1.57
Rb/Sr	0.597	1.680	2.010	0.103	0.167	0.031
Ti/Zr	2.7	3.4	10.8	10.5	4.7	33.6
Zr/Nb	7.2	5.8	13.7	26.3	20.8	30.5
Nb/Y	0.80	0.25	0.44	0.12	0.22	0.18
Zr/Y	5.8	1.4	6.0	3.1	4.5	5.5
FeO-T/MgO	15.23	4.21	3.46	2.48	0.87	2.88

KEY: sh=schist; b=biotite; a=amphibole; p=plagioclase; c=chlorite; e=epidote; m=muoncovite; q=quartz;
cc=carbonate; s=sericite; ND=not detected; NA=not analyzed; major elements=wt.% trace
elements=ppm

Table B2: Accuracy

(169)

SAMPLE					AVG.	R.V.	ERR.
SiO ₂	BCR-1	54.27	54.30	54.27	54.28	54.53	0.46
TiO ₂	BCR-1	2.21	2.23	2.23	2.22	2.26	1.62
Al ₂ O ₃	BCR-1	13.59	13.56	13.61	13.59	13.72	0.97
Fe ₂ O ₃ -T	BCR-1	13.30	13.22	13.30	13.27	12.44	6.69
MgO	BCR-1	4.53	4.18	4.92	4.54	3.48	30.56
CaO	BCR-1	6.99	6.98	7.01	6.99	6.97	0.33
Na ₂ O	BCR-1	4.10	3.82	4.57	4.16	3.30	26.16
K ₂ O	BCR-1	1.73	1.71	1.72	1.72	1.70	1.18
MnO	BCR-1	0.21	0.20	0.20	0.20	0.18	12.96
P ₂ O ₅	BCR-1	0.36	0.36	0.36	0.36	0.36	0.00
LOI	BCR-1	0.62	0.62	0.62	0.62	0.67	7.46
TOTAL	BCR-1	101.91	101.18	102.81	101.97	99.61	2.36
Rb	GS-N			187.2		185.0	1.17
Ba							
Sr	AN-G	76.0	76.2	76.3	76.1	76.0	0.18
Pb	GS-N			51.1		53.0	3.62
Th	GS-N			46.3		44.0	5.14
U	GS-N			11.1		8.0	38.75
V							
Cr							
Ni	G-2	8.4	9.5	8.2	8.7	5.0	73.93
Cu	G-2	8.9	10.4	8.3	9.2	11.0	16.45
Zn	G-2	85.4	87.0	86.2	86.2	85.0	1.40
Ga	G-2	15.5	18.5	18.1	17.4	22.0	21.08
Y	AN-G	8.1	8.1	8.1	8.1	8.0	1.46
Zr	GS-N			213.0		235.0	9.36
Nb	GS-N			23.8		23.0	3.43

AVG.= average, R.V.= recommended value, ERR.= error

KEY: ND=not detected; NA=not analyzed; major elements=wt. %; trace elements=ppm

Table B3: Precision

(170)

SAMPLE					AVG.	S.D.	C.V.
SiO ₂	BCR-1	54.27	54.30	54.27	54.28	0.01	0.03
TiO ₂	BCR-1	2.21	2.23	2.23	2.22	0.01	0.42
Al ₂ O ₃	BCR-1	13.59	13.56	13.61	13.59	0.02	0.15
Fe ₂ O ₃ -T	BCR-1	13.30	13.22	13.30	13.27	0.04	0.28
MgO	BCR-1	4.53	4.18	4.92	4.54	0.30	6.65
CaO	BCR-1	6.99	6.98	7.01	6.99	0.01	0.18
Na ₂ O	BCR-1	4.10	3.82	4.57	4.16	0.31	7.43
K ₂ O	BCR-1	1.73	1.71	1.72	1.72	0.01	0.47
MnO	BCR-1	0.21	0.20	0.20	0.20	0.00	2.32
P ₂ O ₅	BCR-1	0.36	0.36	0.36	0.36	0.00	0.00
LOI	BCR-1	0.62	0.62	0.62	0.62		
TOTAL	BCR-1	101.91	101.18	102.81	101.97	0.67	0.65
Rb	AN-G	2.6	2.1	3.2	2.6	0.42	15.98
Ba							
Sr	AN-G	76.0	76.2	76.3	76.1	0.10	0.14
Pb	AN-G	6.3	4.9	4.5	5.2	0.76	14.58
Th	AN-G	1.7	1.8	2.3	1.9	0.24	12.76
U	AN-G	4.2	3.2	4.1	3.8	0.43	11.18
V							
Cr							
Ni	G-2	8.4	9.5	8.2	8.7	0.58	6.69
Cu	G-2	8.9	10.4	8.3	9.2	0.87	9.41
Zn	G-2	85.4	87.0	86.2	86.2	0.66	0.77
Ga	G-2	15.5	18.5	18.1	17.4	1.34	7.72
Y	AN-G	8.1	8.1	8.1	8.1	0.02	0.25
Zr	AN-G	20.4	20.7	19.7	20.3	0.41	2.03
Nb	AN-G	2.9	3.2	2.7	2.9	0.20	6.85

AVG.= average, S.D.= standard deviation, C.V.= coefficient o

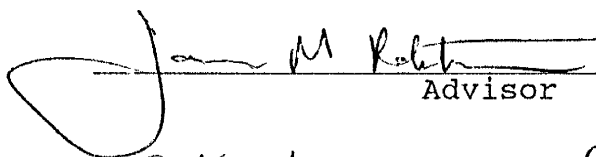
KEY: ND=not detected; NA=not analyzed; major elements=wt. %; trace elements=ppm

Tabel B4: Lower Limit of Detection

Element	ppm
Rb	3.0
Ba	11.0
Sr	3.0
Pb	9.8
Th	8.7
U	3.5
Cr	5.0
Ni	2.0
Cu	5.1
Zn	6.1
Ga	2.7
Y	3.2
Zr	2.5
Nb	2.5

From the New Mexico Bureau of Mines and Mineral Resources x-ray lab.

This thesis is accepted on behalf of the faculty
of the Institute by the following committee:



Advisor

C. K. Mawer (CHRISTOPHER K. MAWER)



June 8, 1988

Date